

Summer 8-22-2018

Characterization of Phosphorylated G Protein Function and Membrane Culstering by Super Resolution Imaging

Sarah A. Alamer

Follow this and additional works at: <https://digitalcommons.library.umaine.edu/etd>

 Part of the [Cell Biology Commons](#)

**CHARACTERIZATION OF PHOSPHORYLATED G PROTEIN FUNCTION AND
MEMBRANE CLUSTERING BY SUPER RESOLUTION IMAGING**

By

Sarah A. Alamer

B.S. King Faisal University, 2008

M.S. University of Maine, 2013

A DISSERTATION

Submitted in Partial Fulfillment of the

Requirements for the Degree of

Doctor of Philosophy

(in Biomedical Science)

The Graduate School

The University of Maine

August 2018

Advisory Committee:

Robert E. Gundersen, Associate Professor, Department of Molecular and Biomedical Sciences, Advisor.

Julie Gosse, Associate Professor, Department of Molecular and Biomedical Sciences

Rebecca J. Van Beneden, Professor, School of Marine Science

Sam Hess, Associate Professor, Department of Physics and Astronomy

Lucy Liaw, Faculty Scientist III, Maine Medical Center Research Institute

Jeff Hadwiger, Associate Professor, Department of Microbiology & Molecular Genetics, Oklahoma State University.

CHARACTERIZATION OF PHOSPHORYLATED G PROTEIN FUNCTION AND MEMBRANE CLUSTERING BY SUPER RESOLUTION IMAGING

By Sarah A. Alamer

Dissertation Advisor: Dr. Robert E. Gundersen

An Abstract of the Dissertation Presented
in Partial Fulfillment of the Requirements for the
Degree of Doctor of Philosophy
(in Biomedical Science)

August 2018

Heterotrimeric G proteins play crucial roles in various signal transduction pathways, where they act as molecular switches in transducing a signal from G protein coupled receptors (GPCRs) at the plasma membrane to downstream effectors. Although their mechanism of action is mostly concentrated at the plasma membrane, their dynamic membrane organization and how it is regulated are not understood. Due to the diffraction limited resolution of fluorescence microscopy, studying the precise organization of membrane proteins can be challenging. In this study, we took advantage of super-resolution fluorescence photoactivation localization microscopy (FPALM) to overcome this challenge. *Dictyostelium discoideum* was used as a cellular model to study G protein function and membrane organization. These cells rely on chemotaxis

toward a secreted chemoattractant, cyclic adenosine monophosphate (cAMP) during the development phase of their life cycle. The G α 2 subunit of *D. discoideum* is required for the chemotactic response. Once activation occurs, G α 2 is known to be phosphorylated on serine 113; however, the role of this phosphorylation remains poorly defined. Exchange of serine residue 113 to alanine causes starved cells to begin the aggregation phase several hours sooner when compared to wild type, while exchanging this serine to aspartic acid (phosphorylation mimic) shows a dramatic decrease in plasma membrane surface localization. At the nanoscale level, images using FPALM show that activation and phosphorylation cause significant changes to G α 2 cluster density in the plasma membrane. Getting these first nanoscale images of G protein provided robust information, which adds to our understanding of the ligand-dependent reorganization and clustering of G α 2 required for precise signaling. Cell fractionation experiments supported this result. In addition, phosphorylation-dependent interaction between phosphorylated G α 2 and *D. discoideum* 14-3-3 protein was detected.

ACKNOWLEDGEMENTS

I first and foremost would like to thank my advisor Dr. Robert Gundersen for welcoming me into his lab and giving me the opportunity to be one of his graduate students. Thank you for your constant feedback, guidance, support, patience and understanding during the past eight years. It has been an enjoyable experience working with you. I also would like to acknowledge my thesis committee members for the time, assistance and guidance that you gave me during my graduate study. Special thanks to Dr. Sam Hess for allowing me to work in his lab and use FPALM for this project. Your kind favors contributed in moving this project forward. I am also very thankful to all his lab members for all the help and support. Nikki and Matt, thank you for your amazing assistance to make this study successful. I am so grateful to the GSBSE program for all the opportunities that helped me grow personally and professionally.

My deepest gratitude goes to my parents for their hard work, struggle, emotional support and encouragement during this journey. Your trust and your belief in me have always been my biggest motivation behind my success. I love you so much!

Thanks to my amazing siblings for standing by my side during this challenging process. Your love and support keeps me always going. I'm blessed to have you in my life. To my little brother, Abdulrahman, thank you for all you had done for my family and me. You may no longer live here with us but you are in my heart and thought forever. We started this Journey together and we wished to finish it together. With all your love and care, here I am, completing this amazing achievement for you and me and all our loved ones. For you and our lovely parents I dedicate this degree.

A very special thanks to the love of my life, Nasser and my wonderful children for all their constant love and support during the grad school years. Nasser, I really appreciate all your patience and hard effort that made things run smoothly. This is an important milestone in my life and I couldn't have done it without you. I am forever indebted. Love you!

For all my friends, Sarah Alrowaished, Linda Bradford, Jessica Piesz, Catherine Frederick, The Office of International Programs, Maginnis lab members, GSBSE students and my friends in Saudi Arabia. You have all helped me in too many ways for which I am more thankful than you'll ever know.

Lastly, I would like to thank the government of Saudi Arabia and my sponsor, King Faisal University, for their financial support during my academic journey.

TABLE OF CONTENTS

ACKNOWLEDGEMENTS.....	ii
LIST OF FIGURES.....	vii
LIST OF ABBREVIATIONS.....	ix
Chapter	
1. CHAPTER 1: INTRODUCTION.....	1
1.1. G-protein Coupled Receptors (GPCRs).....	1
1.2. Overview of Heterotrimeric G Protein Signal.....	4
1.2.1. Mechanism of Action.....	6
1.2.2. Physiological Functions of G Protein and Diseases.....	13
1.3. Cell Membrane Organization and Signal Transduction.....	15
1.4. Cell Motility.....	22
1.5. <i>Dictyostelium Discoideum</i> : An Experimental Model for Cell Motility and Chemotaxis.....	26
1.6. Rationale.....	32
2. CHAPTER 2: MATERIAL AND METHODS.....	33
2.1. Cell Lines, Cell Culture and Development.....	33
2.2. Antibodies and Reagents.....	33
2.3. Plasmid Construction, Mutagenesis and Transformation of <i>D.discoideum</i>	34
2.4. Gel Electrophoresis and Immunoblotting.....	35
2.5. Cell Fractionation and Density Gradient Centrifugation.....	36
2.6. Ga2/14-3-3 Co-Immunoprecipitation.....	37

2.7. Cell Immunostaining and Confocal Imaging.....	37
2.8. Cell Viability Assay.....	38
2.9. Fluorescence Photo-Activated Localization Microscopy (FPALM).....	39
2.9.1. Sample Preparation.....	39
2.9.2. Single-Color FPALM Experimental Setup and Image Acquisition.....	39
2.9.3. Image Rendering and Cluster Analysis.....	41
2.10. Data Analysis and Statistics.....	42
3. CHAPTER 3: FACTORS INVOLVED IN MEMBRANE DISTRIBUTION AND SHUTTLING OF ACTIVATED $\text{G}\alpha_2$ SUBUNIT.....	43
3.1. Background and Hypothesis.....	43
3.2. Results.....	45
3.2.1. Membrane Distribution of Activated $\text{G}\alpha_2$ is Independent of $\text{G}\beta$ and/or cAR1.....	45
3.2.2. $\text{G}\alpha_2$ Translocation is Independent of Raft Organization.....	50
3.2.3. Dissociation-Defect of G protein Heterotrimer Restricted ER to Golgi Translocation.....	52
4. CHAPTER 4: FUNCTIONAL CONSEQUENCE OF $\text{G}\alpha_2$ PHOSPHORYLATION.....	54
4.1. Background and Hypothesis.....	54
4.2. Results.....	56
4.2.1. $\text{G}\alpha_2$ Phosphorylation Regulates its Function.....	56
4.2.2. $\text{G}\alpha_2$ Phosphorylation Regulates its Membrane/ Cytosolic Localization.....	60

4.2.3. Activated and Phosphorylated G α 2 Co-localized With 14-3-3 Proteins.....	64
4.2.4. The Interaction Between G α 2 and 14-3-3 is Activation and Phosphorylation-Dependent.....	66
4.2.5. Phosphorylation of G α 2 Regulates Myosin II Filament Dynamic in the Polarized Cells.....	69
5. CHAPTER 5: MEMBRANE DISTRIBUTION AND CLUSTERING OF ACTIVATED AND PHOSPHORYLATED Gα2.....	71
5.1. Background and Hypothesis.....	71
5.2. Results.....	74
5.2.1. G α 2 Phosphorylation Regulates its Membrane Distribution Pattern.....	74
5.2.2. Membrane Clustering of G α 2 Using High-Resolution Fluorescent Photoactivated Localization Microscopy (FPALM) Imaging.....	76
6. CHAPTER 6: DISCUSSION.....	81
REFERENCES.....	93
BIOGRAPHY OF THE AUTHOR.....	110

LIST OF FIGURES

Figure 1.1.	Phylogenetic relationship of human and mouse G α subunits.....	5
Figure 1.2.	Activation cycle of the heterotrimeric G protein by G protein coupled receptor.....	8
Figure 1.3	The structure of the G α .GDP/G β γ	12
Figure 3.1.	Membrane distribution of G β (YFP) and cAR1(YFP) in OptiPrep density gradient.....	47
Figure 3.2.	Cellular localization and membrane distribution of cAR1-YFP.....	48
Figure 3.3.	Membrane distribution of activated cAR1-YFP, G α 2-YFP and G β -YFP.....	49
Figure 3.4	Membrane distribution of GPI-anchored protein, gp80.....	51
Figure 3.5	Co-localization of G α 2(YFP)-wt and G α 2(YFP)-G207A with calnexin in AX2 cells.....	53
Figure 4.1	Developmental phenotype of g α 2-null cells (MYC2) cells expressing G α 2-wt, G α 2-S113A and G α 2-S113D.....	58
Figure 4.2.	Developmental phenotype at 24hr of g α 2-null cells (MYC2) cells expressing G α 2-wt, G α 2-S113A and G α 2-S113D.....	59
Figure 4.3	Cellular localization of G α 2(S113A)-YFP and G α 2(S113D)-YFP.....	61
Figure 4.4.	Cellular phenotype of G α 2 (S113D)-YFP expressing cells.....	61
Figure 4.5	Membrane and cytosolic distribution of G α 2-YFP.....	63
Figure 4.6	Co-localization of G α 2 and 14-3-3 proteins.....	65
Figure 4.7	Co-immunoprecipitation of G α 2 and 14-3-3 proteins.....	67

Figure 4.8	Expression level of 14-3-3s, G α 2 (S113A)-YFP and G α 2 (S113D)-YFP.....	68
Figure 4.9	Immunostaining of Myosin II in polarized <i>Dictyostelium</i> cells.....	70
Figure 5.1.	Membrane distribution of G α 2(S113A)-YFP and G α 2(S113D)-YFP.....	75
Figure 5.2.	Proper controls for FPALM imaging.....	78
Figure 5.3	Nanoscale membrane cluster morphology of active/inactive G α 2(wt)-YFP.....	79
Figure 5.4	Nanoscale membrane cluster morphology of G α 2(S113A)-YFP and G α 2(S113D)-YFP.....	80
Figure 6.1	Model of G α 2 plasma membrane clustering.....	92

LIST OF ABBREVIATIONS

AC	Adenylyl cyclase
ACS	Auriculo-Condylar Syndrome
AH	α -helical domain
cAMP	Cyclic adenosine monophosphate
cARs	Cyclic AMP receptors
cGMP	Cyclic guanosine monophosphate
Crac	Cytosolic regulator of adenylyl cyclase
DAG	Diacylglycerol
DPLL	Dual lipid modification motif
DTT	Dithiothreitol
FPALM	Fluorescence photoactivation localization microscopy
G-domain	GTPase domain
G-proteins	Guanine nucleotide-binding proteins
GCA	Guanylyl cyclase A
GDI	Nucleotide dissociation inhibitor
GEFs	Guanine nucleotide exchange factors
GPCRs	G protein-coupled receptors
GPI	Glycosylphosphatidylinositol
GRKs	G protein-coupled receptor kinases
GTP	Guanosine triphosphate
HA	Haemagglutinin
IP ₃	Inositol trisphosphate

MAT	Mesenchymal-amoeboid transition
PAK1	p21-activated protein kinase
PC	Phosphatidylcholine
PdsA	Phosphodiesterase
PE	Phosphatidylethanolamine
phdA	PH domain protein A
PI3K	Phosphoinositide-3-kinases
PIP ₂	Phosphatidylinositol 4,5-bisphosphate
PIP2	Phosphatidylinositol 4,5-bisphosphate
PIP ₃	Phosphatidylinositol 3,4,5-trisphosphate
PKC	Protein kinase C
PLA2	Phospholipase A2
PLC-β	Phospholipase Cβ
PS	Phosphatidylserine
PSF	Pre-starvation factor
PTEN	Phosphatase tensin homologue
RGSs	Regulator of G Protein Signaling
Rho	Ras homolog
RTKs	Receptor tyrosine kinases
sGC	Soluble guanylyl cyclase
SIMS	Secondary ion mass spectrometry
TGFb	Transforming growth factor b
TsuA	Tsunami protein

CHAPTER 1

INTRODUCTION

1.1. G Protein-Coupled Receptors (GPCRs)

G protein-coupled receptors (GPCRs) consist of seven transmembrane helices (TM1-TM7) connected by three extracellular loops and three intracellular loops (Baldwin., 1994). GPCRs are the largest family of membrane receptors in eukaryotes (Strader et al., 1994) where they represent 3-4% of the human genome and are targeted by more than 40% of marketed drugs (Drews, 1996). This fact reflects the extremely important role of GPCRs in modulating many physiological processes ranging from cell communication, neurotransmission and cell chemotaxis to the senses of smell, taste and sight (Pierce et al., 2002). These processes can be induced mostly by GPCRs transducing extracellular signals across the cell membrane via guanine nucleotide-binding proteins (G-proteins) (Szczepek et al., 2014; Syrovatkina et al., 2016). A possible GPCR function independent of G protein has also been described (Hall et al., 1999; Zhai et al., 2005).

Shorr et al., 1981 reported the purification of the first GPCR, the β -adrenergic receptor. Since it was the first GPCR to be characterized and structurally determined, the β -adrenergic receptor was a model system for GPCRs family (Cherezov et al. 2007).

The basic structure of the 7TM α - helices with an extracellular amino-terminal segment and an intracellular carboxy-terminal tail is common motif among all the

members of the GPCR family. The length of these receptors can vary between 311 and 1490 amino acid residues. Most of this variation falls on the length of N and C termini (Gentles et al., 1999).

In some of the GPCRs but not all, the C terminus contains a cysteine residue that acts as a palmitoylation site, which regulates the attachment of the GPCRs to the plasma membrane (Chini and Parenti, 2009). The N terminus is a key player in ligand binding and activation processes. This structure for the majority of GPCRs is stabilized by disulfide bonds formed by two highly conserved cysteine residues in the extracellular loops (ECL1 and ECL2) that influence protein folding, which is important for receptor trafficking to the cell surface (Probst et al., 1992; Baldwin, 1994). However, many GPCRs contain non-conserved extracellular cysteine residues that play a role in receptor stabilization as well (Noda et al., 1994). The three intracellular loops contain Ser and/or Tyr residues that are highly involved in GPCR signaling, receptor phosphorylation and desensitization (Baldwin, 1994). A previous study suggested that ICL2 and ICL3 are important for the association of the receptors with G proteins (Itoh et al., 2001)

Agonist binding/activation of GPCRs causes conformational rearrangement of the transmembrane helices that facilitate their interaction with heterotrimeric G protein as well as promote the phosphorylation of the receptors by G protein-coupled receptor kinases (GRKs) and second messenger-dependent kinases, PKA and PKC. GRKs consist of six Ser/Thr protein kinases that selectively enhance their activity by using the N-terminus to form intracellular interactions with the GPCRs (Pingret et al., 1998). It has been shown that upon agonist binding, GPCRs act as guanine nucleotide exchange

factors (GEFs) for the G protein to promote the exchange of bound GDP from G_a to GTP, which in turn transduces the signal to downstream effectors. GPCR phosphorylation then recruits β-arrestin to facilitate the receptor's endocytic mechanism without interfering with G protein coupling to the receptor (Thomsen et al., 2016).

The 1406 GPCRs are classified into six families that share some sequence homology and functional similarity. Family A known as rhodopsin-like is the largest family. Rhodopsin and β-adrenergic receptors belong to this family. Family B known as Secretin-like consist of 60 members that do not share any significant sequence homology. Family C, which is metabotropic glutamate receptors family consist of 24 members. Family D, the Fungal pheromone receptor family comprises pheromone receptors (VNs). Family E, cAMP receptor family (cARs) has four members found in *Dictyostelium discoideum*. Family F, known as serpentine receptor family such as Frizzled/Smoothened receptor play a major role in embryonic development (Gao and Wang, 2006; Tuteja., 2009).

In the social amoeba *Dictyostelium discoideum*, four serpentine cyclic AMP (cAMP) receptors (cARs) have been identified (cAR1, cAR2, cAR3 and cAR4) that show around 54-69% amino acid identity; they are highly homologous. All cARs use cyclic adenosine monophosphate (cAMP) as a ligand however each receptor is expressed in specific stages of the organism's life cycle. They share similar biological function, which is to regulate the expression of certain developmental genes. During *Dictyostelium* development, the expression of cAR1 occurs before and during aggregation. In late aggregation, cAR3 is expressed in the prespore cell population, while after aggregation,

both cAR2 and cAR4 are expressed in the prestalk cells population (Klein et al., 1988; Johnson et al., 1993; Louis et al., 1994; Saxe et al., 1996; Yu and Saxe, 1996). To understand their function, many studies were conducted using cAR knockout cell lines. The *car1*-null cells showed an aggregation-minus phenotype as well as no expression of the essential developmental genes (Sun and Devreotes., 1991). Aggregation and development were normal for *car3*-null cells (Johnson et al., 1993). The development of *car2*-null cells was blocked in the mound stage and abnormal slug morphogenesis was detected using *car4*-null cells. An abnormal reduction in prestalk gene expression was seen in both *car2*- and *car4*-null cell lines (Saxe et al., 1993; Louis et al., 1994). The four *Dictyostelium* cARs however still further require further study to fully understand the specificity of each receptor and its association with specific signal transduction pathways.

1.2. Overview of Heterotrimeric G Protein Signal

In order for GPCRs to mediate downstream signal transduction and regulate many biological functions, a major transducer is needed. Among guanine nucleotide binding proteins, the heterotrimeric G proteins act as molecular switches to transduce the signal initiated from these receptors to downstream effectors (Ross and Gilman, 1980). Many of these effectors have been identified and characterized including adenylyl cyclases, phospholipase isoforms, protein tyrosine kinases and ion channels. Heterotrimeric G proteins localize at the inner leaflet of the plasma membrane and consist of three functional subunits α , β and γ , which bind to each other to form a stable complex in the inactive state of the protein. In human, 35 genes encode G proteins with 16 of them encoding α -subunits, 5 β and 12 γ . G-proteins are recognized by their $G\alpha$

subunits. It is the largest subunit with a molecular weight around 45 kDa. Based on G α subunits sequence and functional similarities, G proteins are classified into four families, Gai, Gaq, Gas, and G α 12 (Figure 1.1). The largest family is Gai which consists of seven members: Gai1, Gai2, Gai3, Gao, Gaz, Gat and Gag. They are expressed in most cell types including neurons, platelets, taste buds, and rod and cone outer segments. The Gaq family consists of four members, Gaq, G α 11, G α 14, and G α 15/16. Both Gaq and G α 11 are ubiquitously expressed. G α 14 is expressed in the kidney, lung, and liver while the expression of G α 15/16 is restricted in hematopoietic cells. The Gas family consists of two members, Gas, which is expressed ubiquitously and Gao β in olfactory neurons. Similarly, two members have been identified for G α 12 family, G α 12 and G α 13 and they are ubiquitously expressed (Syrovatkina et al., 2016).

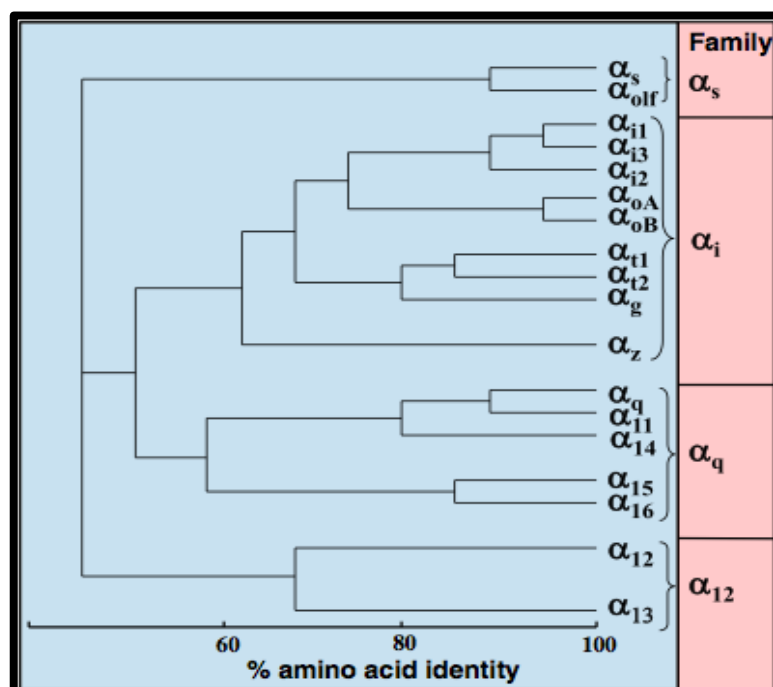


Figure 1.1. Phylogenetic relationship of human and mouse G α subunits. (Syrovatkina et al., 2016).

Five G β subunits and 12 G γ subunits have been identified. The G β subunits share 80 to 90% sequence similarity and they are widely expressed except G β 5, which is highly expressed in the brain. The G γ subunits share 20 to 80% sequence similarity and are widely distributed (Syrovatkina et al., 2016).

1.2.1. Mechanism of Action

Upon ligand binding to the GPCRs, the GDP bound to the α subunit is released, which allows for binding of guanosine triphosphate (GTP). This replacement induces the dissociation of the G α subunit from GPCR and G $\beta\gamma$ complex. Both G α -GTP and G $\beta\gamma$ complex can interact and modulate downstream effectors. These interactions result in dramatic changes in the concentration of intracellular second messengers including Ca $^{+2}$, cAMP, inositol trisphosphates and diacylglycerol. The deactivation process is induced by the GTPase activity of most G α subunits that leads to GTP hydrolysis and converts G proteins from a GTP-bound active state to a GDP-bound inactive state (Figure 1.2).

For most classes of G α subunits, turnover rates are from 2 to 4 min at 30° C. This GDP/GTP cycling of the G α subunit is regulated by three novel factors: Regulator of G Protein Signaling (RGSs) that interacts with G α to stimulate GTP hydrolysis, guanine nucleotide dissociation inhibitor (GDI) and guanine nucleotide exchange factor (GEF). In 1996, the first RGS was discovered in yeast (Chen and Otte, 1982a,b). RGSs specifically and selectively bind G α subunits through a conserved helical domain of approximately 130 amino acids in length, called the RGS domain. There are over 20 RGS family members with a conserved RGS domain which have been classified into 9

subfamilies based on the sequence similarity of this domain (De Vries et al.,2000; Ross and Wilkie., 2000; Siderovski and Willard., 2005). Each subfamily has a distinct N terminal region that is essential for its cellular localization as well as for its functionality and selectivity. A single RGS protein can regulate many types of G α subunits and one G α may be regulated by several RGS proteins. Clear experimental evidences have supported the selective regulation of RGS proteins. Both RGS4 and RGS19 selectively stimulate the GTPase activity of G α i 1,2,3 , G α 0 and G α q-mediated activation of phospholipase C β (PLC- β) (Berman et al., 1996; Hepler et al., 1997; Huang et al., 1997). However, G α q-mediated 5-HT2A receptor signaling is attenuated by RGS2 and RGS7. Both RGS2 and RGS-PX1 were shown to interact with G α s and RGS-PX1 specifically regulates G α s-mediated β 2 adrenergic receptor signaling (Zheng et al., 2001; Roy et al., 2006). Although their major function is stimulating the GTPase activity of G α subunits, RGS have other regulatory roles. It has been shown that RGS inhibit G proteins from binding to their effectors as well as increase the affinity of G α subunits for G $\beta\gamma$ subunits after GTP hydrolysis. Additional regulation has been reported including microtubule dynamics, receptor internalization and protein- trafficking mechanisms in the brain, liver and kidney. However, fuller understanding of their mechanisms of action and their roles in G protein signaling is needed.

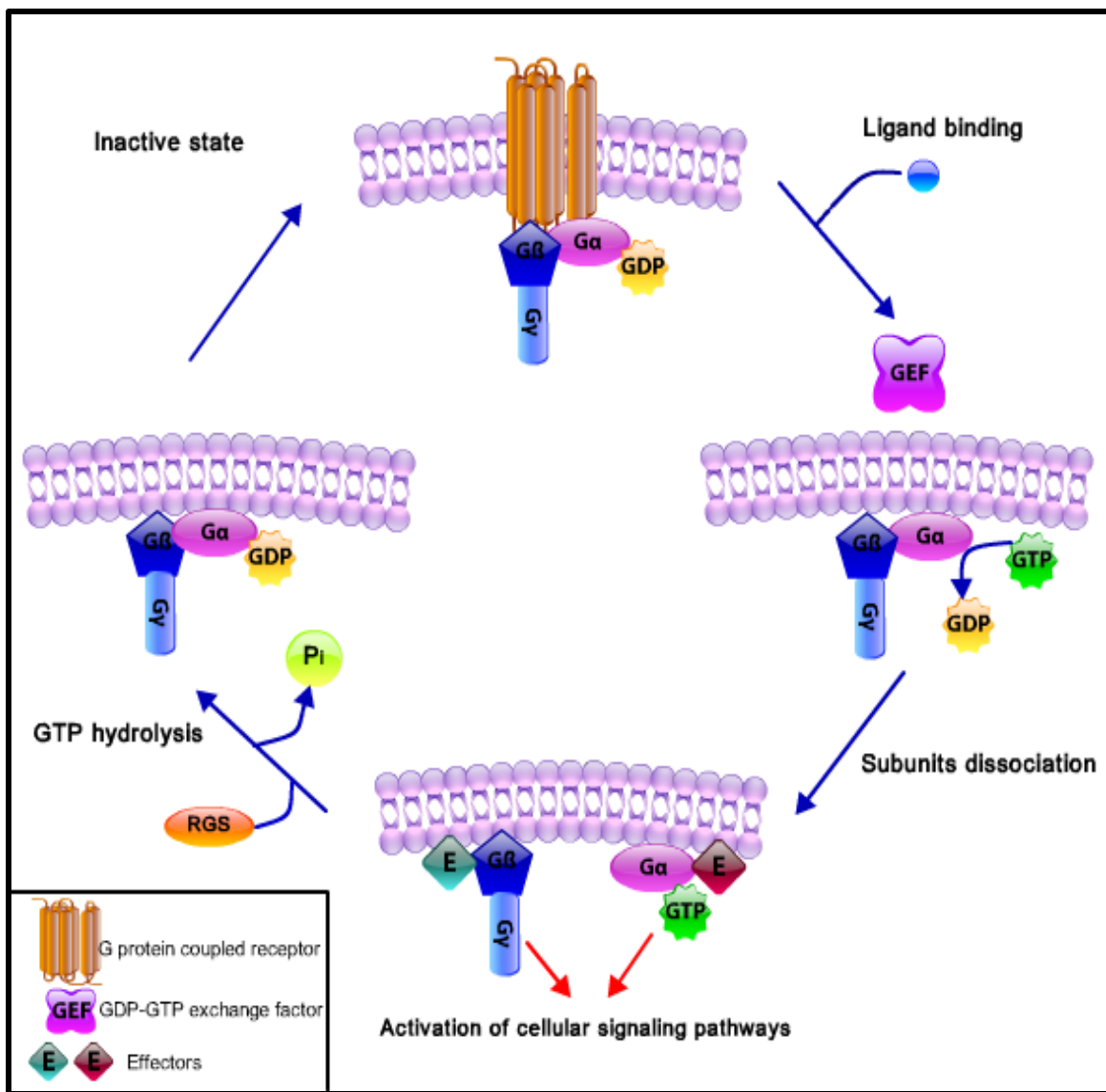


Figure 1.2. Activation cycle of the heterotrimeric G protein by G protein couple receptor. In the living cell, heterotrimeric G protein is bound to the inner membrane leaflet. Ligand binding to the receptor causes its conformational change which in turn allows exchange of GDP for GTP bound to the G_α subunit. This exchange triggers the dissociation of the active G_α-GTP from G_β-G_γ dimer and both can then interact with down stream effectors. This activation is a temporary state and can be shifted to the inactive state of the G protein by GTPase activity of the G_α subunit, which is enhanced by RGS to hydrolyze GTP to the GDP-bound G_α, thus causing it to re-associate with G_β-G_γ dimer.

During this regulated GTP/GDP (active/inactive) cycle, a distinct conformational change of the G protein is formed in each stage (Duc *et al.*, 2017). By the early 90's, the structures of G α subunits in GTP- and GDP-bound forms were described as either a monomer or a G α β γ heterotrimer (Noel *et al.*, 1993; Wall *et al.*, 1995; Lambright *et al.*, 1996). In general, all G α subunits consist of two distinct domains: Ras-like or GTPase domain and a helical domain (Figure 1.3). The Ras-like domain is common to all members of Ras super family. The heterotrimeric GTPase domain is comprised of a six-stranded β -sheet (β 1- β 6) surrounded by five helices (α 1- α 5) in addition to three flexible switch regions (switch I, switch II and switch III) that undergo conformational changes in response to the GTP binding. The N-myristoylated and palmitoylated G protein is associated with the inner leaflet of the plasma membrane through the N-terminus (Ras-domain). The helical domain (AAs; 59-172) is unique to the family of heterotrimeric G proteins and consists of six helices (α A- α F). It is connected to the Ras domain by two polypeptide segments known as linker 1 (switch I) and linker 2 in a way that these two domains form a deep cleft where the nucleotide binds tightly (Lambright, 1994; Nole *et al.*, 1993). GDP binding is stabilized by interactions between the phosphate groups of GDP and the P-loop, the α 1 helix, and switch I of the G α subunit in addition to the interactions between the guanine ring of GDP and the α G helix and strands β 4- β 6 of the G α subunit. On the other hand, GTP binding stabilizes the three flexible regions (switches I, II and III) by connecting them with the γ -phosphate group.

The change in structure between the G α -GDP and G α -GTP, which happens on a microsecond time scale, has been detected by principal component analysis of 53 G α crystallographic structures. This analysis revealed that the conformational change is

concentrated on the three flexible regions (switches I, II and III) of the GTPase domain, which leads to a decreased affinity of $\text{G}\alpha$ -GTP to its GPCR and $\text{G}\beta\gamma$ complex. In addition, a small-scale ($<10^\circ$) rotation of the helical domain is observed. However, a large-scale opening and closing ($>60^\circ$) of the helical domain relative to the GTPase domain has been detected in nucleotide-free $\text{G}\alpha_t$ (Yao and Grant; 2013). Also, a larger-scale (127°) rotation of the helical domain with respect to the GTPase domain was reported in the crystallographic structure of $\text{G}\alpha_s$ in complex with $\text{G}\beta\gamma$ and the $\beta 2$ adrenergic receptor (Westfield et al., 2011).

A recent study on the $\text{G}\alpha$ subunit, $\text{G}\alpha_i$, showed that the GDP-bound form of this subunit is open, dynamic and more flexible while the structure of GTP-bound form is more compact and rigid. This study also showed that the conformational change of this subunit during the GDP/GTP cycle controls its binding with GPCR. The apo form of $\text{G}\alpha_i$ has the highest affinity for the receptor, which is reduced by binding of GDP. This change in the affinity for the receptor is caused by a conformational change concentrated on the helix 5 in GTPase domain, which is the main site for receptor interaction. The results revealed that the activated GPCR binds GDP-bound $\text{G}\alpha$ subunit and promotes a conformational change that leads to the low-affinity state of the protein and influences the apo form to bind GTP (Goricanec et al., 2016). The critical role of the $\alpha 5$ helix in G protein activation by GPCRs has been a recent focus (Shim et al., 2013; Alexander et al., 2014; Dror et al., 2015). An approximately 60° displacement or rotation of the $\alpha 5$ helix was observed upon GPCR binding. It was suggested that this rotation is essential for GPCR-mediated allosteric GDP release by increasing the flexibility of the guanine ring- contacting the $\beta 6/\alpha 5$ loop, which leads to disruption of the connection

between the GDP and the GTPase domain. In addition to the role of the α 5 helix in G protein activation, another rearrangement was detected including the interaction between α 5 helix, β 6/ α 5 loop, α 1 helix, and α G helix (Alexander *et al.* 2014; Dror *et al.*, 2015). Another study conducted by Flock *et al* (2015) described the mechanism of activation where the orientation of the α 5 helix disrupts its contact with the α 1 helix leading to an increased flexibility of the α 1 helix and in turn disrupt the contacts between the α 1 helix and α -helical (AH) domain as well as GDP. Releasing of GDP and separation of the AH domain were observed as a result of this disruption.

The β and γ subunits tightly associated and exist as a constitutive dimer. The 35 kDa β subunit has a unique shape that consists primarily of seven distinctive WD repeats, that are approximately 40 amino acids in length, and form a seven-bladed beta-propeller. Each blade is comprised of four-stranded antiparallel β -sheets (Fong *et al.*, 1986; Neer *et al.*, 1994; Wall *et al.*, 1995). $\text{G}\gamma$ is the smallest subunit of the heterotrimeric G protein with a molecular weight of 8-11KDa. This subunit consists of an N-terminal helix forming a parallel coiled-coil with the N-terminal helix of $\text{G}\beta$ by packing against one side of the propeller, contacting blades 4 and 5. Two conserved regions in the $\text{G}\gamma$ subunit have been identified. The first one is located in the middle and is responsible for its specificity for binding to the different β subunits while the other is a dual lipid modification motif (DPLL), which is a target for the post-translational prenylation and required for membrane association (Trusov *et al.*, 2012).

The crystal structure of the heterotrimeric G protein shows that the $\text{G}\alpha$ subunit interacts with the $\text{G}\beta\gamma$ complex in two major regions: the switch II region of the $\text{G}\alpha$ subunit interacts with the top of $\text{G}\beta$ propeller and the N-terminus of the $\text{G}\alpha$ subunit,

which interacts with the outer strands of blade 1 of G β . Previous data demonstrate a surface area in the G β subunit that mimics the switch II region of the G protein α subunit, known as the “hot spot”. This surface has unique binding properties and undergoes conformational changes allowing target recognition and mediating the interaction between G $\beta\gamma$ and its various binding partners (Scott JK et al., 2001; Davis TL et al., 2005). This discovery is a major breakthrough in pharmacology to allow selective disruption of G $\beta\gamma$ -dependent target recognition and its downstream signal.

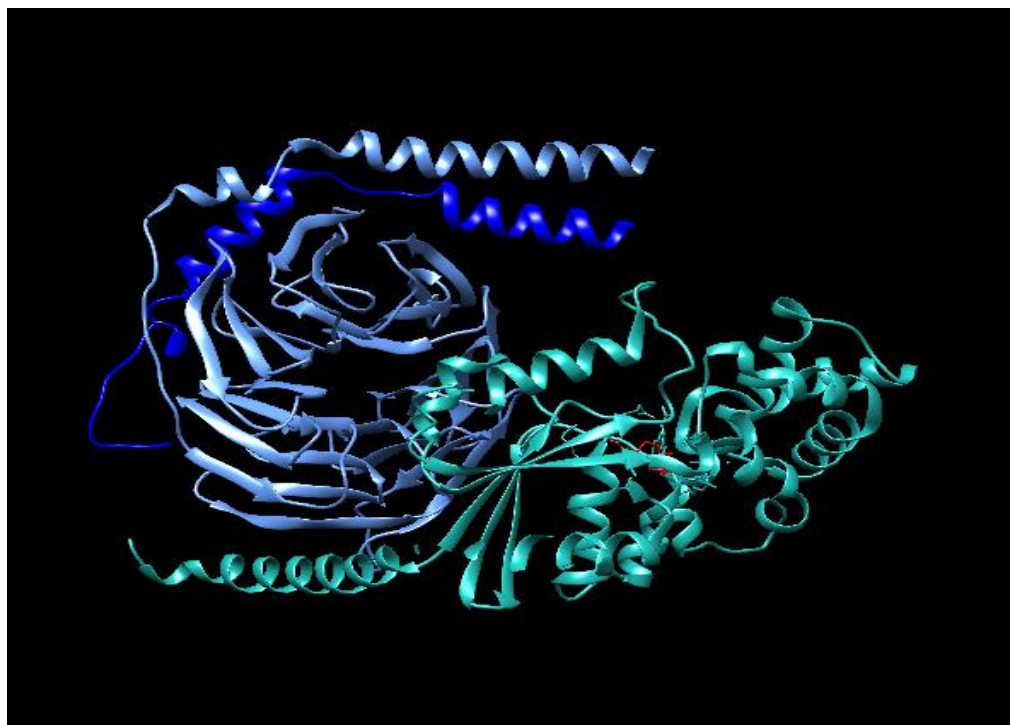


Figure 1.3. The structure of the G α .GDP/G $\beta\gamma$. The largest subunit G α subunit (green) composed of two domains, the GTPase domain (G-domain) and the α -helical domain. The GTPase domain consists of six helices surrounding a six-stranded beta sheet, polypeptide loops and three switch regions. The inactive state of the heterotrimeric G protein is indicated by the GDP (red) binding to this domain. G β (purple) subunit's propeller shape interacts with the G γ subunit (blue) in the N-terminal.

1.2.2. Physiological Functions of G Protein and Diseases

In the G protein field, accumulated data have proven multiple downstream signaling effectors (Wettschureck and Offermanns., 2005). First is Adenylyl cyclase (AC), a well-known enzyme that has a regulatory role in most cells. AC is a specific down-stream effector for both Gas and Gai. These G α families regulate AC differently. Gas stimulates AC to convert ATP into cAMP, which leads to an increase in cAMP level and thereby regulates its downstream proteins including protein kinase A, GEF and cyclic nucleotide-gated channels (Wettschureck et al., 2004; Syrovatkina, 2016). Gai decreases the intracellular cAMP levels by inhibiting AC. A strong contribution of Gas and Gai pathways on cardiac functions has been reported. Loss-of-function mutation in Gas is linked to the genetic disorder Albright's Hereditary Osteodystrophy while mutations in GNAI3, which encodes Gai3, are associated with Auriculo-Condylar Syndrome (ACS) (Marivin et al., 2016).

The G α q family activates phospholipase C (β - isoforms), which catalyzes the hydrolysis of phosphatidylinositol 4,5-bisphosphate (PIP2) into two second messengers: inositol trisphosphate (IP₃) and diacylglycerol (DAG). DAG remains bound to the membrane and activates protein kinase C (PKC), while IP₃ opens the calcium channel IP₃ receptor in the endoplasmic reticulum. This family of heterotrimeric G proteins is well known to regulate a wide range of Ras homolog (Rho)-mediated responses including acetylcholine vesicle release at neuromuscular junctions and the activation of RhoA in smooth muscle cells (Steven et al., 2005; William et al., 2007).

Gαq knockout mice suffer from many defects including craniofacial defects, which are a sign of ACS, cardiac malformation and defective platelet activation. However, gain-of-function mutations in both Gαq and Gαs are linked to some cancers (Syrovatkina et al., 2016). The Gαq is homologous to the Gα2 in *Dictyostelium* as the both proteins activate the down stream effector phospholipase C.

Several proteins have been reported to interact with the Gα12/13 family. RasGAP, Btk family tyrosine kinases, Gap1, cadherins and α-SNAP interact with Gα12. In addition to cadherins and Btk family tyrosine kinases, Gα13 has been detected to interact with p115RhoGEF, radixin, Hax-1, and Integrin $\alpha_{iiib}\beta_3$. Gα13 is essential for blood vessel formation, where gene-deleted mouse embryos have defective vascular systems and the endothelial cells were unable to develop into a vascular system. Gα13 gene-deleted resulted embryo death at E9.5 (Ruppel et al., 2005; Syrovatkina et al., 2016).

Similarly, many downstream effectors of Gβγ have been detected, including cardiac muscarinic-gated inwardly rectifying K⁺ the first direct effector identified for Gβγ, as well as AC, PLCβ, phosphoinositide-3-kinases (PI3K) and voltage-gated Ca²⁺ channels, which mediate calcium ion flux across the plasma membrane (Khan et al., 2013). Besides its many physiological functions, Gβγ has been found to be critical for embryonic neurogenesis. Gβ1-knock-out mice exhibit microencephaly, neural tube defects, abnormal suckling behavior and respiratory defects. In addition, abnormal morphologic changes in neural progenitor cells, impaired neural progenitor cell proliferation and severe brain malformations were also observed (Okae and Iwakura, 2010).

Although there is significant evidence regarding the potential roles of heterotrimeric G protein subunits in diseases, many concerns still need to be addressed. The molecular mechanisms underlying G proteins in many diseases are still undefined.

1.3. Cell Membrane Organization and Signal Transduction

Cells are surrounded by the plasma membrane separating inside from outside. Important to this thesis is the plasma membrane's role in cell-cell communication. Cells receive external signals and must transduce these across the membrane to the inside. Organization and interaction of membrane lipids and proteins has been shown to be critical for signaling and other cellular processes. Thus plasma membrane composition, organization and function have been investigated for decades.

In 1925, E. Gorter and F. Grendel established the bilayer model for the biological membrane by studying lipids extracted from red blood cells. The formation of the bilayer occurs from the natural amphipathic property of the membrane lipids. The hydrophilic heads will always face the aqueous environment in bilayers while the hydrophobic tails will face the inner region away from the water (Gorter and Grendel, 1925). The quick movement and flexibility of lipids are major keys that create a dynamic and fluid membrane. However, the movement of the membrane proteins is relatively slower. This fluid nature of the membrane is known as the 'Fluid Mosaic Model', established in 1972 by Jonathan Singer and Garth Nicolson (Singer and Nicolson, 1972).

The significant advances in biophysical and biochemical techniques have expanded our understanding of the structure of these lipid bilayers. Multiple types of

lipids have been identified including phospholipids, glycolipids (sphingolipid) and sterols. Both phospholipids and glycolipids consist of two fatty acid chains linked to glycerol and a phosphate group. This type of phospholipid is referred to as the glycerophospholipid. Three common kinds of glycerophospholipids have been recognized in cell membrane, phosphatidylcholine (PC), phosphatidylserine(PS) and phosphatidylethanolamine (PE). Glycolipid fatty acid chains are connected to glycerol along with a sugar such as glucose. A third type of membrane lipid is the sterols such as cholesterol, an important component in animal cell plasma membranes. Cholesterol consists of a hydrophilic hydroxyl group, steroid rings structure and hydrocarbon side chain. Cholesterol gives the membrane its thickness and makes it more rigid. In mammalian cells, the lipid composition of the outer leaflet is different from the inner one. While PC and sphingomyelin are the main components of the outer leaflet, PS and PE exist in the inner leaflet (Simons and Van Meer, 1988; Lange et al., 1989; Watson, 2015).

In the late 1980s, van Meer and Simon modified the Fluid Mosaic Model and established a new model for biological membrane compartmentalization where the interaction between the saturated lipid tails with sterols and sphingolipids forms a lipid-rich liquid ordered phase. This was the emergence of the lipid raft hypothesis, which has been subjected to controversial debate in both biomedical and biophysics fields (Simons and van Meer, 1988). In 2006, Pike reported all the outcomes at a Keystone Symposium on Lipid Rafts. The consensus definition of a membrane raft that emerged from the meeting stated that membrane rafts are small (10 – 200 nm), heterogeneous and highly dynamic microdomains (Pike, 2006). In multicomponent lipid membranes, lipids show very complex behavior. The heterogeneity of lipid bilayers influences the

phase transitions and induces lipid-lipid phase separation while the line tension penalizes the interface between two domains (Baumgart et al., 2003). This phase separation is often linked to thermal and conformational changes in the multicomponent lipid membranes and influences small membrane domains formation. Domain-induced budding is one example and was first proposed theoretically in 1992 by Lipowsky. It is a mechanism that facilitates multi-domain formation by bulging of phase separated membrane domains and reduction of the domain boundary, which in turn lowers its edge energy (Hurley et al., 2010).

A second example that facilitates multi-domain formation is membrane curvature, which is induced by the difference between the bending rigidities of the liquid order (Lo) phase and liquid disordered (Ld) phase of the bilayers (Ursell et al., 2009). Many physical mechanisms are involved in stabilizing membrane nano-domains. The existence of line active membrane molecules (linactants) contributes to the membrane heterogeneities. Aggregation of these linactants including hybrid lipids with one saturated and one unsaturated tail, to domain boundaries has been seen to decrease the line tension, which in turn facilitates the formation of membrane domains by one of the above mechanisms as well as stabilizes membrane domain structures (Brewster et al., 2009; Palmieri et al., 2014). This was confirmed using GUVs of four-component lipid mixtures composed of DSPC/(DOPC/POPC)/Chol with varying (DOPC:POPC) fractions at temperature, 23°C. No phase separation was detected with either type I mixture (DSPC/POPC/Chol) or type II mixture (DSPC/DOPC/Chol), when intermediate compositions of fully unsaturated lipid DOPC and the hybrid lipid POPC were made, many patterns of phase separation were detected (Konyakhina et al., 2011).

In 1987, the bilayer curvature coupling mechanism was proposed by Leibler and Andelman. This mechanism requires the lipid composition on the two monolayers to differ from each other, which in turn gives the membrane the tendency to bend in a certain direction, forming a spontaneous curvature. Leibler-Andelman's mechanism leads to membrane domains on the range of 100 nm to micrometers (Leibler and Andelman, 1987).

In 1993, Dan et al. proposed a monolayer curvature coupling mechanism. Depending on the local composition of the monolayer, they will tend to bend inwards or outwards. The coupling of both monolayers produces elastic stress that can be relieved at domain boundaries and leads to membrane domains of 10 nm in size (Dan et al., 1993).

Although lipid-lipid phase separation maybe required for membrane domain formation, lipid-protein and protein-protein interactions can strongly contribute to this phenomenon. The segregation of membrane lipids along with membrane proteins raises an active dynamic platform to regulate many cellular processes including protein clustering, membrane trafficking and plasma membrane signaling. Lipid modifications on proteins such as palmitoylation and Glycosylphosphatidylinositol (GPI) anchors are known as common mechanisms for proteins partitioning into lipid microdomains. The resistance of these domains to detergent solubilization contributed to the discovery of these microdomains and supported the raft phenomenon. It also helps in describing the composition and properties of detergent-resistant membrane fractions (Watson, 2015).

Membrane proteins and lipids are able to diffuse in the bilayer. This concept was shown using a Fluorescence Photobleaching method on lipids and proteins that are tagged with a fluorescent protein. The recovery of fluorescence in a specific area of membrane after photobleaching allows quantification of membrane lipid and protein mobility (Axelrod et al., 1976; Lippincott-Schwartz et al., 2001).

The role of membrane lipids has extended beyond the definition as a platform or barrier. In biological membranes, it has been shown that lipids surround the membrane proteins and modulate their activity. In some cases, lipids regulate specific types of proteins by forming a strong interaction with their hydrophobic transmembrane domains (TMD). This interaction can be long-lived or brief and it is correlated with TMD lengths as well as organelle specificity. One example is the interaction between K⁺ channel and the surrounding membrane lipids, which highly regulate its activity (Valiyaveetil et al., 2002).

Although various data have been generated regarding lipid microdomains over the last 3 decades, a comprehensive picture is still missing. Recent progress in plasma membrane (PM) isolation methodology, lipid analysis as well as the use of superresolution microscopy have confirmed the existence of nano- and micro-scale domains in biological membranes and have improved the understanding of these domains (Lippincott-Schwartz et al., 2001; Hess et al., 2007; Sengupta et al., 2011).

Use of fluorescent lifetime imaging microscopy for live Hela cells stained with the dyes Laurdan and di-4-ANEPPDHQ revealed that ~76% of the plasma membrane was in a liquid order phase (Lo), while the remaining ~24% consisted of a liquid disorder (Ld)

phase (Owen et al., 2012). A breakthrough in the complexity of lipid microdomains was achieved by using high-resolution secondary ion mass spectrometry (SIMS) technique on fibroblast cells revealed that sphingolipids cluster in ~200 nm diameter microdomains, while cholesterol was evenly distributed in the plasma membrane. NanoSIMS Images also showed that these sphingolipid microdomains were not enriched with membrane cholesterol and were not disrupted by cholesterol reduction. However, disruption of the actin cytoskeleton strongly affects sphingolipid membrane organization (Frisz et al., 2012; Frisz et al., 2013; Wilson et al., 2015).

Membrane raft models have been extended after discovering the role of filamentous proteins, including F-actin, in membrane organization. Yethiraj and Weisshaar (2007) were the first to point out the role of the integral membrane proteins and the cytoskeleton on membrane domain stabilization. Their study suggested that integral membrane proteins attached to the cytoskeleton act as blockers that limit the size of lipid domains (Yethiraj and Weisshaar, 2007).

Using a single particle tracking experiment, Kusumi et al., (2005) observed that when membrane proteins are clustered, their hopping rate across the cytoskeleton boundary is highly restricted. This led to their proposal of the Picket Fence Model, which states that membrane molecules are hindered by the transmembrane proteins that act as pickets and the cortical actin network that acts as a fence. Although the role of actin has been recognized in this model, its contribution in membrane organization may be more complicated. Membranes with three-dimensional topographies that were used in the single particle tracking experiments can cause an artificial increase in protein immobilization or clustering.

Further investigation by Goswami et al., (2008) showed that dissociation of GPI-anchored proteins from the underlying cortical actin converted GPI-anchored protein nanoclusters to monomers. In 2012, using high-resolution fluorescence imaging of GPI-anchored proteins, Gowrishankar et al., (2012) described in greater detail the role of actin on the protein nanoclusters. They suggested that the association of GPI-anchored proteins with the cortical actin cytoskeleton is a key factor on the protein nanocluster formation. Their study described the active actin aster model, which states that myosin motors arrange the short and dynamic actin snippets into asters. Associations of membrane proteins with these actin snippets can influence their dynamic clustering. In 2013, Gudheti et al. examined the dynamic clustering of the transmembrane protein haemagglutinin (HA) using super-resolution fluorescence photoactivation localization microscopy (FPALM). The study revealed a positive correlation between HA protein and the underlying cortical actin filaments. The actin-binding protein cofilin was also involved in this dynamic clustering of HA, which led to the suggestion that HA clusters influenced actin organization (Gudheti et al., 2013).

The Phase Switching Model was proposed by Owen and Gaus, 2013. They described the lipid ordered phase as a continuously percolating phase where the interaction between raft proteins is permitted and this phase surrounds islands of the disordered phase, acting as boundaries to inhibit protein-protein interaction. Under physiological changes to the actin cytoskeleton, these two phases can switch from one to another (Owen and Gaus, 2013; Rayemann et al., 2017).

Over the past decade, many biochemical and biophysical techniques have been used to examine cell membrane organization. However, deep understanding of cell membrane dynamics and structure is still needed.

1.4. Cell Motility

In every living system, from simple to complex, the ability to move are imperative. In the smallest structural and functional living unit, the cell, migration is an evolutionarily conserved mechanism from protozoa to mammals. The first detection of cell migration was at the beginning of the 17th century by Antony van Leeuwenhoek by looking into a drop of water using glass bead. The swimming cells that he observed were believed to be ciliated protozoa. Today the discovery of more powerful tools makes the study of cell migration more convenient. Depending on the cell type and the surrounding environment, cells can move in a variety of different ways. Multiple distinct migration modes of cells have been detected and each has a crucial role in many physiological perspectives.

The slow mesenchymal cell migration is a well-known locomotion strategy of fibroblast and keratocytes. In this type of movement, cells elongate and adopt a spindle-like shape that engages the focal adhesions in the extracellular matrix, which associate with actin-rich lamellipodia or filopodia. This lamellipodia-based cell is characterized by the presence of actin stress fibers and has an important role in embryogenesis and tissue regeneration.

In contrast, the amoeboid-like movement is a fast locomotion strategy in eukaryotic cells and unicellular organisms. Unlike crawling or swimming of protozoa using cilia and flagella, there are no specialized locomotive structures for the amoeboid

movements of cells. Their movement involves the entire cell using an extension of cytoplasmic projections called pseudopodia and forms focal adhesion with its environment. It is an essential mechanism in human leucocytes, including neutrophils, for proper immunological functions (Friedl and Wolf, 2010).

Amoeboid-like movement is a more common locomotion than mesenchymal cell migration and engages other locomotion sub-types. Bleb-based migration is a distinct subtype that occurs in certain types of cells and has been less studied compared to lamellipodia- and pseudopodia-based cell migration. Blebs appear as spherical expansions of the plasma membrane that form by cytoplasmic hydrostatic pressure, which is induced by actomyosin cortex contraction. Over the past decade, blebs have attracted much attention in the cell migration field. It is an essential locomotion strategy of apoptosis and cytokinesis. Also, it is a major strategy for primordial germ cells (PGCs) in zebrafish and some leukocytes (Charras and Paluch, 2008). Although some cell types use exclusively either lamellipodia or pseudopodia, there are certain types of cells that are able to switch between both modes in order to select the most efficient locomotion modes for the given environment. This switching phenomenon is known as the mesenchymal-amoeboid transition (MAT) (Tozluoglu et al., 2013; Taddei et al., 2013; Liu et al., 2015). During the stage of zebrafish gastrulation is an example, where Wnt signaling can control the balance between three different locomotion modes for successful lateral mesendoderm progenitors (Weiser D.C et al., 2007). Many types of cancer cells are also able to switch between two modes. However, their movement has to be directed in order to metastasize. This directional movement of cells, known as chemotaxis, helps them to sense, polarize and respond directionally to a chemical

gradient i.e., chemoattractants. In addition to the mesenchymal-amoeboid transition, blebs and pseudopods show cooperation during chemotaxis (Tyson et al., 2014). The external stimulants converted into internal signals that in turn influence the complex subcellular process of cytoskeletal proteins and their interactions, which perform the motile responses (Swaney et al., 2010).

Chemotaxis is now generally recognized as an important regulator of many physiological and pathological processes. Leukocytes, a powerful feature of host defense, exit the bloodstream and are chemotactic toward a site of infection or inflammation. Production of a chemokines in this site serves as an attractant that guides leukocyte recruitment. In wound healing, the migration of epithelial cells and keratinocytes takes place in addition to other critical signaling events (Rot and Von Andrian, 2004; Nourshargh and Alon, 2014).

Although both types, amoeboid and mesenchymal cells undergo directional migration, they differ in their chemotactic behavior (Vorotnikov and Tyurin-Kuzmin., 2014). Over the past decades, much has been learned about chemotactic migration of amoeboid cells. It mostly came from using the lower eukaryotic amoeba *Dictyostelium* as a model organism for studying chemotaxis. It has provided significant insights into chemotactic behavior and the common signal transduction that is involved in this action, which are mostly conserved in many cell types of higher eukaryotes including amoeba-like neutrophils (Drayer and Van Haastert, 1994).

On the other hand, the mechanisms that regulate mesenchymal cell chemotaxis are much less understood. The difference between chemotactic behavior in both cell types is based on the signal pathways and the feedback mechanisms that amplify the

chemotactic signals. Unlike the membrane feedback mechanism that exists in amoeboid cells, mesenchymal cell feedback functions in the cytosol (Schneider and Haugh, 2005).

Cell chemotaxis is adaptable, precise and a very tightly regulated mechanism. However, any deregulation or reprogramming of chemotaxis pathways influences the development and progression of many human diseases. Excessive chemotaxis of leukocytes leads to chronic inflammatory diseases including asthma, atherosclerosis and arthritis (Zernecke and Weber, 2010; Sadik and Luster, 2012). The reprogramming of chemotaxis pathways of tumor cells in the surrounding microenvironment is the core key of tumor dissemination during progression and successful cancer metastasize (Bravo-Cordero et al., 2014). Thus, it is important to study signaling regulation involved in cell-directed migration. Activation of seven-transmembrane-spanning GPCRs that express on the surface of amoebae-like cells are known as major regulators of this dynamic process. One of the main classes of GPCRs that initiate chemotaxis in tumor cells is the chemokine receptor. Currently, more than 50 types of chemokines and chemokine receptors have a major role in cancer and 30% of these are involved in cell chemotaxis. Chemokine receptor CXCR4 and its ligand CXCL12 are one of the most widely studied in cancer metastasis. Signaling through this ligand and receptor is involved in around 11 types of cancer (Lazennec and Richmond., 2010). However, growth factors acting on receptor tyrosine kinases (RTKs) and cytokines such as transforming growth factor b (TGFb) as well as extracellular matrix proteins function as chemoattractants for mesenchymal cell. After the external signal is picked up by these receptors it is transmitted to the cytoskeleton. From the middle of the 20th century, it

has been generally accepted that coordination of cytoskeletal dynamics and reorganization is required for cell migration. Actin filaments, myosin and microtubules have been recognized as major regulators of cell shape and motility (Etienne-Manneville, 2014; Le Clainche and Carlier, 2008; Devreotes and Horwitz, 2016). The connection between actin and microtubules is regulated by the small GTPases Rho, Rac and Cdc42 (Ridley et al., 2003; Vorotnikov and Tyurin-Kuzmin, 2014). These regulators are common in the two cell migration modes, amoeba-like cells and mesenchymal cells.

Actin filaments (F-actin) are polar fibers that result from the polymerization of actin monomers under the control of nucleation and elongation factors (Carlier et al., 2015). The dynamic assembly and disassembly of actin allow cells to extend pseudopodia or lamellipodia at the leading edge, polarize and move. In a wide range of cells, including *D. discoideum*, leukocytes and neurons, studies have been shown that actin filaments and actin-associated proteins undergo wave-like movement. The generation of this wave involves in a positive and negative feedback mechanism. The contribution of the actin wave in cell migration has been a recent area of interest (Inagaki and Katsuno, 2017).

1.5. *Dictyostelium Discoideum*: An Experimental Model for Cell Motility and

Chemotaxis

Dictyostelium discoideum is a social amoeba that belongs to the Amoebozoa. The vast majority are haploid, feed on bacteria and divide by mitosis. *D. discoideum* cells are amazingly similar to animal cells. *Dictyoselium* are able to perform many

processes including phagocytosis, pseudopod-based cell motility and chemotaxis. A wide range of methodologies have been developed for use on this species including genetic transformation, molecular genetic and cell biology techniques. *Dictyostelium* can be easily grown in liquid culture and takes only a few days to reach high density. Also of great benefit, its haploid genome has been sequenced (Eichinger et al., 2005). It is a suitable model for homologous recombination and insertional mutagenesis techniques to disrupt and identify any gene, respectively (Bagorda et al., 2006). The amoebae can be easily transfected with tagged proteins for fluorescence purposes. An online resource, 'Dictybase', is available and offers many *Dictyostelium* cell lines that have already been transfected or mutated and as well as numerous plasmid constructs. Dictybase also provides a wealth of information about *Dictyostelium* and the experimental processes (Kreppel et al., 2004). These features mark *D. discoideum* as a popular and suitable model to study genes involved in signal transduction and development. It is also considered as a good model to study many processes linked to many human diseases including mitochondrial diseases, cell motility-related pathologies, lysosomal-related disorders and cancer.

In the absence of nutrients (bacteria), starved *Dictyostelium* cells enter the development phase where approximately 10^5 to 10^6 cells aggregate together by chemotaxis to form a mound, which in turn develops through different stages to form at the end of this process a multicellular structure called the fruiting body. The fruiting body consists of stalk cells filled with spores. This is a mechanism of cell survival after food source depletion. The transition from growth (vegetative) to multicellular development requires the ability of amoebas to monitor their own cell density and many regulatory

cell signals are involved in this transition. The vegetative cells secrete pre-starvation factor, PSF, at a constant rate. This factor is a glycoprotein and acts as a quorum-sensing factor directing gene expression relative to cell density (Clarke et al., 1987). As the bacteria level goes down, the PSF level goes up, which leads to the expression of the protein kinase, YakA (Souza et al., 1998). This protein kinase inhibits binding of the translational repressor PufA to the 3'-end of the catalytic subunit of cAMP-dependent protein kinase (PKA) (Souza et al., 1999). The expression of all the aggregation-dependent genes is thus induced by PKA. This includes the cAR , AC, acaA and the extracellular cAMP phosphodiesterase pdsA (Schulkes and Schaap, 1995). Also, the starved cells express conditioned medium factor (CMF), which is necessary for CarA-mediated signal transduction (Yuen et al., 1995). The three proteins, CarA, AC A and phosphodiesterase (PdsA), are essential to generate cAMP pulses. Cyclic AMP is a key component in *Dictyostelium*'s developmental life cycle. It acts as a cell chemoattractant and up-regulates the expression of the genes required during and after aggregation (Othmer and Schaap., 1998; Cai et al., 2014).

Chemotaxis-driven aggregation in *D. discoideum* is characterized by three distinct steps: Motility, directional sensing and polarity. Motility starts as the food source is depleted where *D. discoideum* moves and extends uniform size pseudopodia in random directions in the absence of stimuli. Their behavior looks somewhat like ice-skating. In the initial presence of a cAMP gradient, cells show a global response and the cAR1 receptors increase allosterically over the cell. The receptors undergo phosphorylation, which leads to a fivefold decrease in cAMP binding (Caterina et al., 1995; Hereld et al., 1994). Later, the cells will be able to directionally sense the cAMP gradient and the response

will accumulate at the initial site of receptor activation but be inhibited across the rest of the cell. Adaptation to this mechanism (local excitation, global inhibition) allows cells to respond to the difference in receptor occupancy, leading to transduction of a response into an internal signal. Receptor-cAMP binding results in activation of the heterotrimeric G protein triggering the dissociation of $\text{G}\alpha_2$ from the $\text{G}\beta\gamma$ complex (Xu et al., 2005). This is followed by recruitment of phosphatidylinositol 3- kinase (PI3K) from the cytosol to the plasma membrane with its accumulation at the leading edge of the chemotactic cell, while the phosphatase tensin homologue (PTEN) localizes to the rear of the cell. This distribution of both proteins is considered as a key factor in the regulation of phosphoinositol lipid synthesis and degradation at the leading edge and at the back of the chemotactic cells, respectively. The PI3K enzyme catalyzes the phosphorylation of Phosphatidylinositol 4,5-bisphosphate (PIP_2) to phosphatidylinositol 3,4,5-trisphosphate (PIP_3) within 5 seconds upon cAMP stimulation (Funamoto et al., 2002). Interestingly, the PTEN distribution in cAMP gradient is different than its distribution in a less polarized cells (resting cells) and uniformly stimulated cells. As some of the proteins exist in the plasma membrane in the resting cells, a fraction of PTEN translocates from the plasma membrane to the cytosol after uniform stimulation (Bretschneider et al., 2016).

PIP_3 is involved in cell directional sensing as this lipid accumulates in the leading edge where the extracellular cAMP level is highest (Huang et al., 2003). Leading edge accumulation of PIP_3 leads to actin polymerization and pseudopodia extension in the correct direction. Also, the re-localization of PI3Ks and PTEN increases the localization of PH domain-containing effectors such as cytosolic regulator of adenylyl cyclase

(Crac), protein kinase BA (PKBA), and PH domain protein A (phdA) at the front as well as increases the actin-binding proteins in the front cell cortex. PI3K null cells show a dramatic decrease in PIP₃ production and a defect in both chemotaxis and developmental processes (Huang et al., 2003; Luo et al., 2003). Although the intracellular signaling events involved in chemotaxis are activated at the leading edge, neither the cAR1 nor the G-proteins are found accumulated in that region. They display a uniform distribution along the plasma membrane (Xiao et al., 1997; Servant et al., 1999; Jin et al., 2000). However, in $\alpha 2$ -null cells (MYC2) cells or β -null cells (LW6), cAMP does not induce actin polymerization and/or activation of down stream effectors including ACA, soluble guanylyl cyclase (sGC), guanylyl cyclase (GCA) or PI3K which leads to an aggregation-minus phenotype (Huang et al., 2003; Kumagai et al., 1991; Wu et al., 1995; Zigmond et al., 1997). ACA is a major regulator of the production and secretion of cAMP (Pitt et al., 1992). Activation of ACA is mediated by PIP₃ accumulation and PKB activation. These data indicated that $\alpha 2$ is necessary for multicellular development upon starvation, where MYC2 cells are able to grow normally as vegetative amoebae and survived as unicellular form upon starvation (Chen et al., 1994).

Cell polarity is the third step of chemotaxis that allows a directional persistence of the cell even in the absence of any stimuli. Cells elongate in this process, which involves some signaling molecules and the cytoskeleton. The actin cytoskeleton, cyclic guanosine monophosphate (cGMP) signaling and microtubules have been shown as major regulators for cell polarity. Cells treated with latrunculin (an inhibitor of actin polymerization) showed a polarity defect (Janetopoulos et al., 2004). Accumulation of

cGMP led to excessive Myosin II association with cell cortex, which led to increased cell polarization. Activation of the G protein induced the phosphorylation of myosin II heavy chain by MHCKs and is the key factor that promotes myosin II disassembly and opposes cGMP-mediated Myosin II assembly (Bosgraaf and Van Haastert., 2006). The Tsunami protein (TsuA) and PTEN are other examples, where cells lacking either of these proteins were able to move but showed a defect in polarity, which led to an aggregation-minus phenotype (Iijima and Devreotes, 2002; Tang et al., 2008). Despite the amount of generated data, the molecules responsible for initiating cell polarization are still unknown. PTEN dephosphorylates phosphotyrosine in D3 position of PI(3,4,5)P₃. In PTEN-null cells, PH domain-containing proteins were highly accumulated in the plasma membrane and are not restricted in the leading edge. These cells also extend pseudopodia in every direction, which indicates PIP₃ degradation is reduced in these cells. (Huang et al., 2003; Luo et al., 2003). In contrast, *Dictyostelium* cells lacking PI3Ks are able to perform chemotaxis in extreme cAMP gradients. These data indicate that another pathway acts in parallel with PIP₃ signaling during cell chemotaxis. It was speculated that phospholipase A2 (PLA2) could be involved, as cells lacking both PLA2 and PI3K showed chemotactic defects stronger than cells lacking either one of them.

In addition to the PTEN, both myosin II and actin-binding protein Cortexillin I also localize in the back of chemotactic cells and they all mediate the back contraction. In 2005, Veltman et al. found that the leading edge was enriched with the soluble guanylyl cyclase, the enzyme that catalyzes cGMP synthesis. This evidence suggests that cross-talk exists between the front and the back edge of the chemotactic cell to provide proper movement.

1.6. Rationale

A current concept in cell membrane organization describes the clustering of the membrane lipids and proteins in nanoscale domains. Organization of these molecules in clusters is a phenomenon, which is believed to have different influence on different proteins including the efficiency of cell signaling (Lang and Rizzoli, 2010).

Understanding of their dynamic regulation is still limited due to the constraints of experimental approaches used to detect individual signaling molecules. Recent development of biophysical techniques in microscopy has improved the resolution and advanced our understanding of such phenomena (Lang and Rizzoli, 2010; Curthoys et al., 2015). G α 2 subunit resides mostly in the plasma membrane presumably associated with the inner leaflet. Our previous work using cell fractionation techniques suggested a possibility of a non-random distribution and dynamic clustering of this protein in the plasma membrane. However, how the activation of G α 2 affects this clustering is unknown.

Activation of G α 2 results in its phosphorylation on serine 113 (Chen et al., 1994). Phosphorylation is a very common mechanism in regulating protein functions (Nishi et al., 2011). To date, the role of the phosphorylation in G protein signaling, membrane clustering and protein-protein interaction is not understood. In this study, we used a combination of molecular genetics, biochemical and biophysical techniques to gain a deeper understanding of the role phosphorylation plays in G protein signaling, membrane clustering and 14-3-3 protein interaction.

CHAPTER 2

MATERIALS AND METHODS

2.1. Cell Lines, Cell Culture and Development

The wild type, *D.discoideum* axenically growing strain AX2, the $\alpha 2$ - null cell line (MYC2) and β -null cell line (LW6) were used in this study. MYC2 (Chen et al., 1994) and LW6 (Wu et al., 1995) was kindly supplied by Peter N. Devreotes (Johns Hopkins University Medical School). Cells were grown in HL-5 medium (1% dextrose, 1% proteose peptone, 0.5% yeast extract, 3.6mM KH₂PO₄, 3.6mM Na₂HPO₄ and 41 μ M dihydrostreptomycin) at 22°C (Watts and Ashworth, 1970). $\alpha 2$ (wt), $\alpha 2$ (S113A) and $\alpha 2$ (S113D) were expressed in $\alpha 2$ -null (MYC2) background. All the transfected cells were maintained constantly in G418- containing media at a concentration of 20 μ g/ml.

For development, cells were washed in development buffer (DB) (5 mM NaH₂PO₄, 5 mM Na₂HPO₄, 2 mM MgSO₄, 0.2 mM CaCl₂). Cells were starved in DB at 2x10⁷ cells/mL for 4-5 hrs on an orbital shaker. After an hour of starvation, cells were pulsed with 100 nM cAMP every 6 minutes (Gundersen, 1997).

2.2. Antibodies and Reagents

IR Dye 680 RD goat anti-rabbit (C60329-15; 1.0 mg/ml) from LI-COR. GFP ABfinity recombinant rabbit monoclonal AB (G10362; 0.2 mg/ml) from Life Technologies. CAGE 590 anti-rabbit from Abberior. Alexa Fluor 647-conjugated goat anti-mouse IgG (A-21235; 2 mg/ml) from Invitrogen. Alexa Fluor 633-conjugated goat anti-rabbit IgG (A-21070; 2mg/ml) from Life Technologies. Mouse IgG2a anti-Myosin II (56-396-5) (31 μ g/ml) from DSHB Hybridoma by Gerisch. Polyclonal anti-rabbit 14-3-3

was kindly provided by Douglas N. Robinson (Department of Pharmacology and Molecular Sciences, Johns Hopkins University School of Medicine, Baltimore, MD). 14-3-3 antibody was generated as described previously (Zhou et al., 2010). Chameleon Duo pre-stained protein ladder (C60825-03) from LI-COR. Phosphate Buffered Saline (PBS) from Lonza. Phosphatase inhibitor cocktail (034M4009V) and protease inhibitor (S8820) were obtained from Sigma. Bovine serum albumin, fract V (041501) and glycine (124594) were acquired from Fisher.

2.3. Plasmid Construction, Mutagenesis and Transformation of *D. discoideum*

The point mutations (S113A and S113D) were initially created in Ga2/pAPI, a modification of pBluescript II KS- (Stratagene, La Jolla, CA) using oligonucleotide-mediated, site-directed mutagenesis. The mutant α-subunit was removed from pAP1 with the restriction endonucleases BgIII and BamHI and cloned into the BgIII site of the *D. discoideum* expression vector, pJKI (Pitt et al., 1992). Ga2(wt)-YFP construct was kindly supplied by Peter N. Devreotes (Johns Hopkins University Medical School). The protein was cloned into the CV5 vector, an extra-chromosomal plasmid with an actin 15 expression promoter. The point mutations (S113A and S113D) were created into this CV5 vector that expresses eYFP using oligonucleotide-mediated, site-directed mutagenesis. DNA sequencing of clones was performed by the University of Maine DNA Sequencing Center. Plasmid DNA was transfected into *Dictyostelium* cells, AX2 and Ga2-null cell line (MYC2) via electroporation. For transformation, cells were washed in 10 mL of electroporation buffer (EB, 1mM Na/K phosphate buffer pH 6.3 and 250 mM sucrose) and resuspended at 2x10⁷ cells/mL of EB. 0.5ml of the cells were

incubated with 5 μ g of plasmid DNA for 3-5 minutes on ice. 450 μ l of the later sample was added to a sterile electroporation cuvette and electroporation was carried out using a Bio-Rad Gene Pulser set at 1.2 kV, 200 ohms resistance and 3 μ F capacitance. The electroporation time constant should be between 0.5 and 0.6. The electroporation cuvette was placed on ice for 10 min. After 10 minutes, the cells were removed to a Petri dish containing 2 μ l of healing solution (100 mM CaCl₂, 100 mM MgCl₂). The cells were incubated with healing solution for 15 minute at 22°C then 12 mL of HL-5 medium was added. After 24 hours, the transformants were selected with 20 μ g/ml G418 and 50 μ l of heat-killed *O.p.* was added to promote the growth of the transfected cells.

2.4. Gel Electrophoresis and Immunoblotting.

For gel electrophoresis, protein samples were separated by 10% SDS-PAGE (1.5 mm thick gels). Electrophoresis was carried out at a constant current of 24 mA for 1.5 hr. Proteins were then transferred from the gel to nitrocellulose paper at a constant current of 100 mA for 1.5 hr. For immunoblot analysis, the nitrocellulose paper was incubated in blocking solution containing 5% bovine serum albumin (BSA) in Tris-buffered saline with 0.1% Tween 20 (TBST) overnight. The following day, an hour incubation with primary antibody was performed in 2% blocking solution at 1:2000 dilution for the Ga2 peptide antiserum and for 14-3-3 antiserum. The secondary antibodies were added at 0.2 μ g/ml (1:5000). Blots were washed and imaged using LI-COR clx imaging system. The total proteins amount was detected using bradford assay for the five fractions (5%; 24 μ g, L; 40 μ g, 20%; 30 μ g, 35%; 34 μ g, 45%; 80 μ g).

2.5. Cell Fractionation and Density Gradient Centrifugation

Aggregation competent cells at a density of 3×10^8 (2×10^7 cells/mL) were starved for 4 to 5 hr, then lysed on ice at 5×10^7 cells/mL using base buffer (20 mM Tris-HCl, pH 7.4, 250 mM sucrose, containing 1 mM MgCl₂ and 1 mM CaCl₂ plus 2X protease inhibitor (Sigma). Cell lysates were lysed by forcing the cells through a 3 µm pore Nucleopore filter. Cell lysates were centrifuged at 12,000 rpm (~17,500 xg) for 10 minutes at 4°C. 100µl of the supernatant was taken to detect the YFP protein composition. The resulting pellet was resuspended in 1.5 ml of base buffer containing protease inhibitor and sonicated with a Branson Sonifier 405 on ice with 10 pulses (3 seconds for each to prevent heat generation), duty cycle of 40% and an output of 4 (Harris et al., 2001A). The sonicated sample was centrifuged at low speed (1000 xg) for 5 minutes. 100µl aliquot of the cell membrane sonicate, low-speed supernatant was taken and the YFP protein composition in each was detected with a microplate reader (Synergy 2; Biotek) using excitation and emission wavelengths of 485 and 528 nm, respectively.

Microdomain isolation was performed in an 0.5 mL ultracentrifuge tube using a 50µL aliquot of the cell membrane sonicate, low-speed supernatant mixed with 150µl of 60% Optiprep in base buffer (to final concentration of 45%). This was overlaid with 120µL each of 35%, 20% and 5% Optiprep in base buffer. The gradient was centrifuged at 67,000 rpm (~200,000 xg) for 1 hour at 4°C in a Beckman Optima TLX ultracentrifuge in a TLA120.1 rotor. The low-density membrane fraction (L) was found between the 5% and 20% layers. The clearly visible L fraction was drawn off with a micropipet and was generally 50 µL in volume. Each of the other layers was sampled. 50 µL aliquots of

each fraction was taken, and mixed with an equal volume of base buffer. Yellow fluorescent protein (YFP) was detected with a microplate reader.

2.6. G α 2/14-3-3 Co-immunoprecipitation

Co-Immunoprecipitation was performed based on the number of cells and as described previously (Zhou et al., 2010). Cells (6×10^7) expressing any of G α 2(wt), G α 2(S113A) or G α 2(S113D) were starved in DB at 2×10^7 /ml with cAMP pulsing for 4-5 hr. Cells were then centrifuged and lysed in 600 μ L lysis buffer (50 mM Tris pH 7.4, 150 mM NaCl, 0.1% NP-40, 1 mM ATP, 1 mM MgCl₂, 2x protease inhibitor, 1x phosphatase inhibitor). Lysates were incubated in ice for 10 min then centrifuged at (16,000 xg).. A 300 μ L of supernatant was collected and added to the previously 2 hr incubated mixture (50 μ L of protein A-agarose beads + 5 μ L antibody). All three were incubated for 2 hr at 4°C on a rotating mixer. Finally, the beads were washed three times with 1 mL of cold TBS, 50 μ L of 1X sample buffer was added and the sample was heated at 95°C for 4 min. 50 μ L of supernatant was mixed with 50 μ L 2X sample buffer and around 10% of the 300 (the volume used for immunoprecipitation) was taking from this mixture to detect protein concentration.

2.7. Cell Immunostaining and Confocal Imaging

For immunostaining cells expressing G α 2(wt)-YFP, G α 2(S113A)-YFP or G α 2(S113D)-YFP were starved on 25 mm No. 1.5 glass coverslips in DB buffer for 4 to 5 hr. Cells were either treated with 2 mM caffeine for 15 min or stimulated with 10 μ M cAMP for 1 min. Caffeine blocks the cAMP-dependent activation of the adenylate cyclase, which lead to block cAMP production (Brenner and Thomas, 1984). Cells were

then fixed for 10 minutes in 2% or 4% paraformaldehyde for 14-3-3 proteins staining and myosin II staining respectively. Cells were then permeabilized with 70% acetone for 1-2 minutes and washed three times with 1X PBS/.05% Tween 20 containing 0.3 M glycine. Samples were blocked with 2% BSA for 30 minutes and then incubated with primary anti-rabbit 14-3-3 AB (1:600) or anti-mouse Myosin II AB (4ug/ml) in 0.5% BSA for 1.5 hr. After three washings with PBS/.05% Tween 20, samples were incubated with anti-rabbit secondary antibody coupled to Alexa Fluor 633 at 10 μ g/ml (1:200) or anti-mouse secondary antibody coupled to Alexa Fluor 640 at 10 μ g/ml (1:200) in 0.5% BSA for 40 minutes. Cells were washed with PBS/.05% Tween 20 three times then images were acquired by sequential scanning to avoid fluorescence crossover on a confocal microscope Olympus FluoView TM FV1000 with a 100X oil immersion objective lens. For negative controls, *Dictyostelium* cells were starved and fixed as above and then we performed a secondary staining with Alexa Fluor 633 or Alexa Fluor 640 for fixed cells without primary staining.

2.8. Cell Viability Assay

Gα2(S113A)-YFP- or Gα2(S113D)-YFP-expressing MYC2 cells were starved in 24-well plates at a density of 1x10⁷ cells/well in 0.5 ml DB for 4-5 hr. Cells were then mixed with 0.4% trypan blue at a final concentration 0.1%. Cells were then manually counted with a hemocytometer. Viable cells were colorless, and dead cells were blue. To calculate the percentage viability, the live cell count was divided by the total cell count.

2.9. Fluorescence Photo-Activated Localization Microscopy (FPALM)

2.9.1. Sample Preparation

Cells expressing Ga2(wt)-YFP, Ga2(S113A)-YFP or Ga2(S113D)-YFP were starved on glass coverslips, # 1.5, 25mm in DB buffer for 4-5 hrs. For Ga2(wt)-YFP, cells were either treated with 2 mM caffeine for 15 min or stimulated with 10 µM cAMP for 1 min after starvation. Cells were then fixed in 4% PFA and permeabilized with 70% acetone for 1-2 minutes. After three washes with 1X PBS/.05% Tween 20 containing 0.3 M glycine, samples were blocked with 2.5% BSA for 45 min. Samples were then stained with anti-GFP rabbit antibody (1:400) in 0.5% BSA for 1.5 hr and washed three times with 1X PBS/.05% Tween 20. Secondary staining was performed in the dark. Anti-Rabbit IgG-Abberior CAGE 590 antibody (1:1000) was used. Samples were stained with CAGE 590 in 0.5%BSA for 40 min then washed three times with 1X PBS/.05% Tween 20. Samples were kept in the dark until imaging. For negative controls, *Dictyostelium* cells were starved and fixed as above without any staining to detect the levels of background and non-specific labeling. Also, we performed a secondary staining with CAGE 590 for fixed cells without primary staining.

2.9.2. Single-Color FPALM Experimental Setup and Image Acquisition

A key factor for FPALM imaging is using photoactivatable or photoswitchable fluorescent probes, such as the CAGE dye to improve resolution by controlling the density of activated molecules. These probes are characterized by their ability to switch from an inactive dark state to an active fluorescent state when illuminated with a particular wavelength of light. Two lasers were used for FPALM imaging, an activation

laser 405 nm diode laser (FBB-405-050-FSFS-100, RGBBlase LLC, Fremont, CA) to convert inactive (nonfluorescent) molecules to an activated state and a readout laser 561 nm to drive the activated molecules to emit light. Both lasers are combined using multiple silver mirrors and a dichroic mirror (Z405RDC, Chroma, Rockingham, VT) and then passed through a convex lens ($f=+350\text{mm}$) (Thorlabs, Newton, NJ) to be focused in the back focal plane of the objective lens (60X 1.4 NA oil-immersion) within the microscope (IX71, Olympus America, Melville, NY). The intensities of both lasers were controlled using motorized neutral density filter wheels (FW 102B, Thorlabs, Newton, NJ). Electronic shutters (SH05, TSC001 Thorlabs, Newton, NJ) were also used to block/unblock the lasers. The intensity of the readout laser was $\sim 10 - 15 \text{ kW/cm}^2$ at the sample.

The emitted fluorescence was collected by the objective lens and filtered through the dichroic mirror (T565LP, Chroma, Rockingham, VT) and the long pass emission filter (LP02-561-RU-25, Semrock, Rochester, NY) located in the same filter cube of the microscope. The collected light was then passed through a notch filter (NF03-405E-25 and 561 Notch, Semrock, Rochester, NY) to attenuate any remaining activation or readout laser, followed by a 605/70 emission filter (Chroma) and two lenses ($f +200\text{mm}$ and $f=+400 \text{ mm}$) (Thorlabs, Newton, NJ). These two lenses were arranged as a $\sim 2x$ or $2.67x$ telescope to form an image on the sensor of an EMCCD camera (iXon+DU897DCS-BV, Andor Technology, South Windsor, CT) (Hess et al., 2006).

Laser beam image profiles were captured by illuminating an aqueous solution of Rhodamine B (RB; Sigma Aldrich, St. Louis, MO). Samples were imaged at $\sim 50\text{Hz}$

with 200 EM gain. Ten thousand frames were recorded for each data set. All images were saved in TIF format. To reduce background signal and focus on the surface of cell, images were taken using total internal reflection fluorescence (TIRF).

2.9.3. Image Rendering and Cluster Analysis

For an image series, the background was subtracted from each frame using a rolling ball algorithm (Sternberg, 1983) and positive intensity peaks with at least one pixel above a minimum threshold were fitted to a two-dimensional Gaussian to determine the x and y coordinates, amplitude, $1/e^2$ radius, and offset of each point spread function (PSF). PSFs were then toleranced to select for molecules with the best fitting parameters. Clusters were analyzed as described previously (Gudheti et al., 2013) by breaking data sets into chunks of 40,000 molecules and using single-linkage cluster analysis (SLCA) with a maximum linking distance (R_{max}) of 50 nm. For clusters with a minimum of 10 molecules, densities and areas were determined by binning molecules into a fine grid, convolving each localized point with a circle of radius R_{max} , and then using the regionprops function in Matlab. Cluster areas and densities were normalized on a per cell basis and binned into histograms.

2.10. Data Analysis and Statistics

All statistical analyses for protein distribution and cell fractionations experiments were performed with JMP Statistical Software. Statistical significance was analyzed with Student's *t*-test. Each experiment was repeated at least three times and the values

represent the mean \pm SD. Quantification of the Western blot data were performed by measuring the intensity of the bands using ImageJ analysis program. For the co-immunoprecipitation data, band intensity was normalized to the total input of three independent experiments. Statistical significance was analyzed with Student's *t*-test. For localization study, quantification of fluorescence images was done using Pearson correlation coefficients colocalization plugin of Fiji software for two independent experiments. Statistical significance was analyzed with Student's *t*-test. Myosin II immunostaining data was analyzed using the Z-Project of Fiji software. Every confocal Z stacks were converted to average intensity projection. Line plot of fluorescence intensity across the cell (from the back to the front) was performed and the data was import into Excel worksheet. The average of myosin II staining intensity for 1.5 μ m in the back vs 1.5 μ m in the front of the cells for two independent experiments was measured. Using JMP software, statistical significance between the back and the front of the cells was determined by Student's *t*-test for G α 2 (WT) expressing cells and by Wilcoxon Signed Rank Test for G α 2(S113A) and G α 2(S113D) expressing cells.

CHAPTER 3

FACTORS INVOLVED IN MEMBRANE DISTRIBUTION AND SHUTTLING OF ACTIVATED $\text{G}\alpha_2$ SUBUNIT

3.1. Background and Hypothesis

Our previous work using cell fractionation and density gradient centrifugation indicated that $\text{G}\alpha_2$ is non-randomly distributed in cell membranes, and is regulated by different factors including the activation/deactivation process, monomer/ heterotrimer formation and lipid modification of the protein (Alamer, Kageyama, Gundersen, 2018). Cell fractionation and density gradient centrifugation using Optiprep generated nice floating band (Low density fraction) between 20% to 5% fraction. More detailed about the technique can be found in Material and Methods. Activated $\text{G}\alpha_2$ significantly shifted out of the low-density fraction and an increase of the protein level was detected in a higher density fraction. Using cells expressing a GTPase hydrolysis deficient mutant, $\text{G}\alpha_2$ -208, which represents the active and monomer, $\text{G}\alpha_2$ -208 showed a significant increase in the 20% fraction compare to $\text{G}\alpha_2$ -wt.

The data suggested that monomer and active $\text{G}\alpha_2$ move to a heavier microdomain before translocation to the cytosol or internal membranes. Although activation of $\text{G}\alpha_2$ may be considered a major regulator in this process, additional factors can be involved. Previous studies demonstrated that the cyclic AMP receptor (cAR1) and $\text{G}\beta\gamma$ along with $\text{G}\alpha_2$ remain associated when inactive (Janetopoulos et al., 2001). The diffusion rates of the cAR1, $\text{G}\alpha_2$ and $\text{G}\beta\gamma$ have been determined previously (de

Keijzer et al., 2008; van Hemert et al., 2010). The mobility of the G protein subunits was heterogeneous. Probably, the slow mobility fraction resulted from the existence of these subunits in low-density microdomains. Interestingly, stimulation with cAMP increased the mobility of the receptor in the leading edge. Moreover, they found that the mobility of the receptor resulted in its dissociation from $\text{G}\alpha_2$ subunit (de Keijzer et al., 2008). To further understand the cause of activated $\text{G}\alpha_2$ membrane redistribution, both cAR1 and $\text{G}\beta$ were examined. In this study, we hypothesized that cAR1 and $\text{G}\beta$ may be involved in the active $\text{G}\alpha_2$ membrane distribution.

Another factor considered in this study involves $\text{G}\alpha_2$ membrane distribution in various sized microdomains. It is known that the size of these microdomains is dynamically regulated by external signals, such as those triggered by ligand binding or antibodies. Generally low-density microdomains appear to be small in size and enriched with signaling proteins. However various signals can cause the small domains to fuse forming ‘platforms’ thought to be important for amplifying the signal (Lingwood and Simons, 2010). Thereby, the shifting of $\text{G}\alpha_2$ after cAMP stimulation observed in density gradients may result from membrane domains reorganization. This possibility was tested using the phospholipid-anchored membrane glycoprotein gp80 for comparison. In contrast to the monomer and active $\text{G}\alpha_2$, using a dissociation-defect mutation, $\text{G}\alpha_2$ (G207A), showed poor localization to low density microdomains and most of the protein appeared to be in the highest-density fraction, 45% (Alamer, Kageyama, Gundersen, 2018). This mutation causes a block in dissociation of $\text{G}\alpha_2$ subunit from the $\beta\gamma$ dimer. However, the $\text{G}\alpha_2$ subunit in this mutant still undergoes GTP-GDP exchange (Lee et al., 1992). Confocal imaging showed that most of the protein appeared to be attached to the

internal membranes. The question then is why are the majority of these proteins in the non-raft membrane? This question raised the possibility that these proteins accumulated in the ER, as a previous study in the small G-protein (H-Ras) described. It was shown that active H-Ras transmits its signal from the plasma membrane and while in transit to the endoplasmic reticulum (ER) before reaching the Golgi apparatus (Lorentzen et al., 2010). In this study, we hypothesized that a block in dissociation of $\text{G}\alpha_2$ subunit from the $\beta\gamma$ dimer causes accumulation of the protein in ER membranes.

3.2. Results

3.2.1. Membrane Distribution of Activated $\text{G}\alpha_2$ is Independent of $\text{G}\beta$ and/or cAR1

As a previous study from our laboratory indicated, palmitoylation/depalmitoylation and activation/deactivation cycles of $\text{G}\alpha_2$ control its membrane distribution and microdomain association. Whether cAR1 and/or $\text{G}\beta\gamma$ might regulate $\text{G}\alpha_2$'s dynamic association with membrane upon cAMP binding has not been examined. In order to determine whether cAR1 and/or $\text{G}\beta\gamma$ can influence $\text{G}\alpha_2$ membrane distribution, AX2 cells expressing cAR1-YFP and $\text{G}\beta$ null cells (LW6) expressing $\text{G}\beta$ -YFP were used. Their cellular localization was detected using confocal microscopy (Figure 3.1A). Cell fractionation and Optiprep density gradients were applied to each cell line to examine active/inactive state on protein membrane distribution pattern. To test the inactive state, cells were treated with 2mM caffeine for 15-20 minutes to inhibit cAMP production. The quantitative analysis showed that $59\pm1\%$ of $\text{G}\beta$ -YFP and $48\pm8\%$ of cAR1-YFP accumulate in the low-density fraction. However, stimulation with 10 μM of cAMP for one minute before lysing the cells to induce the active state for the proteins showed

51±3 % of G β -YFP and 42±8% of cAR1-YFP in the low-density fraction (Figure 3.1B,C). Similar to the G α 2-wt-YFP, G β -YFP is significantly shifted (around 9%) out of the low-density fraction after cAMP stimulation. The change observed for cAR1-YFP was not significant. However, unlike the G α 2 and G β subunits, cAR1 was observed at an increased level in the lightest (5%) fraction. Coomassie blue staining for AX2 expressing cAR1-YFP showed a level of proteins exist in 5% fraction (Figure 3.2A). The addition of 10 mM dithiothreitol (DTT) to inhibit cAMP phosphodiesterase during cAMP stimulation (10 min.) further increased the clustering of the receptor in this fraction (Figure 3.2B). In order to determine if the 5% fraction might contain vesicles from ER, immunostaining using the ER marker Calnexin antibody was performed. Fluorescent images showed no colocalization of cAR1 and calnexin (Figure 3.2C) confirming that the 5% fraction does not contain ER vesicles. It has been known that lipid microdomains exist in membranes of many cellular organelles including endosomes, which is the receptor's destination after internalization. This is evidence that 5% fraction represents lighter microdomains that exist in vesicles such as endosomes (Rajendran and Simons, 2005). For further understanding of the activation-dependent membrane distribution, we statistically compared all the three proteins (G α 2, G β and cAR1) side by side after cAMP stimulation. It is clear that each protein follows a certain path (Figure 3.3). cAR1 significantly increases in the 5% fraction, while G β significantly increases in the 45% fraction compared to the G α 2. These data indicate that the membrane clustering pattern of activated G α 2 is independent of G β and/or cAR1.

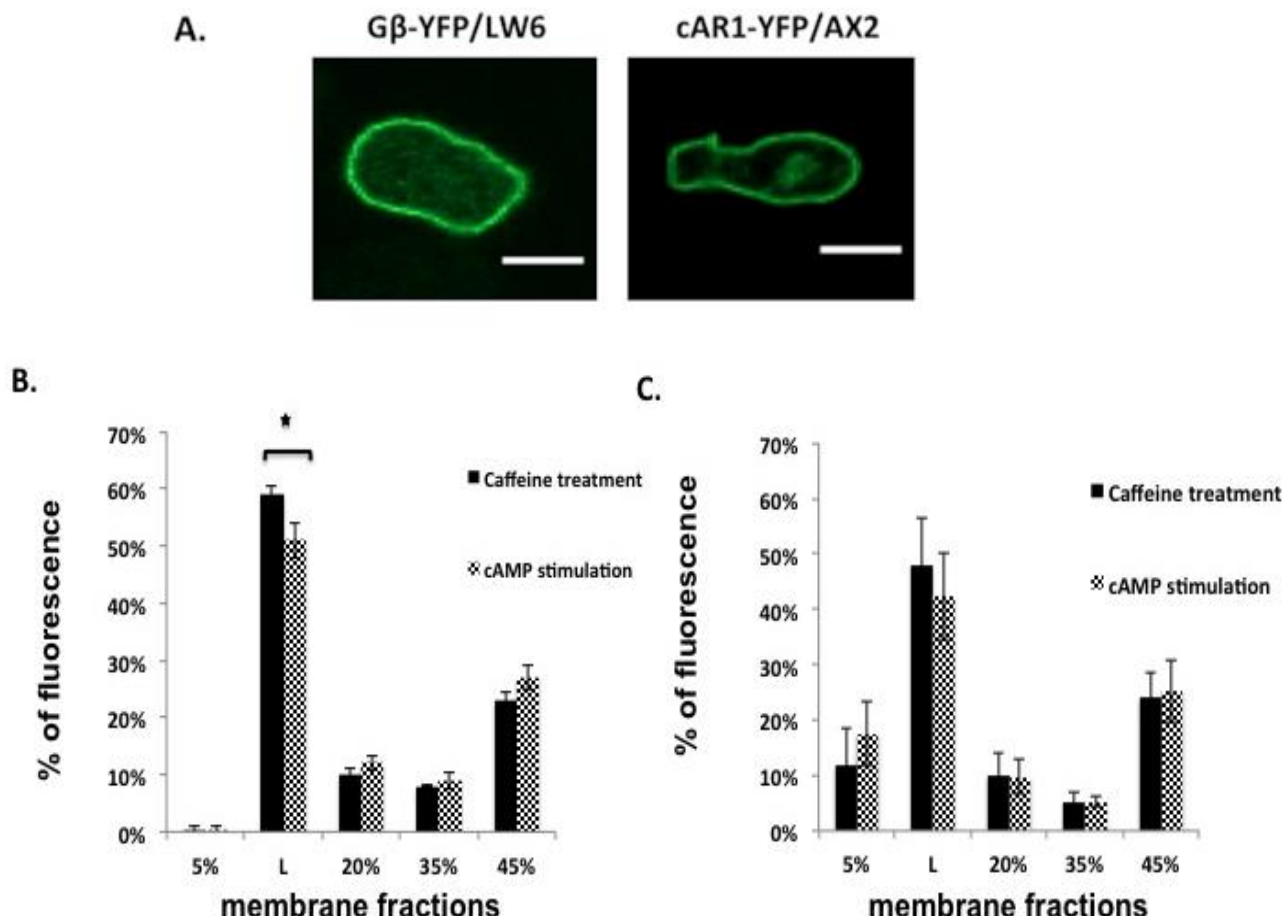


Figure 3.1. Membrane distribution of G β (YFP) and cAR1(YFP) in OptiPrep density gradient. A. G β null cell line (LW6) expressing G β -YFP and AX2 cells expressing cAR1-YFP were starved for 5hr and imaged with an Olympus 1000 confocal microscope. The laser (515 nm) was set to 550 hv at 5%. Scale bars are 5 μ m. B-C. Both cells were starved for 5 h, lysed and the membrane fraction for two samples, caffeine treated (2mM for 15 min) and cAMP stimulated (10 μ M for 1 min) samples were subjected to OptiPrep gradient centrifugation as described in the MATERIALS AND METHODS. The fluorescence of 50 μ l from each fraction mixed with an equal volume of base buffer was detected by a plate reader (Synergy 2; Bitek). L: low density fraction, (n=3; t-test *p < 0.05).

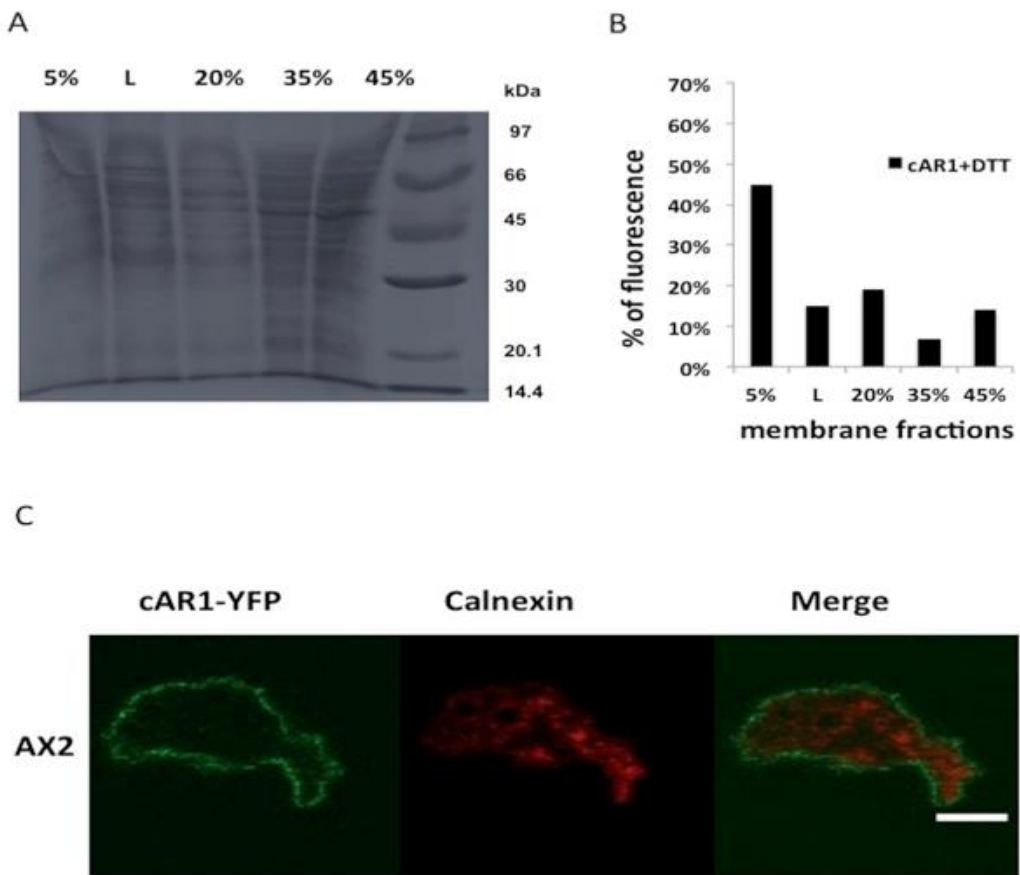


Figure 3.2. Cellular localization and membrane distribution of cAR1-YFP. A-B. AX2 cells expressing cAR1-YFP were starved with cAMP pulsing for 5hr .For A. Cells lysed and membranes fraction subjected to OptiPrep gradient centrifugation as described in MATERIALS AND METHODS. 50 μ l aliquots of each fraction was taken and mixed with an equal volume of 2X SDS sample buffer. The samples heated for 4 minutes and then subjected to SDS-PAGE and detected by Coomassie staining. Protein amount in each fraction was determined as described in Material and Methods. For B .Starved cells treated with 10mM DTT and stimulated with 10 μ M cAMP in lysis buffer for 10 minutes prior to the cell homogenization. Membrane fraction was subjected to Optiprep gradient centrifugation and the florescence in each fraction detected by plate reader. C. Cells expressing cAR1-(YFP) were starved on glass coverslips in DB buffer for 5hr. Cell then uniformly stimulated with 10 μ M cAMP for 1 min, fixed with 1.5% paraformaldehyde for 10 minutes and permeabilized with 70% acetone for 2 minutes. Cells stained with anti-calnexin – ER membrane marker antibody followed by anti-mouse secondary antibody coupled to Alexa Fluor 640. Scale bar is 5 μ m.

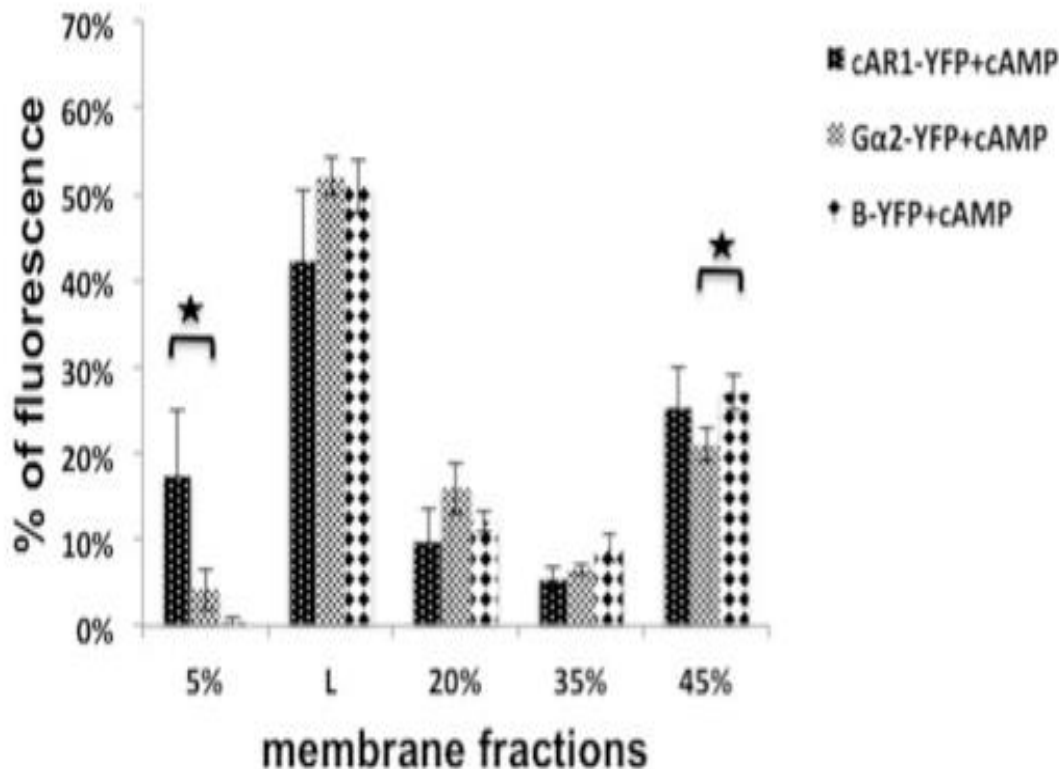


Figure 3.3. Membrane distribution of activated cAR1-YFP, G α 2-YFP and G β -YFP. Cells expressing either cAR1-YFP, G α 2-YFP or G β -YFP were starved for 4hr-5hr with cAMP pulsing. In lysing buffer, cells were stimulated with cAMP then lysed after 1 minute. Membrane fractions were subjected to OptiPrep gradient centrifugation as described in MATERIALS AND METHODS and the fluorescence detected by plate reader. (*t*-test * $p < 0.05$).

3.2.2 Gα2 Translocation is Independent of Raft Organization

Another factor that may be involved in membrane microdomain clustering of Gα2 is signal-dependent membrane reorganization. If Gα2 shifting after cAMP stimulation is based on membrane reorganization and lipid microdomains clustering, it should be detected with the lipid raft marker gp80. In order to test this possibility, two samples of AX2 cells were starved for ~ 7hr. First one sample was treated with caffeine for 15-20 min and the other one was stimulated with 10 μM cAMP for 1 min before lysing the cells. Optiprep density gradient centrifugation was applied and the level of lipid raft marker gp80 in the low-density fraction for both samples was examined. Immunoblot analysis showed no significant difference of the gp80 level between both samples (Figure 3.4). The data indicated that the shifting of the Gα2 out the low-density fraction is independent to membrane reorganization and lipid microdomain clustering but it is based on specific translocation/clustering of the Gα2.

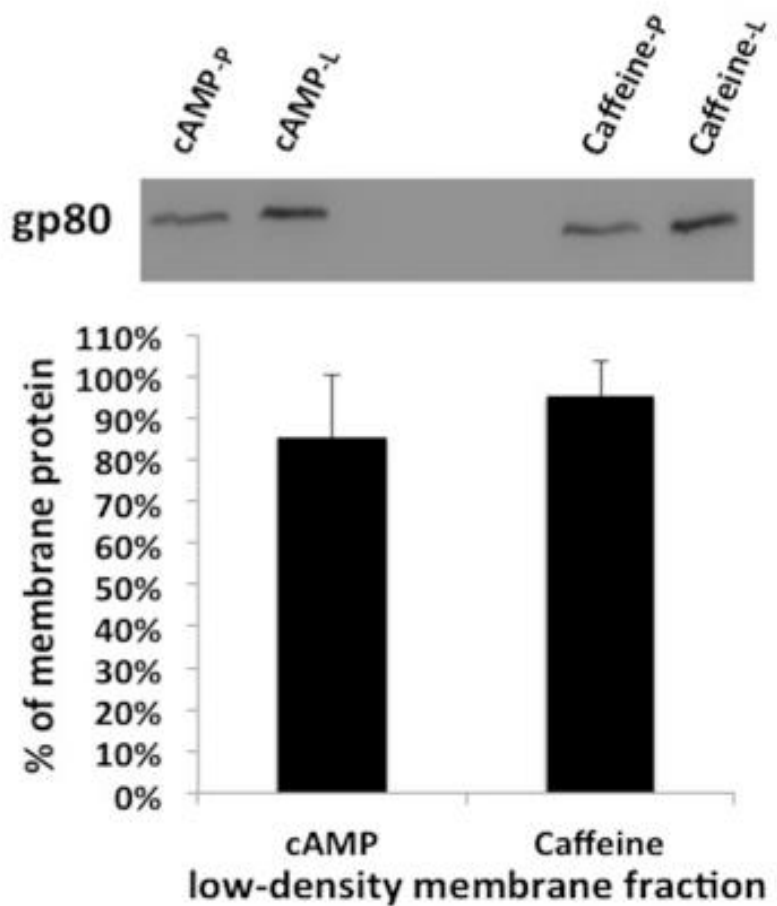


Figure 3.4. Membrane distribution of GPI-anchored protein, gp80. AX2 cells were starved for ~7hr with cAMP pulsing. To block the activation, cAMP pulsing was stopped and the cells incubated with 2mM caffeine for 15-20min prior to the cell homogenization and membrane fractionation. To induce the activation state of G protein signal, cells were stimulated with 10 μ M of cAMP in the lysis buffer then lysed after 1 minute. Membrane fraction for both samples was subjected to Optiprep density gradient centrifugation. Membrane fraction (sonicated pellet; P) and low density fraction (L) from both samples (caffeine treated and cAMP stimulated) were mixed equally with 2X SDS sample buffer, heated and then 50 μ l (40 μ g of protein) was loaded onto the SDS-PAGE for gp80 detection. The band intensity reading of 50 μ l of the pellet (cAMP-P and caffeine-P) was corrected for the total volume that was used for the Optiprep density gradient centrifugation. The graph represents the average of three independent experiments \pm S.D. The difference was not significant (*t*-test $P=0.18$).

3.2.3 Dissociation-Defect of G Protein Heterotrimer Restricted ER to Golgi

Translocation

The dissociation-defect mutation of $\text{G}\alpha_2$ ($\text{G}207\text{A}$) showed poor localization to the low density fraction with most of the protein present in the 45% fraction. In order to understand $\text{G}\alpha_2$ membrane localization and shuttling inside the cell, it is important to know whether this protein exists in the membrane of an organelle that does not have microdomains such as ER or if it is accumulating in non low-density membrane part of Golgi apparatus. This was testing by using AX2 expressing $\text{G}\alpha_2(\text{YFP})\text{-wt}$ and $\text{G}\alpha_2(\text{YFP})\text{-G}207\text{A}$. Cells were fixed, permeabilized and then stained with antibody against the ER marker calnexin (Muller-Taubenberger et al., 2001). Imaging revealed that $\text{G}\alpha_2(\text{YFP})\text{-G}207\text{A}$ co-localizes with calnexin to a greater extent than $\text{G}\alpha_2(\text{YFP})\text{-wt}$ (Figure 3.5). The immunostaining data with the ER marker, calnexin suggests that the 45% fraction contains ER membrane. The accumulation of $\text{G}\alpha_2\text{-G}207\text{A}$ in the ER can be evidence that a monomeric $\text{G}\alpha_2$ is required for translocation from the ER to Golgi where heterotrimer normally formation occurs (Michaelson et al., 2002).

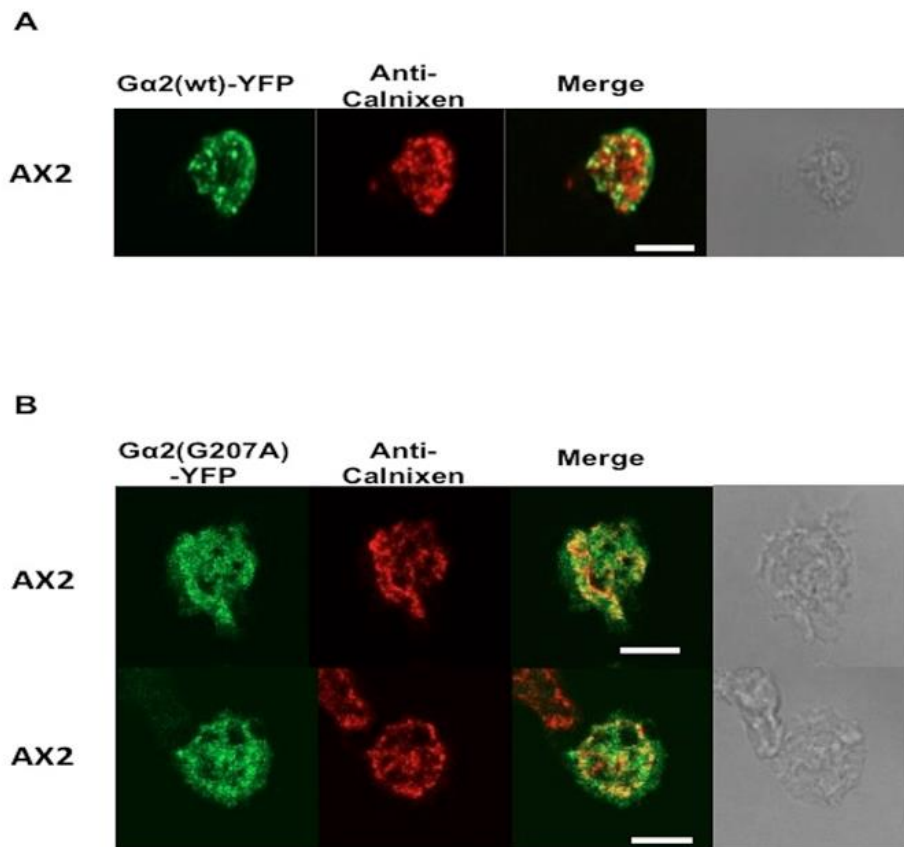


Figure 3.5. Co-localization of Gα2(YFP)-wt and Gα2(YFP)-G207A with calnexin in AX2 cells. AX2 cells expressing A. Gα2 (YFP)-wt and B. Gα2 (YFP)-G207A were allowed to attach to the glass coverslips and then starved in DB buffer for 5 hr. Cells were then fixed and permeabilized as described in MATERIALS AND METHODS. Cells were then stained with anti-calnexin – ER membrane marker antibody followed by anti-mouse secondary antibody coupled to Alexa Fluor 640. Scale bars 10 μm.

CHAPTER 4

FUNCTIONAL CONSEQUENCE OF $\text{G}\alpha_2$ PHOSPHORYLATION

4.1 Background and Hypothesis

G protein-mediated signaling is subject to regulation by many factors that can directly or indirectly modify G proteins and alter their structure and function. Serine or tyrosine phosphorylation that adds a negative charge and installs hydrogen bond acceptor oxygens, appears to have an important aspect in such regulation. Previous studies demonstrated that several G protein α subunits are substrates for serine and/or tyrosine phosphorylation by protein kinases including protein kinase C, p21-activated protein kinase (PAK1), cGMP-dependent protein kinase and Src family non-receptor tyrosin kinases. Stimulation of thyrotropin releasing hormone (TRH) receptors that express in *Xenopus* oocytes induces serine phosphorylation of the $\text{G}\alpha_q$ family protein, $\text{G}\alpha_{16}$. Phosphorylation of $\text{G}\alpha_{16}$ blocks TRH responsiveness, which suggested that a feedback inhibitory loop is initiated after $\text{G}\alpha_{16}$ phosphorylation. Both members ($\text{G}\alpha_{15}$ and $\text{G}\alpha_{16}$) of $\text{G}\alpha_q$ family expressed in hematopoietic cells are regulated by PKC phosphorylation, which indicates a mechanism for autoregulation of the receptor-activated $\text{G}\alpha_{15}/\text{G}\alpha_{16}$ transduction pathway (Aragay and Quick, 1999).

In platelets, stimulation with thrombin or phorbol ester induces serine phosphorylation of $\text{G}\alpha_{12}$, $\text{G}\alpha_{13}$ and $\text{G}\beta\gamma$ by protein kinase C. It has been shown that phosphorylation of these subunits affects $\text{G}\beta\gamma$ - subunit binding, prevents receptor re-association and, therefore, attenuation of the signal (Lounsbury et al., 1991; Lounsbury et al., 1993; Fields and Casey, 1995; Kozaza and Gilman, 1996; Offermanns et al., 1996). Glick and his colleagues have found that PKC-mediated $\text{G}\beta\gamma$ phosphorylation

reduced the ability of RGS to accelerate GTPase activity of this G subunit but the exact mechanism is not clear (Glick et al., 1998). In transfected HEK-293 cells, PAK1 is implicated in $\text{G}\alpha\gamma$ phosphorylation, which inhibits $\text{G}\beta\gamma$ and RGS binding (Wang et al., 1999). On the other hand, protein kinase C-mediated serine phosphorylation of $\text{G}\alpha_i$ attenuates the inhibition of adenylyl cyclase mediated by opiate signaling in neuroblastoma/glioma (NG-108-15) cells (Strassheim and Malbon, 1994). Chinese Hamster Ovary (CHO) cells express multiple members of $\text{G}\alpha$ family that subjected to serine phosphorylation by cGMP-dependent protein kinase. Phosphorylation of $\text{G}\alpha_i$ by cGMP-dependent protein kinase blocks pertussis toxin-sensitive hormone receptor signaling and attenuates calcium influx. This led to the assumption of that $\text{G}\alpha_i$ phosphorylation affects its binding with down-stream effectors (Pfeifer et al., 1995).

In contrast, tyrosine phosphorylation is a regulator of both $\text{G}\alpha_s$ and $\text{G}\alpha_q/11$. Phosphorylation of $\text{G}\alpha_s$ increases GTP binding and adenylyl cyclase activity indicating that phosphorylation leads to $\text{G}\alpha_s$ activation (Poppleton et al., 1995). Similarly, phosphorylation of $\text{G}\alpha_q/11$ regulates its association with the receptor, which in turn regulates the activation of $\text{G}\alpha_q/11$ protein (Liu et al., 1996; Umemori et al., 1997). Although a number of studies have demonstrated that multiple mammalian G protein α -subunits undergo phosphorylation, gaps in this knowledge still exists.

In *Dictyostelium*, phosphorylation of $\text{G}\alpha_2$ is temporary and occurs upon cAMP binding to the surface cAMP receptor (cAR1). $\text{G}\alpha_2$ phosphorylation was identified on Serine 113 within the helical domain. However, the role of phosphorylation in regulating $\text{G}\alpha_2$ function and interaction with partners is not known. In this context, the 14-3-3 protein family, present in all eukaryotes, has become a recent focus for its

phosphoprotein interactions/binding. It is a highly conserved protein family that functions as scaffolding protein to regulate the activity of binding partners and to play an important role in cytoskeletal regulation (Smith et al., 2011). 14-3-3 proteins are implicated in regulating various signaling pathways including nuclear factor- κ B (NF- κ B) signaling, TGF- β signaling, small G protein Rnd3 and some of the regulators of G protein signaling (RGS) family (Benzing et al., 2000; Tang et al., 2016; Riou et al., 2013; Ye et al., 2016). However, nothing is known about the regulatory role of the 14-3-3 proteins on heterotrimeric G proteins signaling.

Since phosphorylation requires an activated $G\alpha 2$, we hypothesized that a phosphorylation-dependent mechanism of regulation exists to regulate $G\alpha 2$ -mediated signaling and interaction with 14-3-3 proteins.

4.2 Results

4.2.1 $G\alpha 2$ Phosphorylation Regulates its Function

The importance of phosphorylation on protein functions is widely accepted (Smith et al., 2011). However, little is known about role of $G\alpha 2$ phosphorylation in *Dictyostelium*. In 1994, a study from our laboratory found that activation of $G\alpha 2$ causes a phosphorylation of serine 113 (Chen, Devreotes, Gunderson, 1994). In order to address the regulatory role of this modification, PCR site-directed mutagenesis was applied using pJK1 and pCV5 plasmid encoding $G\alpha 2$ and $G\alpha 2$ tagged YFP, respectively. The serine 113 was replaced with alanine, generating $G\alpha 2$ (S113A) as a means to block $G\alpha 2$ phosphorylation. A phosphomimetic mutant was also generated by

changing the serine to an aspartic acid, Ga2 (S113D). Each of these constructs was transferred into AX2 and *ga2*-null (MYC2) cell line (Gundersen, 1997).

The developmental phenotype of Ga2-S113A was examined using time-lapse imaging during *Dictyostelium's* developmental life cycle (20hr) in DB plate (Figure 4.1A). The results showed that Ga2-S113A/MYC2 cells initiate aggregation phase and mound formation ~4hr earlier than Ga2-wt/MYC2 cells (Figure 4.1B). At the end of the life cycle, both cell lines formed fruiting bodies at approximately the same time (Figure 4.1A). In addition, streaming was clearly different in Ga2-S113A. Ga2-S113A formed aggregates significantly smaller than Ga2-wt (Figure 4.1C).

Ga2-S113D/MYC2 revealed only one difference from Ga2-wt/MYc2 cells during development on DB agar. Ga2-S113D cells stream similar to the Ga2-wt (Figure 4.1A) and both aggregate in around 8 hr (Figure 4.1B). However, Ga2-S113D culmination was delayed (~30 hr) (Figure 4.2A). The differences observed between the Ga2 mutants and wild type were not related to protein expression levels, as each cell line shows equivalent Ga2 expression on immunoblots of whole cells lysate (Figure 4.2B).

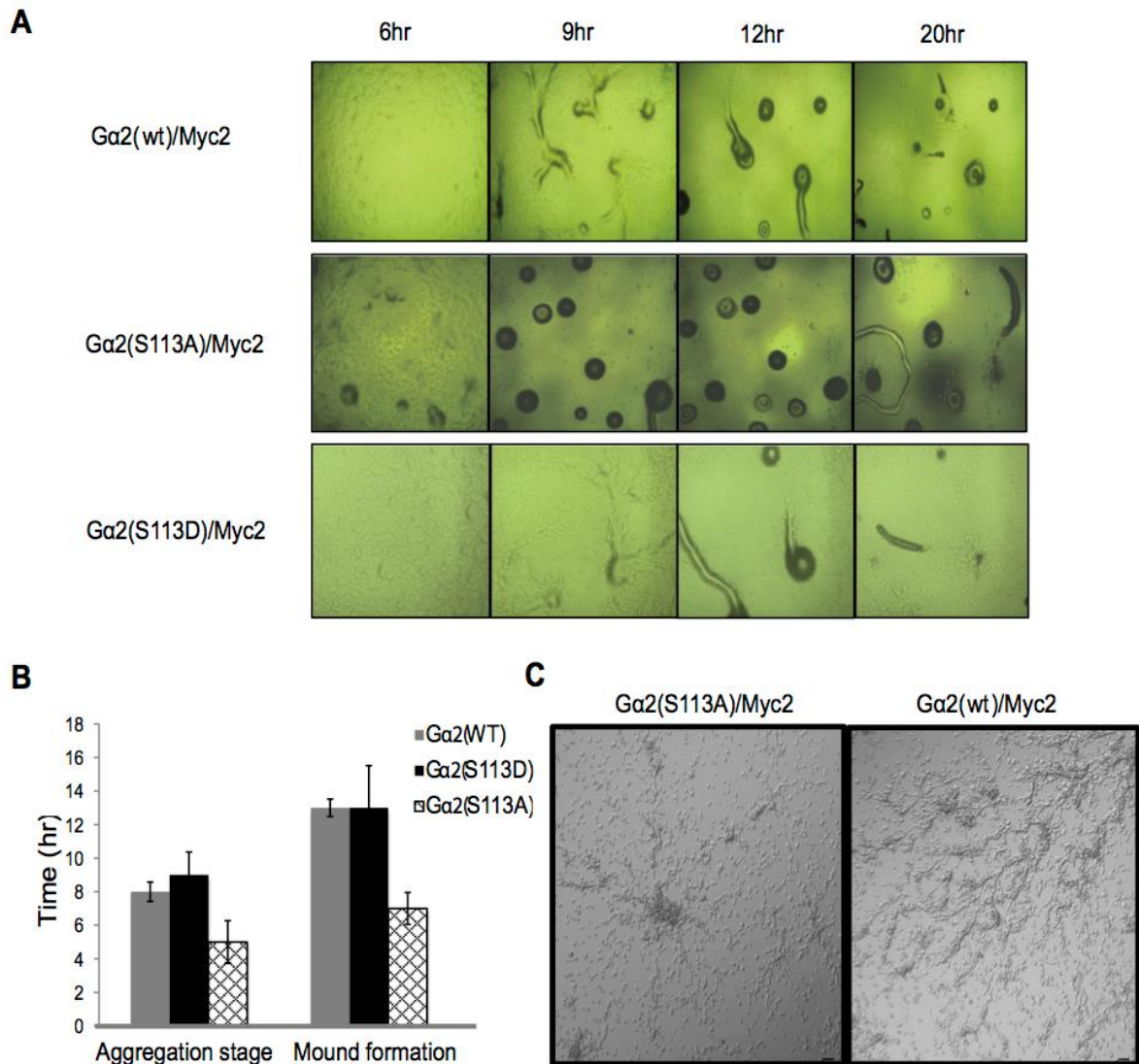


Figure 4.1. Developmental phenotype of *gα2*-null cells (MYC2) cells expressing Gα2-wt, Gα2-S113A and Gα2-S113D. A. Time-lapse imaging for *gα2*-null cell line expressing Gα2-wt, Gα2-S113A or Gα2-S113D. Cells were plated onto DB (7% agar) plates at 2×10^7 cells per plate (100 mm dia.) and allowed to proceed through development for 24 hr. Images were acquired every 6 min using Nikon Eclipse E200 fitted with a Spot idea camera and 40X magnification. B. The average time of the aggregation stage and mound formation of three independent experiments (± 10 min) for each cell line. C. *gα2*-null cell line expressing Gα2-wt, Gα2-S113A were starved at 2×10^7 cells/ml of DB on a shaker (@125 rpm) with cAMP pulsing (100 μ m) for 2hr. Cells were then removed to a glass bottom plate for another 2-3hr and imaged with an Olympus Fluoview FV1000 confocal microscope (10X). Scale bars are 5 μ m.

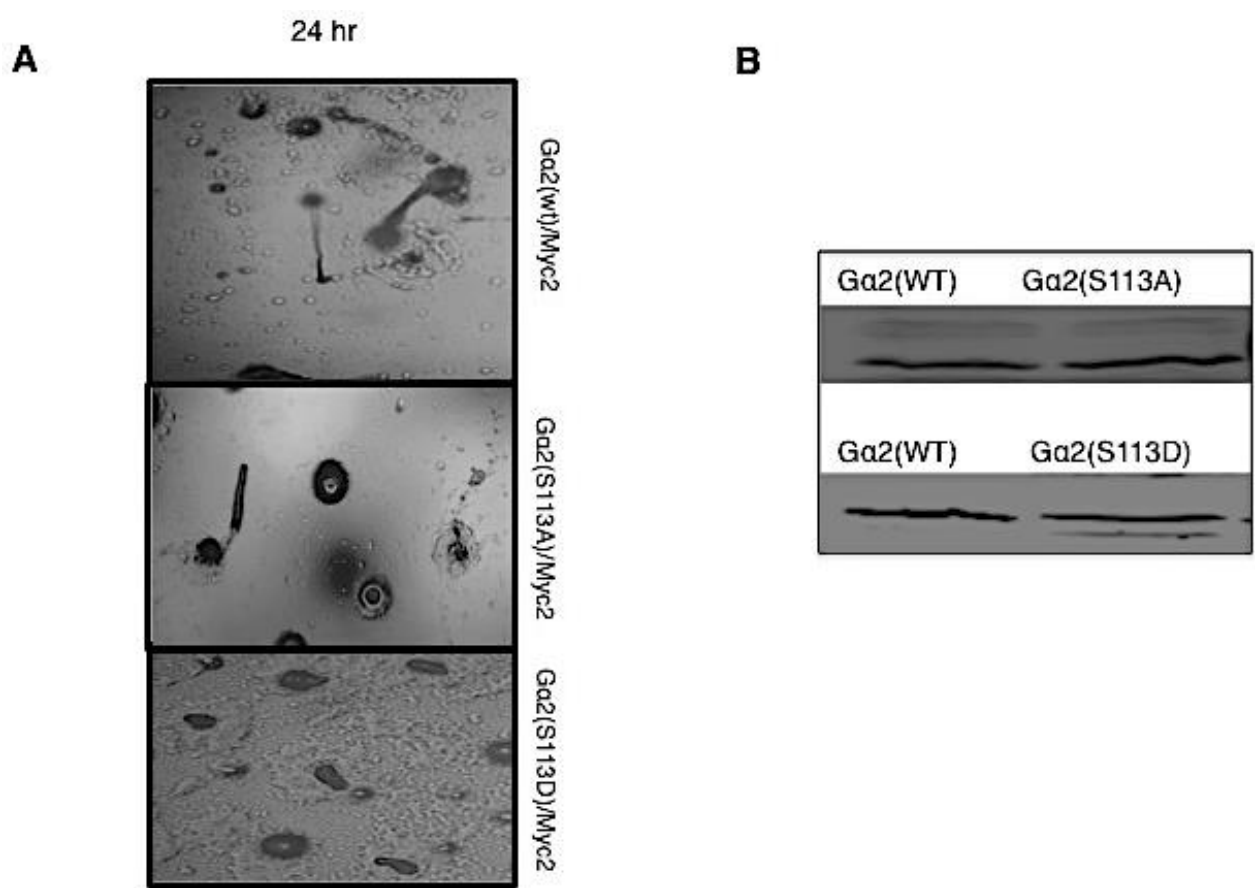


Figure 4.2. Developmental phenotype at 24hr of $\alpha 2$ -null cells (MYC2) cells expressing Ga2-wt, Ga2-S113A and Ga2-S113D. A. Cells were plated onto DB (7% agar) plates at 2×10^7 cells per plate (100 mm dia.) and allowed to proceed through development. Images were acquired after 24 hr using a Nikon Eclipse E200 fitted with a Spot idea camera (40X). B. The blots show the expression level of Ga2-wt, Ga2-S113A or Ga2-S113D in $\alpha 2$ -null cell line. 25 μ l of whole cell lysate was mixed with 1X SDS sample buffer, heated for 4min and loaded into SDS-PAGE and immunoblotted as described in MATERIALS AND METHODS.

4.2.2 Gα2 Phosphorylation Regulates Its Membrane/ Cytosolic Localization

Cellular localizations for Gα2(S113A)-YFP and Gα2(S113D)-YFP were detected using confocal microscopy. Cells were starved for 4hr in DB buffer before imaging. The images showed that the phosphorylation blocked mutant Gα2(S113A)-YFP is uniformly distributed across the plasma membrane similar to the Gα2(wt)-YFP, while most of the phosphomimetic Gα2(S113D)-YFP expressing cells showed non-uniform distribution of the protein across the plasma membrane (Figure 4.3). The reason for this distinctive distribution is not clear. It is also noteworthy that some of Gα2(S113D)-YFP expressing cells frequently produced extracellular vesicles after starvation (Figure 4.4A). In order to rule out cell apoptosis, a cell viability assay was performed for both Gα2(S113A)-YFP and Gα2(S113D)-YFP. Results showed no significant difference between the two cell types (Figure 4.4B).

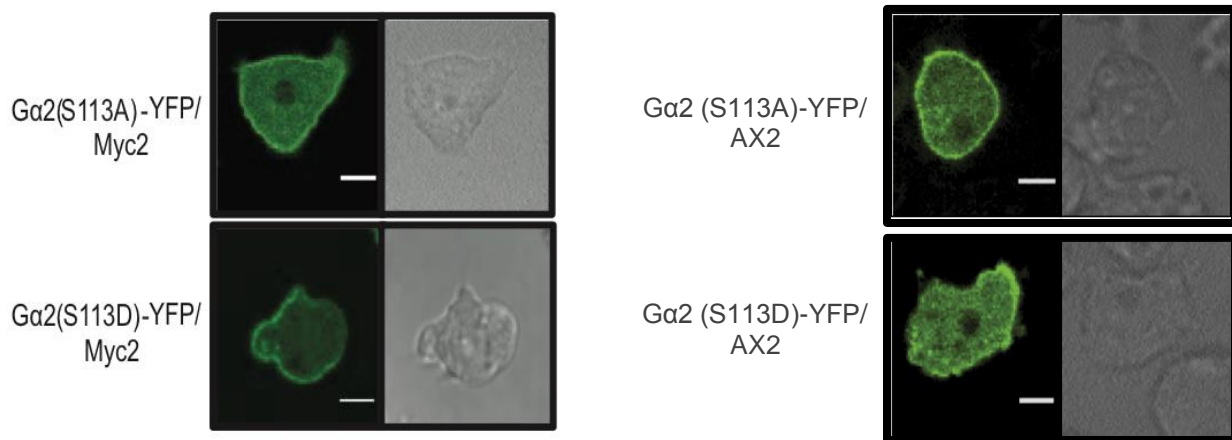


Figure 4.3. Cellular localization of $\text{G}\alpha_2(\text{S}113\text{A})\text{-YFP}$ and $\text{G}\alpha_2(\text{S}113\text{D})\text{-YFP}$. Cells were starved in glass bottom plates for 4-5 hr then imaged with 1000 confocal microscope (100X). The laser (515 nm) was set to 550 hv at 5%. Scale bars are 5 μm

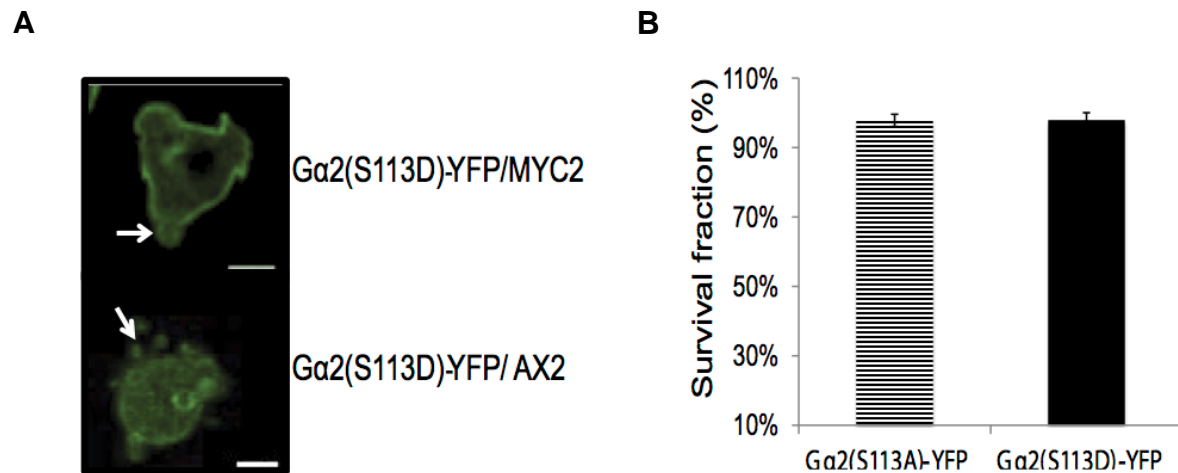


Figure 4.4. Cellular phenotype of $\text{G}\alpha_2$ (S113D)-YFP expressing cells. A. Ax2 cells and Myc2 cells expressing $\text{G}\alpha_2$ (S113D)-YFP produce extracellular vesicle (white arrows) after 4-5 hr starvation. Scale bars are 5 μm . B. Cell viability of $\text{G}\alpha_2$ (S113A)-YFP and $\text{G}\alpha_2$ (S113D)-YFP expressing cells. Cells were starved at $2 \times 10^7/\text{ml}$ in DB then mixed with trypan blue at a final 0.1%. The number of cells were counted using hemocytometer. The graph represent the average of three independent experiments \pm S.D. The difference was not significant (t -test $P=0.47$)

To examine the partitioning of the $\text{G}\alpha_2$ -YFP constructs following lysis, the supernatant and pellet fractions was assayed for YFP fluorescence as detected by microplate reader. Cells starved for 4 to 5 hr with cAMP pulsing were lysed as described in the Material and Methods. The $\text{G}\alpha_2$ (wt)-YFP 17,000 xg pellet fraction yielded $45\pm 2\%$ of the total fluorescence with $55\pm 2\%$ in the supernatant fraction (Figure 4.5A). The reason for detecting less $\text{G}\alpha_2$ -(wt)-YFP in pellet fraction may result from binding of cAMP to the receptor, which promotes $\text{G}\alpha_2$ shuttling from plasma membrane to the cytosol. In the case of $\text{G}\alpha_2$ (S113A)-YFP, $53\pm 3\%$ of $\text{G}\alpha_2$ (S113A)-YFP was detected in pellet fraction and $47\pm 3\%$ of the protein was in the supernatant (Figure 4.5A), a significant difference from $\text{G}\alpha_2$ -(wt)-YFP. To determine if blocking the phosphorylation might be affecting the GTPase activity of $\text{G}\alpha_2$ -S113A which in-turn may affect the lysis distribution of $\text{G}\alpha_2$ -(S113A)-YFP. The pellet and supernatant distribution of the GTPase hydrolysis deficient mutant $\text{G}\alpha_2$ (208)-YFP was examined for comparison (Figure 4.5B). $\text{G}\alpha_2$ (208)-YFP shows $35\pm 2\%$ in the pellet fraction and $65\pm 2\%$ in the supernatant fraction. Similar to the wild type, less $\text{G}\alpha_2$ (208)-YFP was detecting in pellet fraction. These data suggested that phosphorylation of $\text{G}\alpha_2$ affects it's membrane/cytosolic distribution independently of GTPase hydrolysis. Treating cells with 2 mM caffeine to block cAMP production by *Dictyostelium* increased levels in the lysis pellet for both $\text{G}\alpha_2$ (wt)-YFP and $\text{G}\alpha_2$ (S113D)-YFP, while the levels of $\text{G}\alpha_2$ (S113A)-YFP were unchanged (Figure 4.5C), indicating that activated $\text{G}\alpha_2$ (S113A)-YFP may reside in the plasma membrane longer than $\text{G}\alpha_2$ (wt)-YFP and $\text{G}\alpha_2$ (S113D)-YFP.

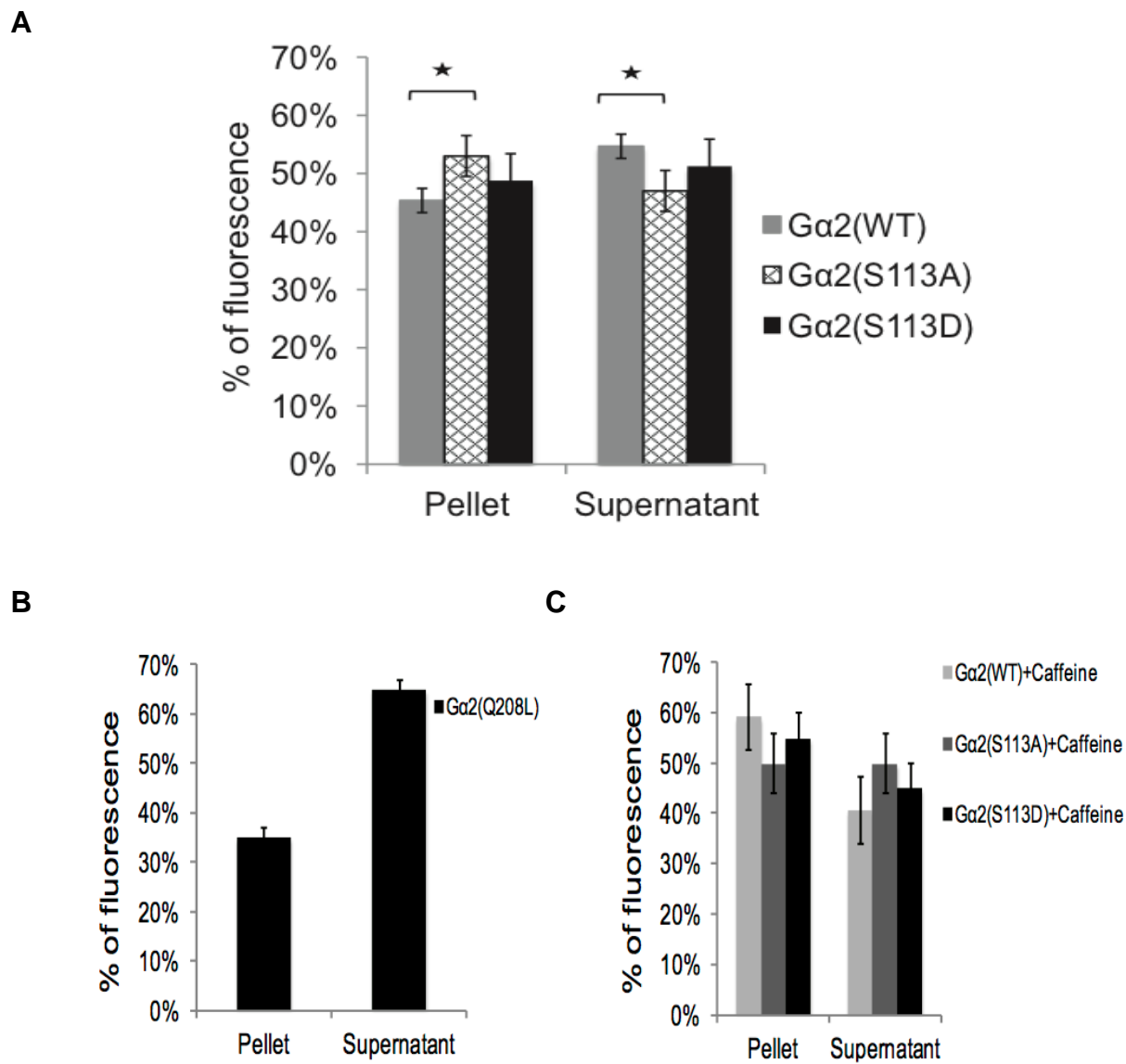


Figure 4.5. Membrane and cytosolic distribution of Ga2-YFP. 3×10^8 cells expressing either Ga2 (wt)-YFP, Ga2 (208)-YFP, Ga2 (S113A)-YFP or Ga2 (S113D)-YFP were starved for 4hr-5hr with cAMP pulsing. Cells were filter lysed. Sample preparation was performed as described in MATERIAL AND METHODS under cell fractionation and density gradient centrifugation. The fluorescence intensity reading of 100 μ l of the pellet and supernatant fractions was detected using a plate reader and corrected for the total volume. The values represent the mean \pm S.D. of three experiments. A. Membrane distribution of Ga2 (wt)-YFP, Ga2 (S113A)-YFP or Ga2 (S113D)-YFP in untreated cells (*t*-test **p* < 0.05). B. Ga2 (208)-YFP membrane distribution. C. Membrane distribution of Ga2 (wt)-YFP, Ga2 (S113A)-YFP or Ga2 (S113D)-YFP in caffeine treated cells.

4.2.3 Activated and Phosphorylated Gα2 Co-localized With 14-3-3 Proteins.

The above data showed that phosphorylation of Gα2 regulates its membrane/cytosolic distribution. This led us to identify a partner that can participate in such action. 14-3-3 protein is a potential partner as it is known to bind phosphoserine-containing motifs in their target. It is a highly conserved adaptor protein in eukaryotic cells and plays a role in the intracellular trafficking of membrane proteins (Smith et al., 2011). In *Dictyostelium*, 14-3-3 is reported to be localized in cell cortex and contribute to signaling pathways that involve microtubules, myosin II and Rac (Zhou et al., 2010). In this study, we aimed to test if Gα2 phosphorylation regulates specific protein-protein interaction with 14-3-3 during chemotactic signal transduction. Initially, we examined the co-localization between Gα2-YFP and 14-3-3 proteins using immunofluorescence. Cells expressing Gα2(wt)-YFP, Gα2(S113A)-YFP or Gα2(S113D)-YFP were starved on glass coverslips for 4-5 hr. Cells expressing Gα2(wt)-YFP were treated with 2mM caffeine for 15 min to block the activation or stimulated with 10μm cAMP for 1min to activate Gα2. Cells were then fixed and immunostained with anti-14-3-3 Ab followed by Alexa fluor 633. In cAMP-stimulated cells, activated Gα2(wt)-YFP (green) co-localized more with 14-3-3 proteins (red) compare to the in active Gα2(wt)-YFP in caffeine-treated cells (Figure 4.6A). This is consistent with the results obtained from imaging Gα2(S113D)-YFP and Gα2(S113A)-YFP. The merged images show an increase of the co-localization between Gα2(S113D)-YFP and 14-3-3s compared to Gα2(S113A)-YFP (Figure 4.6A). Quantification of co-localization using Pearson's correlation coefficient further confirmed the significant co-localization of the activated and phosphorylated Gα2 with 14-3-3 proteins compare to the inactive or non-phosphorylated (Figure 4.6B).

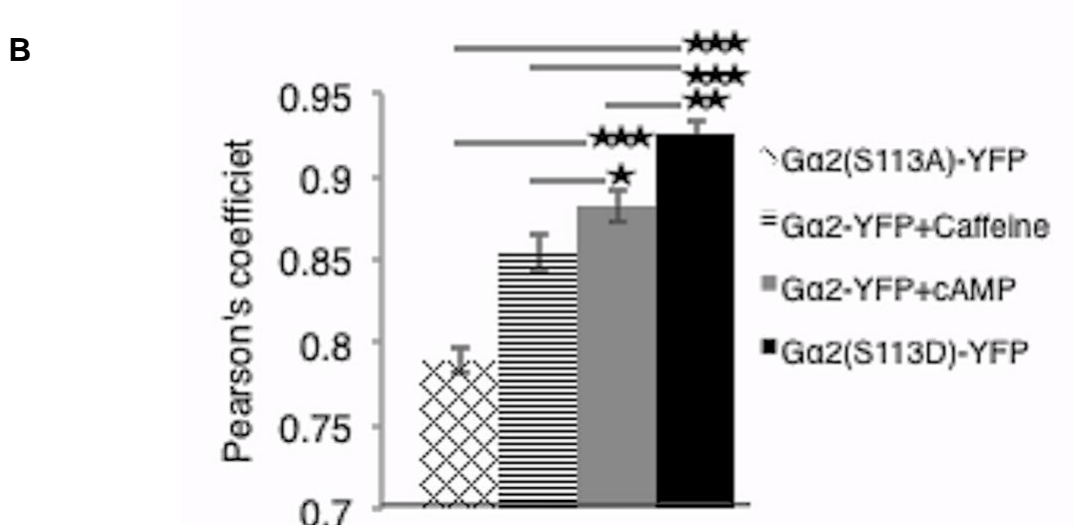
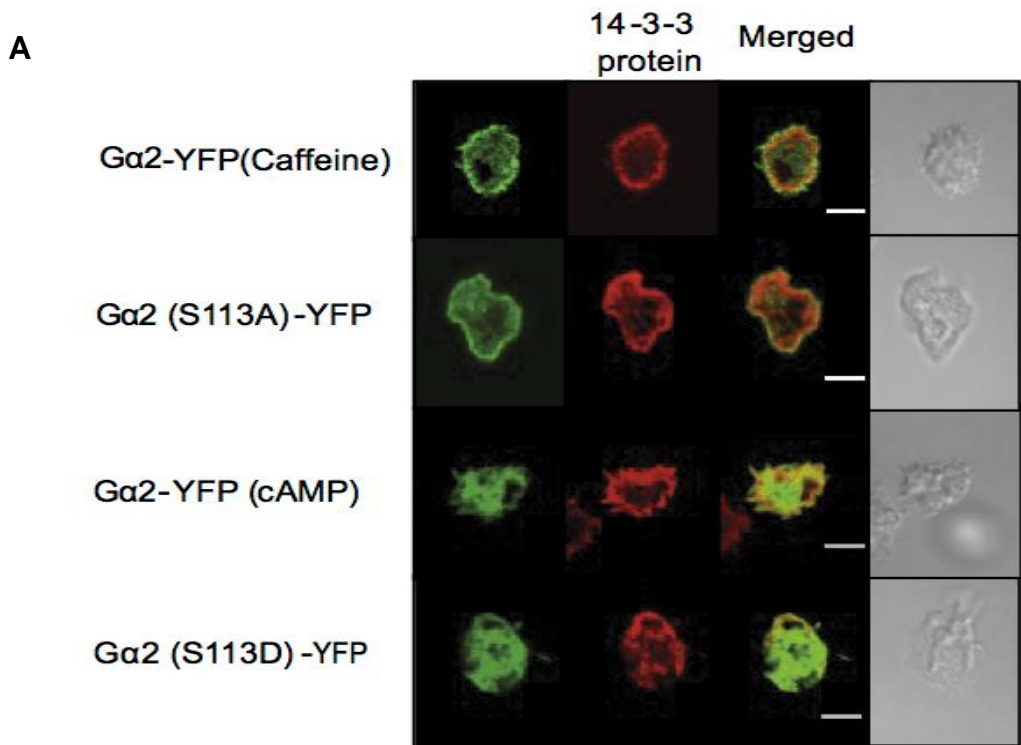


Figure 4.6. Colocalization of Gα2 and 14-3-3 proteins. A. Cells expressing Gα2(wt)-YFP, Gα2(S113A)-YFP and Gα2(S113D)-YFP were starved on glass coverslips for 4-5hr. Gα2(wt)-YFP expressing cells were then treated with caffeine for 15 min to block the activation or stimulated with cAMP for 1 min followed by PFA fixation, permeabilization and 14-3-3 staining as described in Material and Methods. Scale bars 5 μm. B. Plot shows the mean of Pearson's correlation coefficients for the colocalization analysis of two independent experiments (n=25; t-test *p < 0.05, **p < 0.01, ***p < 0.0001).

4.2.4 The Interaction Between G α 2 and 14-3-3 is Activation and Phosphorylation-Dependent

Next we examined whether G α 2 interact with 14-3-3 using co-immunoprecipitation for Myc2 cells that express G α 2-wt, G α 2-S113A or G α 2-S113D. Negative controls IPs were performed with Myc2 strain expressing G α 2-wt (Figure 4.8A). Polyclonal antibody directed to endogenous G α 2 was used to pull down the complex and 14-3-3 was detected by western blotting using 14-3-3-specific antibody. The results showed that stimulation with cAMP influenced the interaction of 14-3-3s with the activated G α 2. This interaction was significantly decreased after caffeine treatment (Figure 4.7A,C). Similarly, 14-3-3 significantly interacts with phosphomimic G α 2, G α 2-S113D compared to the phosphorylation blocked G α 2-S113A (Figure 4.7A,C). The reciprocal interaction was performed with G α 2(S113A)-YFP and G α 2(S113D)-YFP constructs for technical issue. Both constructs express 14-3-3 at a similar level (Figure 4.8B). Also, the expression level of both constructs was detected using a plate reader (Figure 4.8C). Similar results were obtained as the phosphomimic G α 2; G α 2(S113D)-YFP shows significantly more interaction with 14-3-3s compare to the phosphorylation blocked G α 2, G α 2(S113A)-YFP (Figure 4.7B,D).

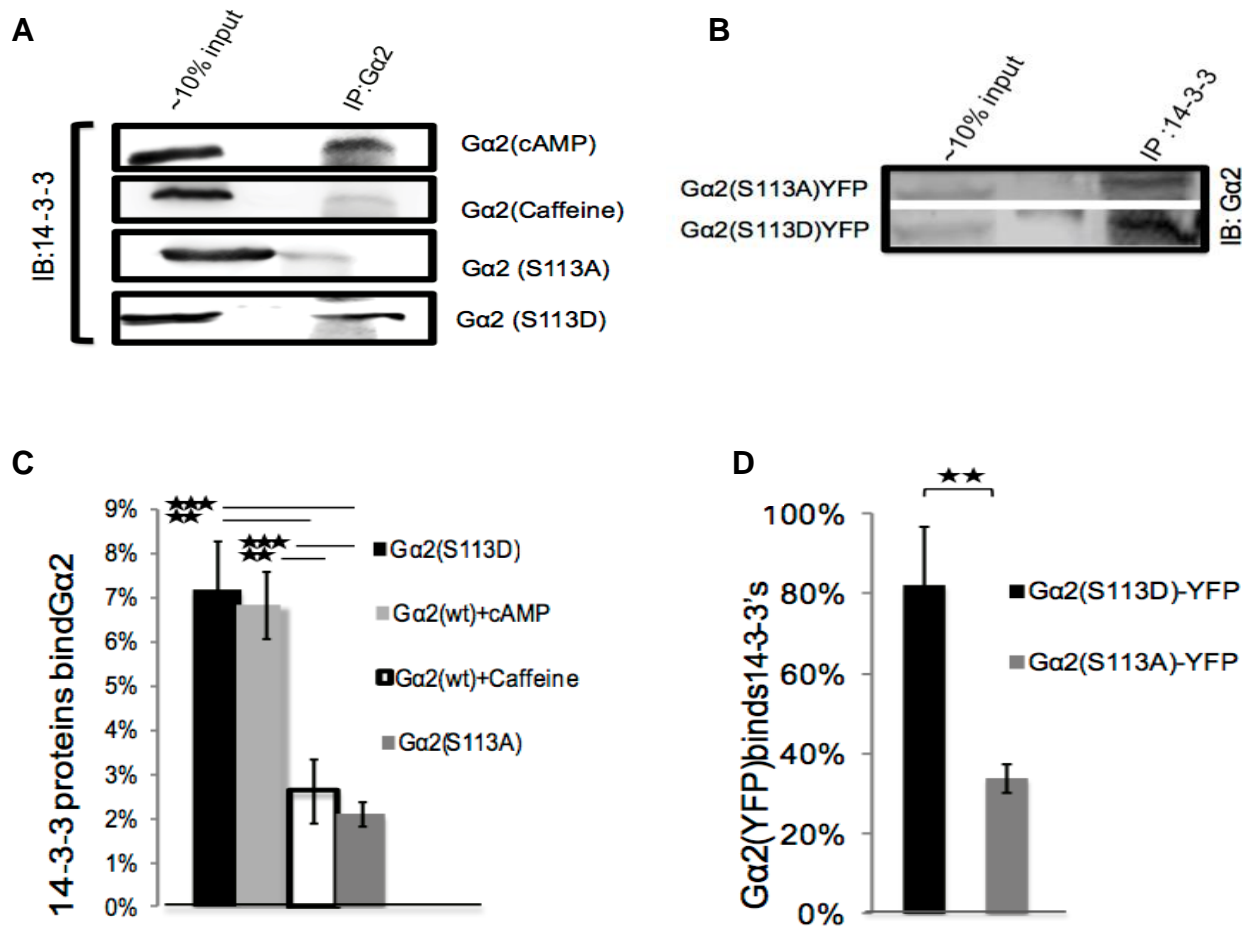


Figure 4.7. Coimmunoprecipitation of Ga2 and 14-3-3 proteins. A. Co-IP of Ga2-wt, Ga2-S113A and Ga2-S113D in MYC2 cells, where IP was performed with anti-Ga2 antibody followed by immunoblotting with 14-3-3 antibody. The first line is the input corresponds to ~10% of the total volume used for the Ga2 pull-down step. The second line represents the total 14-3-3 in lysate that incubated with the beads and antibodies B. Reverse Co-IP of Ga2(S113A)-YFP and Ga2(S113D)-YFP, where IP was performed with 14-3-3 antibody and then precipitates were blotted with anti-Ga2 antibody. The first line is the input corresponds to ~10% of the total volume used for the 14-3-3 pull-down step. The second line represents the total Ga2-YFP in lysate that incubated with the beads and antibodies C. The graph represents the average (%) of the band intensity of 14-3-3, normalized to the total input (100%) of three independent experiments \pm SD. D. represents the average (%) of the band intensity of Ga2-YFP, normalized to the total input (100%) of three independent experiments \pm SD (t -test $^{**}p < 0.01$, $^{***}p < 0.0001$).

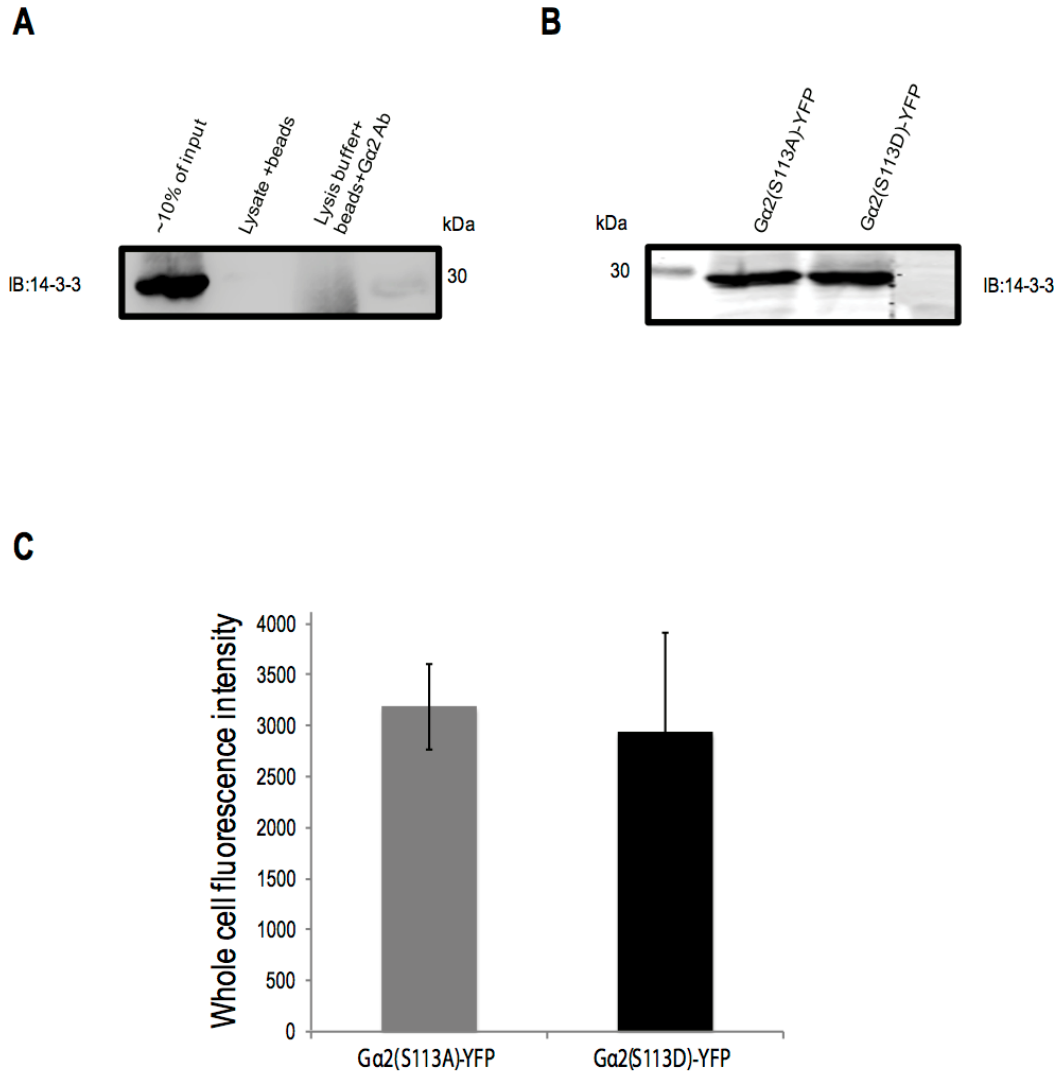


Figure 4.8. Expression level of 14-3-3's, Gα2 (S113A)-YFP and Gα2 (S113D)-YFP. A. The blot shows Co-IP controls of Gα2-wt expressing cells. The first line represents the level of the 14-3-3's in 10% of the lysate input that generated as described in MATERIALS AND METHODS. The second line represents the lysate that incubated with the beads only, and the third line represent the lysis buffer that incubated with beads and anti-Gα2 antibody. B. The level of the 14-3-3's in 10% of the lysate input of Gα2 (S113A)-YFP and Gα2 (S113D)-YFP expressing cells. C. The average of the expression level of Gα2 (S113A)-YFP and Gα2 (S113D)-YFP in whole cells ($\sim 1 \times 10^7$ cells). The fluorescence intensity detected by plate reader. The graph represent the average of three independent experiments \pm SD. The difference was not significant (t test P=0.35)

4.2.5 Phosphorylation of Gα2 Regulates Myosin II Filament Dynamic in the Polarized Cells

In *D.discoideum*, myosin II has a major role in regulating cell chemotaxis (Heid et al., 2004). cAMP stimulation of starved *D.discoideum* cells leads to myosin II filament formation in the cell cortex. Activation of specific kinases stimulate myosin II disassembly in the front of the polarized cells while keep assembled filaments protected in the back of the cells to maintain cell polarization during the chemotactic response (Abu-Elneel et al., 1996; Silveira et al., 1998; Chung and Firtel, 1999) . The precise regulatory mechanism for myosin II assembly/disassembly is not fully understood. Recent study confirmed that 14-3-3s binds myosin II in vegetative cells (Zhou et al., 2010). Since an interaction between phosphorylated Gα2 and 14-3-3s has been observed during cell development, we investigated whether Gα2 phosphorylation could have a potential regulatory role on myosin II assembly in polarized cells.

Immunostaining of myosin II in cells expressing Gα2(wt)-YFP, Gα2(S113A)-YFP and Gα2(S113D)-YFP was applied. Cells were starved for 4-5hr on glass coverslip in DB buffer, fixed and stained with antibody targeted to myosin II as described in Material and Methods section. As previous studies confirmed, our data showed that myosin II filaments accumulate in the back of the polarized cells that express Gα2(wt)-YFP (Figure 4.9A-C). Cells expressing Gα2(S113A)-YFP showed a decrease of myosin II filament disassembly in the front of the polarized cells and became indistinguishable from the myosin II filaments in the back (Figure 4.9D-F).However, cells expressing Gα2(S113D)-YFP showed high level of Myosin II filaments in the back of the cells (Figure 4.9G-I) and the difference between the back and the front is significant (Figure

4.9.l). These data suggested that Ga2 phosphorylation regulates directly/indirectly myosin II assembly/disassembly in polarized cell.

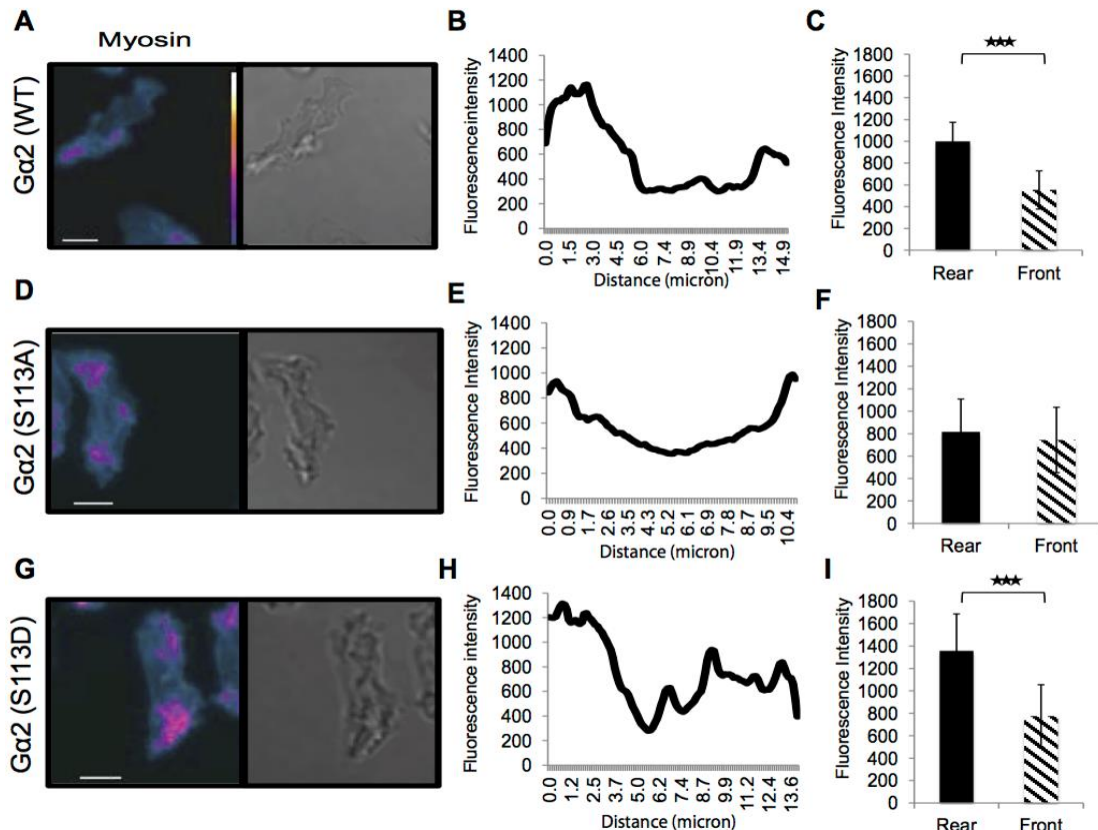


Figure 4.9. Immunostaining of myosin II in polarized *Dictyostelium* cells. Cells were allowed to attach to glass coverslips and then starved in DB for 4 to 5 hr followed by PFA fixation, permeabilization and myosin II staining as indicated in Material and Methods section. Images were taken with a confocal microscope. Every confocal Z stacks were then converted to average intensity projection view using the Z-Project of FIJI before they analyzed. A. Myosin II localization in MYC2 cells expressing Ga2(wt)-YFP. B. Line plot of Myosin II staining intensity across the cell from the back to the front for the cell presented in A. C. The graph shows the average of myosin II staining intensity \pm SD for 1.5um in the back vs 1.5 μ m in the front for MYC2 cells expressing Ga2(wt)-YFP (n=23). D. Myosin II localization in MYC2 cells expressing Ga2(S113A)-YFP. E. Line plot of myosin II staining intensity across the cell from the back to the front for the cell presented in D. F. Graph shows the average of Myosin II staining intensity \pm SD for 1.5 μ m in the back vs 1.5 μ m in the front for MYC2 cells expressing Ga2(S113A)-YFP (n=39). G. Myosin II localization in MYC2 cells expressing Ga2(S113D)-YFP. H. Line plot of myosin II staining intensity across the cell from the back to the front for the cell presented in G. I. The graph shows the average of Myosin II staining intensity \pm SD for 1.5 μ m in the back vs 1.5 μ m in the front for MYC2 cells expressing Ga2(S113D)-YFP (n=44).

CHAPTER 5

MEMBRANE DISTRIBUTION AND CLUSTERING OF ACTIVATED AND PHOSPHORYLATED G α 2

5.1 Background and Hypothesis

Protein cellular localization and posttranslational modifications are considered two key elements for precise signal transduction. Although localization of many signal-related molecules in the plasma membrane (PM) is necessary for their function, it is widely accepted that membrane-associated proteins are non-randomly distributed. PM is well known to be heterogeneous and partitioned into compartments by the actin cytoskeleton, where the membrane proteins fluctuate between fast random motion (Brownian motion) and slow diffusing due to molecular interactions /complexes formation. Clustering or complex formation of membrane molecules in membrane domain is a general phenomenon that has been observed in many cell types. Although this has been an active area of research for more than two decades, the reasons behind the formation of protein clusters or factors may involve in their regulation and stabilization are still not fully understood. Membrane lipids, receptors clusters and adapters proteins all are factors proposed in regulation of membrane-associated protein microclusters (Bunnell et al., 2002; Campi et al., 2005; Cebecauer et al., 2009; Cebecauer et al., 2010; Douglass and Vale, 2005). The formation of membrane protein clusters has been shown to be crucial for their functions. The small GTPase protein, Ras, which serves as a master regulator of signaling pathways involved in many cellular processes was detected by transmission electron microscopy (TEM) to form nanoclusters in the inner- leaflet of PM (Murakoshi et al., 2004; Prior et al., 2003). Stimulation of

lymphocytes causes T- and B-cell receptors to form microclusters with nearby signaling molecules in the plasma membrane. Lck Src-family tyrosine kinase is recruited to phosphorylate TCR clusters. Then, a second kinase, Zap70 is recruited to that clusters in order to phosphorylate linker for activation of T cells (LAT), an adaptor molecule for downstream signaling. Moreover, Syntaxins 1 and 4 have been found to form different clusters and Paxline was shown to form clusters in living cells as well.

Although various methods including biochemical techniques have been used to study this dynamic phenomenon of membrane protein clustering, the conclusion of the data was missing precise quantification. Diffraction limited resolution was a strong limitation in fluorescence microscopy, which prevents imaging the precise plasma membrane dynamic structures and details.

The recent development in the super-resolution light microscopy methods provides essential advantages and a strong tool for analyzing complex cellular structures and dynamic properties of protein clusters, which had not been recognized before by any other microscopic tools. Influenza hemagglutinin (HA) protein membrane dynamic clustering is one example of well-studied protein by super resolution microscopy. It has been shown that membrane distribution and clustering of HA protein is crucial for the protein function to mediate membrane fusion and entry of influenza virus (White et al., 1982; Takeda et al., 2003; Hess et al., 2006; Hess et al., 2007). However, there is no single reason for protein cluster formation or a specific factor involved in this dynamic that has been proposed to date. Previous studies in this area show different effects of protein clustering, which suggests that it may depend on the individual proteins. Membrane clustering of Ras protein appears to facilitate rapid

propagation of receptor signals to downstream effectors while lymphocytes T and B receptors microclusters were expected to sustained signaling that is required for lymphocyte differentiation (Yokosuka et al., 2005; Depoil et al., 2008).

Early evidence suggested that the actin cytoskeleton acts to restrain plasma membrane proteins by forming fences in the plasma membrane that hold transmembrane proteins. This is not the case with syntaxins clustering, where inhibiting actin cytoskeleton did not change the motility of the protein; however, it was affected by cytoplasmic SNARE motifs deletion instead (Sieber et al., 2007).

In *Dictyostelium*, Gα2 is essential for cell chemotaxis and development life cycle via transducing the signal from membrane receptor to the downstream effectors. No evidence has been described yet about their membrane organization and the factors being involved. Our previous work using cell fractionation and gradient density centrifugation indicated that Gα2 membrane-distribution is ligand-dependent mechanism (Alamer , Kageyama , Gundersen, 2018). Since activated Gα2 undergo phosphorylation (Gundersen and Devreotes, 1994), we hypothesized that Gα2 phosphorylation may be involved in membrane distribution and clustering of Gα2. This hypothesis was tested using both cell fractionation and super-resolution FPALM imaging.

5.2 Results

5.2.1 Gα2 Phosphorylation Regulates its Membrane Distribution Pattern

To further examine how phosphorylation might control membrane distribution of Gα2, cell fractionation and density gradient centrifugation was applied for Gα2(S113A)-YFP and Gα2(S113D)-YFP. Since our previous study detected a significant change in membrane distribution and microdomain localization of G protein after cAMP stimulation, we asked whether phosphorylation of Gα2 could contribute in this distinctive distribution. As described in Material and Methods, 17,000 xg pellet fractions were sonicated and subjected to Optiprep density gradient centrifugation. Five fractions (5%, L(low-density fraction), 20%, 35%, and 45% were collected and analyzed for fluorescence intensity using a microplate reader. Similar to the inactive Gα2(wt)-YFP, the quantitative analysis shows that $59 \pm 6\%$ of Gα2(S113A)-YFP is located in the low-density fraction (Figure 5.1A). Treatment of these cells with either 2 mM caffeine or 10 μM cAMP for 1 min did not change the Optiprep distribution of Gα2(S113A)-YFP (Figure 5.1B). This suggests that low-density fraction localization of Gα2(S113A)-YFP is independent of an activation/deactivation dynamic. In comparison, just $32 \pm 6\%$ of Gα2(S113D)-YFP was found in the low-density fraction and a higher proportion in the 20% fraction (Figure 5.1A). Gα2(S113D)-YFP cells treated with 2 mM caffeine showed even further increase in 20% fraction (Figure 5.1C). These data suggest that the shifting of the activated Gα2-wt out of the low-density fraction (L) observed in our previous study (Alamer, Kageyama, Gundersen, 2018) is phosphorylation-dependent.

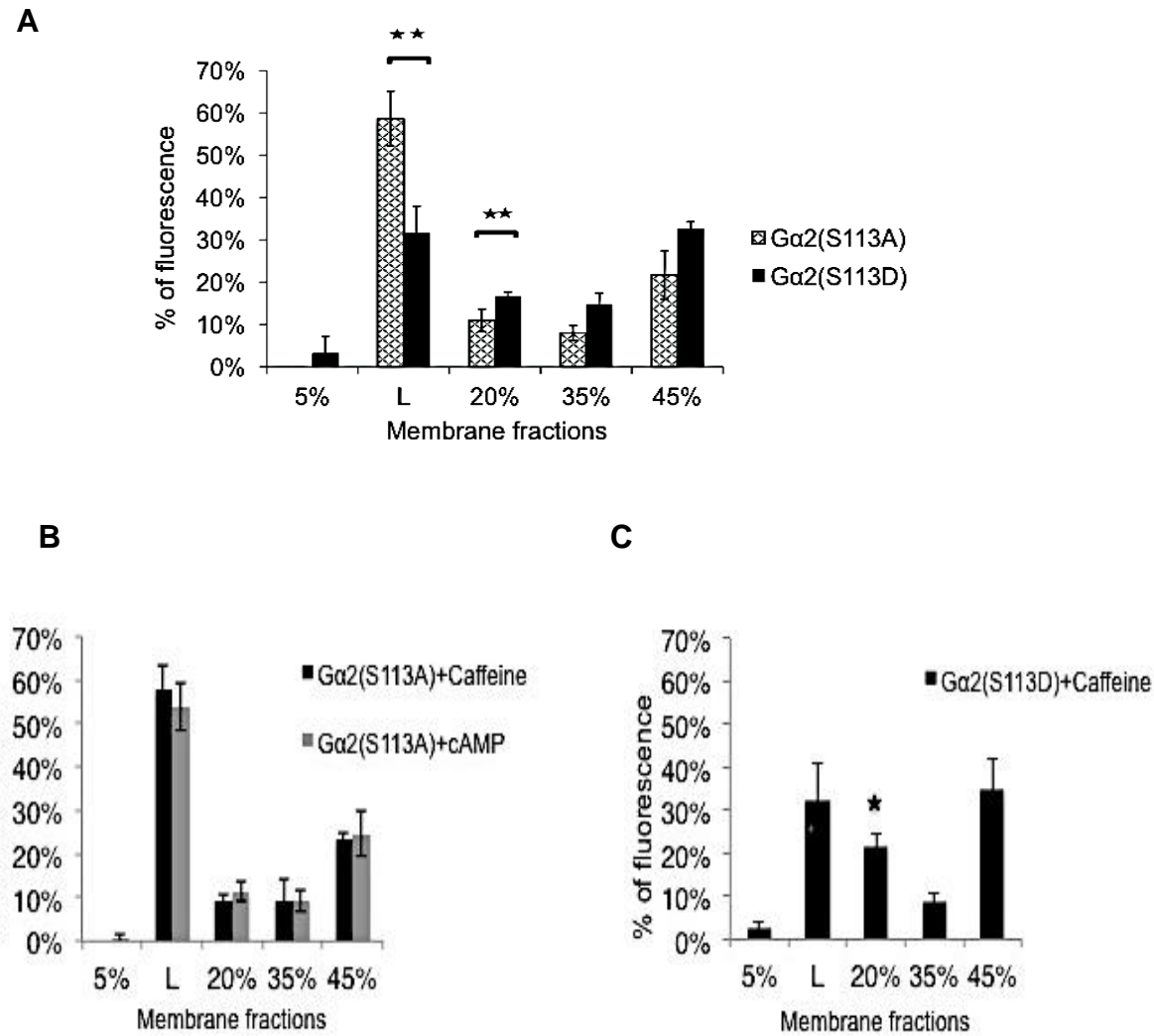


Figure 5.1. Membrane distribution of Ga2(S113A)-YFP and Ga2(S113D)-YFP. The pellet fraction (membrane fraction) subjected to OptiPrep gradient centrifugation as described in the MATERIALS AND METHODS. 50 μ l from each fraction was mixed with an equal volume of base buffer and the fluorescence was detected by a plate reader. The graphs represent the average of three independent experiments \pm SD. L: low density fraction. A. Membrane distribution of Ga2(S113A)-YFP and Ga2(S113D)-YFP in untreated cells (t -test ** p < 0.01). B. Ga2 (S113A)-YFP expressing cells were treated with caffeine for 15 min after starvation or stimulated with 10 μ M cAMP in lysis buffer for 1 min before they lysed. C. Ga2 (S113D)-YFP expressing cells were incubated with caffeine for 15 min after starvation before they lysed (* p < 0.05 compared with the untreated cells)

5.2.2 Membrane Clustering of Ga2 Using High-Resolution Fluorescent Photoactivation Localization Microscopy (FPALM) Imaging.

The distribution pattern of the Ga2 in the low density fraction that was detected using cell fractionation technique and density gradient centrifugation led us to hypothesize that phosphorylation may regulate Ga2 clustering in the plasma membrane in order to control signaling. Although a significant amount of information has been generated using such biochemical techniques, there is still a need of precise details to better understand the distribution of Ga2 and how it is regulated by phosphorylation at a single molecule level in the plasma membrane of a single cell instead of averaging the data from a large number of cells. This study took the advantage of super resolution FPALM to further our knowledge of Ga2 membrane clustering. In *Dictyostelium*, using FPALM is a new and unique technique capable of testing the indicated hypothesis. FPALM enhances the resolution by imaging only a small subset of molecules in the sample at a given time, which allows each individual molecule to be identified and localized (Hess et al., 2006).

For sample staining, the GFP primary antibody was used with a photoactivatable CAGE 590 dye-conjugated secondary antibody. Fluorescent imaging of Ga2-wt-YFP (green) co-localized with Ga2-wt-YFP stained with GFP primary antibody and Alexa fluor 633 (red) (Figure 5.2 A). The single-color FPALM was acquired using a 405 nm diode laser to activate the labeled molecule and a 561 nm laser to read out active molecules. Both beams were focused at the back aperture of a 60 \times /1.4 NA oil-immersion objective lens and images were taken using total internal reflection fluorescence (TIRF) to minimize the detected background fluorescence. Ten thousand

frames were recorded at ~ 50Hz and 200 EM gain for each data set. More details about FPALM imaging and analysis are described in the Material and Methods section. MYC2 expressing Gα2(wt)-YFP, Gα2(S113A)-YFP or Gα2(S113D)-YFP were starved for 4 to 5hr on glass coverslips, fixed and stained as indicated in the Material and Methods section. For the Gα2(wt)-YFP, cells were treated either with 2mM caffeine for 15 min to block possible activation or stimulated with 10 μM cAMP for 1 min to trigger the signal before PFA fixation. The effect of activation/deactivation and phosphorylation/dephosphorylation on the morphology of Gα2 membrane clusters was examined (Figure 5.3A-B) (Figure 5.4A-B). Clusters were analyzed using single-linkage cluster analysis (SLCA) (Gudheti et al., 2013). Changes in three different parameters including number of clusters per cell, cluster density and cluster area were identified. Specifically, Gα2(S113A)-YFP shows a larger number of clusters per cell compared to the other cell lines (Figure 5.4A). Cluster density of Gα2 was significantly increased in both cAMP stimulated samples and Gα2(S113D)-YFP compare to caffeine treated samples and Gα2(S113A)-YFP, respectively (Figure 5.3D) (Figure 5.4D). Cluster area of Gα2 was increased in cAMP stimulated samples compared to the caffeine treated sample, though differences were not significant at the P=0.05 level (Figure 5.3C). However, no change was detected in cluster area between Gα2(S113A)-YFP and Gα2(S113D)-YFP (Figure 5.4C).

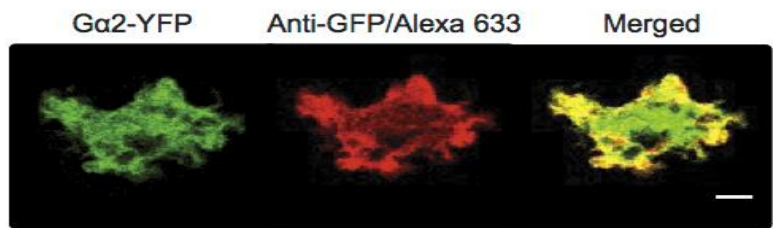
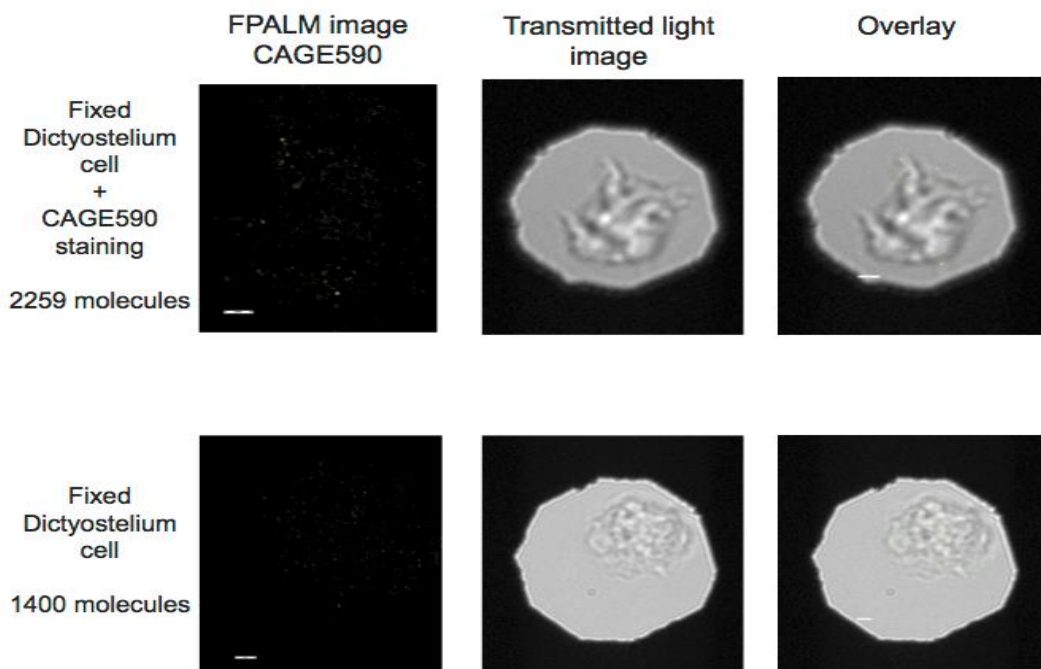
A**B**

Figure 5.2. Proper controls for FPALM imaging. A. Gα2 (wt)-YFP expressing cells were allowed to attach to the glass coverslips and then starved in DB buffer for 4-5 hr. Cells were then fixed and permeabilized as described in MATERIALS AND METHODS. Samples were then stained with anti-GFP rabbit antibody followed by anti-rabbit secondary antibody coupled to Alexa Fluor 633. Scale Bars 5 μm. B. Top panel represents the signal from the negative control for FPALM imaging. Cells were starved as indicated in (A). Cells were then fixed, permeabilized and stained with secondary CAGE590 only. Bottom panel represents the autofluorescence from cells that starved and fixed in similar way to the original samples without immunostaining.

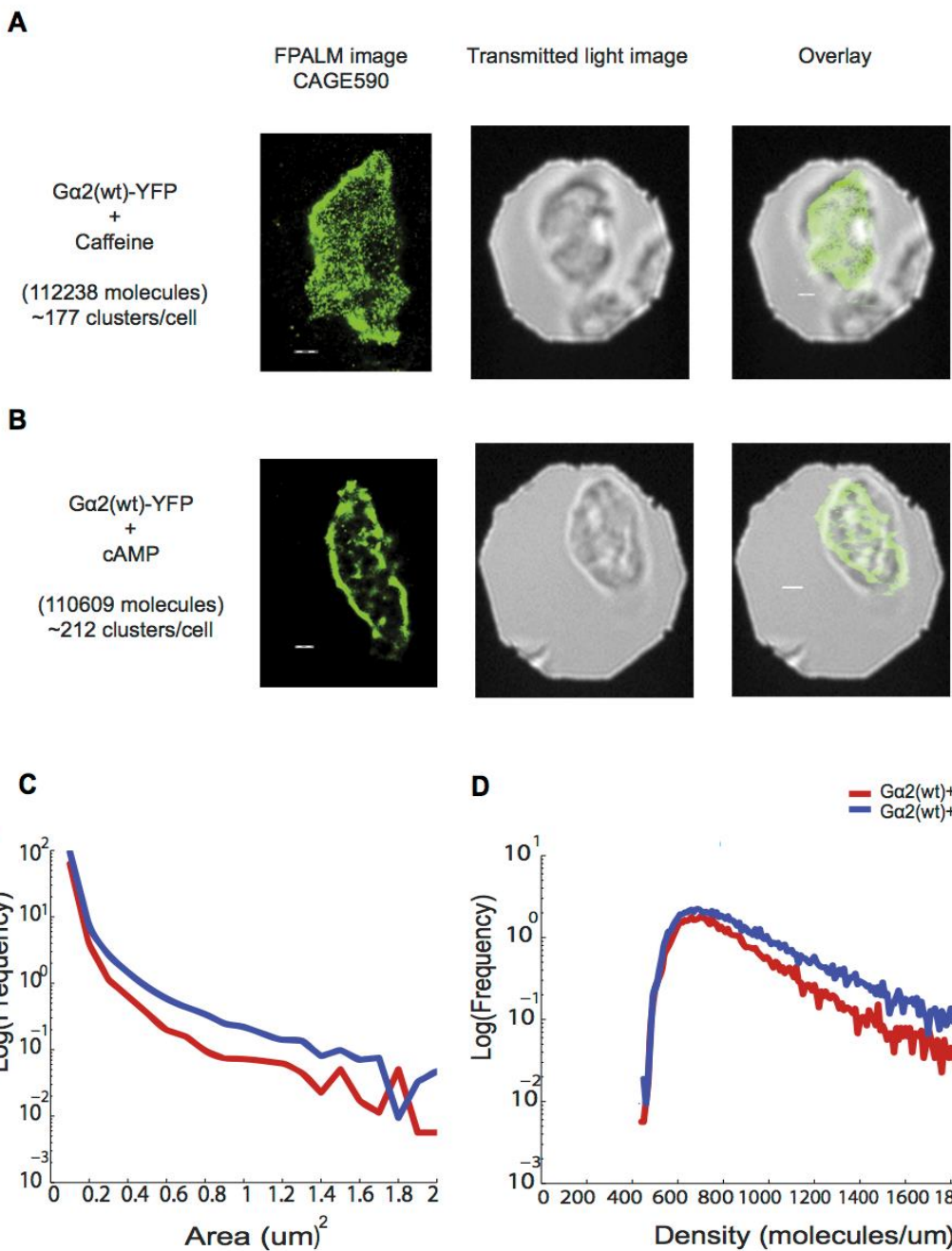


Figure 5.3. Nanoscale membrane cluster morphology of active/inactive Ga₂(wt)-YFP. Membrane clusters of Ga₂(wt) stained with CAGE590 were imaged by single-color FPALM. 7x10⁵ cells were starved on glass coverslip for 4-5hr. Cells were then treated with caffeine for 15 min (A) or stimulated with cAMP for 1 min (B) followed by PFA fixation and staining as described in Material and Methods section. Scale bars are 1 μ m. C. The graph represent the cluster area of in active Ga₂(wt) (red) and active Ga₂(wt) (blue) (P value = 0.05). D. The graph represent the cluster density of in active Ga₂(wt) and active Ga₂(wt) (P value = 0.0001)

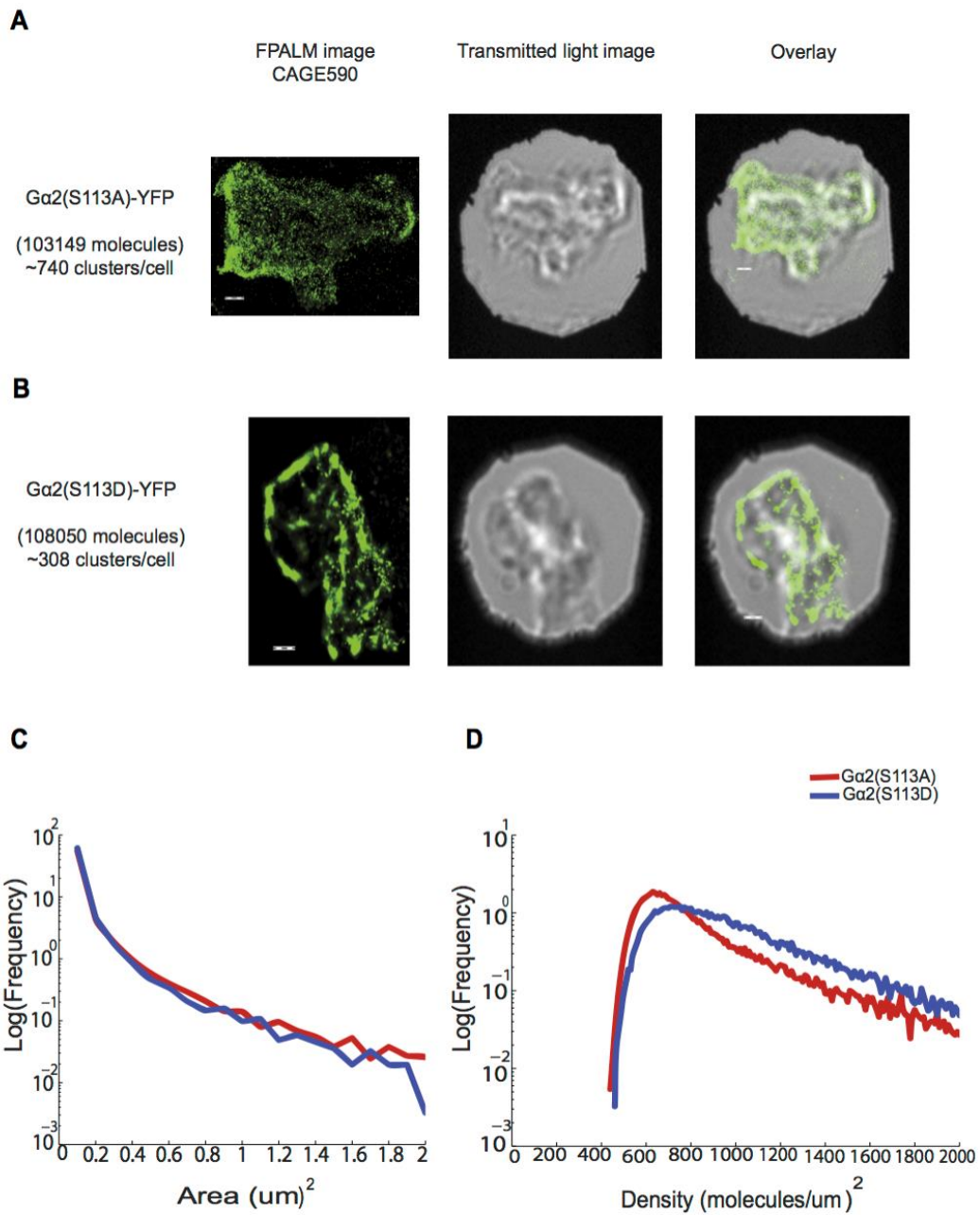


Figure 5.4. Nanoscale membrane cluster morphology of Ga₂(S113A)-YFP and Ga₂(S113D)-YFP. Membrane clusters of Ga₂(S113A)-YFP (A) and Ga₂(S113D)-YFP (B) stained with CAGE590 were imaged by single-color FPALM. 7x10⁵ cells were starved on glass coverslip for 4-5hr. Cells then fixed then stained as described in Material and Methods section. Scale bars are 1μm. C. The graph represent the cluster area of Ga₂(S113A)-YFP(red) and Ga₂(S113D)-YFP(blue) (P value = 0.77). D. The graph represent the cluster density of Ga₂(S113A)-YFP and Ga₂(S113D)-YFP (P value = 0.010)

CHAPTER 6

DISCUSSION

Over the past several decades, directed cell migration has been a major focus in biomedical research due to its importance in many cellular processes, including the migration of neutrophils to the sites of inflammation, organ development during embryogenesis and cancer metastasis. Therefore, understanding the signals that control cell chemotaxis becomes a priority.

In *Dictyostelium discoideum*, the G protein-mediated signal regulates both chemotaxis and its developmental life cycle via the G protein α -subunit, Ga2 (Kumagai et al., 1991). In this study, major factors possibly involved in membrane translocation, clustering and cellular localization of Ga2 were characterized. Based on our observations on Ga2 distribution under various conditions, the presence of cAMP has a significant effect in membrane microdomains localization of Ga2. The Ga2 protein level was decreased in low-density microdomains after cAMP stimulation compared to the caffeine treated sample (Alamer, Kageyama, Gundersen, 2018). This shifting of the Ga2 out of the low-density (L) fraction after cAMP stimulation resulted in a small increase of Ga2 in the 20% fraction.

To further understand the cause of activated Ga2 membrane redistribution, both cAR1 and G β were tested (Figure 3.1). Our data showed that stimulation with cAMP cause a significant increase of cAR1 and G β in the 5% fraction and 45% fraction, respectively compare to the Ga2 (Figure 3.2). This supports our conclusion that translocation of activated Ga2 is independent of cAR1 and/or G β complex. The high

level of cAR1 in the lower density fraction, 5% is evidence of a dynamic membrane distribution of the receptor and the importance of these domains on receptor function. A previous study on a chemokine receptor, a member of the GPCRs family, had shown that after receptor phosphorylation, β -arrestin is recruited to desensitize the receptors by blocking their interaction with G-proteins. Receptor internalization then was initiated via clathrin-mediated endocytosis (Lefkowitz and Whalen, 2004). On the other hand, Jiao et al., 2005, emphasized the critical role of the ligand-induced microdomain partitioning of chemokine receptor as this microenvironment may be necessary for receptor/G protein interaction in delivering precise G-protein-dependent signaling. Our data showed that cAR1 localized in both low-density fraction (L) and 5% fraction, which suggested that each fraction may reflect the specific function of the receptor. The localization of the receptors into the low-density fraction (L) can be necessary for receptor/G protein interaction and the localization into 5% fraction can be necessary for receptor internalization. Additional characterization of the critical role of these domains on cAR1 signal is needed.

In contrast to the membrane distribution of monomer $\text{G}\alpha 2$, a mutation that locks the heterotrimeric even with activation ($\text{G}\alpha 2$, $\text{G}\alpha 2(\text{YFP})$ -G207A) showed poor localization to the plasma membrane and low-density microdomains with most appearing attached to internal membranes. The immunostaining data with the ER marker, calnexin suggests that the 45% fraction contains ER membrane. The accumulation of $\text{G}\alpha 2$ -G207A in the ER can be evidence that a monomeric $\text{G}\alpha 2$ is required for translocation from the ER to Golgi where heterotrimer formation occurs (Michaelson et al., 2002). The trafficking pathway for the heterotrimeric G proteins still

remains unresolved. Our cell fractionation and gradient centrifugation data support a model for G protein trafficking in which active and monomer Ga2 moves from low-density microdomains to heavier membrane microdomains and/or the ER before returning to the Golgi apparatus to bind G β γ , consistent to that described for the small G-protein, H-Ras (Lorentzen et al., 2010).

These data may also address an unresolved observation in G protein signaling in *Dictyostelium*. Activation of Ga2 acts on its downstream effector, phosphatidylinositol-phospholipase C (PLC) with an activity peak around 5-10 seconds. G β γ , on the other hand has an activity peak around 1 to 2 minutes for its activation of adenylyl cyclase (Okaichi et al., 1992). The mechanism responsible for blocking re-association of the heterotrimer thus allowing β γ to function is undefined. Data presented here suggest the possibility that activation of the G protein may cause translocation of Ga2 to a different membrane microdomain before rebinding the G β γ dimer.

Eliminating the contribution of cAR1, G β γ and ligand-dependent microdomains reorganization on membrane dynamic distribution of Ga2 raised the possibility of another factor being involved. Binding of the chemoattractant cAMP to the cAR1 receptor activates Ga2 which also causes its phosphorylation within 1-2 minutes (Gundersen and Devreotes, 1990). Besides Ga2, many mammalian G protein α -subunits that undergo phosphorylation have been identified in the last two decades including Gq, Gi, Gt, Go, Gs, G12/13 and Gz (Chen and Manning, 2001). However, a gap of knowledge regarding the functional significance of such modification still exists.

In this study, we successfully mutated the phosphorylation site (serine 113) and created two constructs, phosphorylation blocked Ga2 (Ga2-S113A) and a

phosphorylation mimic of Ga2 (Ga2-S113D) to gain more understanding of the functional role of this modification. Time-lapsed imaging of developing *Dictyostelium* cells shows that blocking Ga2 phosphorylation led to an early onset to the aggregation of these cells when compared to Ga2-WT and Ga2-S113D. Cell fractionation data shows Ga2-S113A significantly increase in pellet (membranes) fraction compared to the Ga2-wt. A higher presence in the plasma membrane can be reasoned to lead to increased signaling and early aggregation. This suggested that Ga2 phosphorylation stimulates an inhibitory feedback mechanism promoting plasma membrane dissociation of the protein independent of its GTPase activity (Figure 4.5).

Unlike Ga2-S113A, cells expressing Ga2-S113D aggregate in a time similar to the wild type. However, Ga2-S113D culmination was delayed, around 4 hr. Another point of interest is that a number of cells were unable to proceed to the aggregation stage; the reason is still unknown. This can be linked to the cellular localization that has been detected for the Ga2(S113D)-YFP (Figure 4.3). The expression profile of Ga2 in developing *Dictyostelium* cells has two peaks. The first one is in the early development stage and the second one is in the later stages of development (Kumagai et al., 1991). *Dictyostelium* is a common research model has been used to study cellular signals that involved in both chemotaxis and development as most of the regulatory genes are conserved between *Dictyostelium* and mammals. Beside the regulatory role of Ga2 phosphorylation on chemotaxis, it is possible that Ga2 phosphorylation regulates the later stage of development which caused the delay of Ga2(S113D) culmination. However, this assumption has not yet been examined.

Using cell fractionation and density gradient centrifugation, G α 2(S113A)-YFP is seen to accumulate in a low-density membrane fraction independent of the activation/deactivation process. However, G α 2(S113D)-YFP is significantly shifted to a heavier fraction. G protein acts on transducing the signal from the membrane receptor to the downstream effectors. Although their dynamic mechanism of action concentrated in the plasma membrane, there is a lack of knowledge about how the protein behaves in that specific location. Due to the methodological limitation, studying membrane protein can be challenging. In this study we used the advantage of photoactivatable fluorophore CAGE dye and super resolution microscopy technique FPALM for the first time on G protein using *Dictyostelium* cells to further understand the role of activation and phosphorylation. Using this technique is a powerful way to provide information not only about precise membrane localization but also their specific distribution and clustering and if it can be regulated. Super resolution imaging FPALM revealed a unique clustering pattern of the protein under four different conditions, which emphasize the non-random distribution of the protein in the plasma membrane. Cluster analysis suggested that activated and phosphorylated G α 2 tend to form denser clusters in the plasma membrane. This can be critical for their functional dynamic and membrane association as roughly 700 less dense clusters per cell were detected in cells expressing G α 2(S113A)-YFP. A slight change, though not significant, was detected on G α 2 cluster area after cAMP stimulation ($P=0.05$). The activated G α 2 but not G α 2-S113D tended to form bigger clusters. These data suggested that another factor could be involved in this complex dynamic of G protein in plasma membrane.

The role of cytoskeleton in plasma membrane organization has been studied extensively (Kusumi et al., 2012). It has been known that PM compartmentalization is essential for many processes including signal transduction (Jaqaman and Grinstein, 2012). The involvement of actin membrane skeleton in PM compartmentalization is well established (Murase et al., 2004; Kusumi et al., 2012). Also, the contribution of microtubules has been reported (Jaqaman et al., 2011). In *D.discoideum* cells, actin is concentrated in the leading edge of the polarized cell (Yumura and Fukui, 1998). Using latrunculin A to disrupt actin filamentous network causes *D.discoideum* cells to round up and inhibits cell chemotaxis while these cells still could sense a cAMP gradient. It has been shown that, the plasma membrane localization and shuttling of Ga2 were not affected by latrunculin A treatment (Elzie et al., 2009). This did not rule out that the dynamic clustering of Ga2 can be affected. Further studies using super resolution imaging to address this point is needed. The data generated with FPALM imaging is consistent with the cell fractionation and density gradient centrifugation results. The corroborating results for these two disparate biochemical and biophysical techniques provides confidence in the conclusion that Ga2 phosphorylation leads to movement between two different membrane fractions in the cell.

The Ras family of small GTPases is one of the most studied examples of clustered membrane-associated proteins. Their clustering is controlled by distinctive factors including GDP/GTP exchange, post-translational modifications and their hypervariable region (HVR) (Henis et al., 2009; Prior et al., 2003; Tian et al., 2007). After activation, GTP binding to Ras protein immobilized the protein which led to the suggestion of that large activated complexes were formed (Murakoshi et al., 2004). Two

types of Ras clusters have been identified: cholesterol-sensitive and cholesterol-independent (Henis et al., 2009). Any disruption of Ras membrane-clustering abolishes the downstream signaling (Cho, 2006; Plowman et al., 2005; Tian et al., 2007). Using fluorescence recovery after photobleaching (FRAP) and electron microscopy to study the clustering of dually palmitoylated H-Ras revealed that exchange of GDP for GTP decreases cholesterol-sensitive clusters allowing the hypervariable linker domain to form the cholesterol-independent clusters of the protein which in turn provides precise RAS signal (Rotblat et al., 2004). Ras protein share a structural similarity and common mechanisms with G α subunit (Gerwert et al., 2017). Our data show different density clustering for nonphosphorylated and phosphorylated G α 2. It remains unknown if the heterotrimeric G protein clusters seen here are similar to those seen with Ras. Data presented here suggested that the phosphorylation site of the G protein may work in a manner similar to the HVR region of Ras, which influences the formation of the cholesterol-independent clustering. It has been proposed that the increased local concentration of proteins by cluster formation increases the likelihood of interaction between pathway components and thus speeds up the pathway output (Cebecauer et al., 2010). Once this clustering occurs, any positive feedback signal may keep clusters intact independent of external stimulus. Thus, transiently induced clustering can become more stable in the presence of external or internal fluctuations and provide high-fidelity signaling (Harding and Hancock., 2008)

Work by Douglass and Vale (2005) showed that protein-protein interaction can facilitates the formation and stabilization of membrane protein clustering. Within the last two decades, the active role of scaffolding proteins in regulating cell signaling has

started to emerge (Good et al., 2011; Garbett and Bretscher, 2014). The role of scaffolding proteins has been detected in many signaling pathways including G protein-based signaling (Andreeva et al., 2007). Many scaffolding proteins have been identified in the recent years. In this study, the involvement of 14-3-3 as a scaffold protein for Ga2 subunits was examined. The large number (~700) of less dense clusters per cell for the Ga2(S113A)-YFP support our expectation of the existing of scaffolding proteins that are phosphorylation dependent. The 14-3-3 proteins are a family of conserved regulatory proteins that act as phosphoprotein-interacting proteins. They bind phosphorylated serine or threonine and participated in many phosphorylation-based signaling pathways (Smith et al., 2011). *Dictyostelium* presents an advantage in that they contain just one isoform of 14-3-3 compared to seven in mammalian cells. Co-immunoprecipitation detected an interaction between activated and phosphorylated Ga2 with 14-3-3. Although, the results estimate that only 8% of the total 14-3-3 protein interacts with activated and phosphorylated Ga2, this could be very significant knowing that only 10% of 14-3-3 is detected in the membrane fraction (Zhou et al., 2010). However, the reciprocal interaction detected 82% of phosphorylated Ga2 interacting with 14-3-3. The interaction between 14-3-3s and the regulator of G protein signaling proteins (RGSs) is well established. Benzing and his colleagues (2000) detected around 70% of RGS3 interact with 14-3-3, while only 15% of 14-3-3 that form a complex with RGS3. Since co-immunoprecipitation can also detect indirect interaction, there is a possibility of the complex that was detected in this study is through an intermediary binding of RGS. Thereby 14-3-3s may serve as scaffolding protein to bind the phosphorylated G protein with the specific RGS to modulate their activity and regulate the signal. Little is known

about the specific RGS that regulates Ga2 function; however, Sun and Firtel (2003) have identified a novel RGS domain-containing protein kinase (RCK1) that interacts with Ga2 after cAMP stimulation to attenuate the signal. Similar to Ga2-S113A, rck1 null cells aggregate faster than wild-type cells (Sun and Firtel, 2003), suggesting that block the phosphorylation of Ga2 may prevent RGS binding.

Fluorescence colocalization results support the conclusion of 14-3-3 protein and Ga2 interaction, as these two proteins were significantly colocalized under phosphorylation and activation conditions. Previously, it has been shown that 14-3-3 is localized mainly in the cell cortex (Zhou et al., 2010). However, cell cortex localization of 14-3-3 was dramatically decreased in Ga2(S113D)-YFP expressing cells compared to the other cell lines. It may also be implied that 14-3-3 plays a role in the translocation of phosphorylated Ga2 from the plasma membrane to the internal membrane as demonstrated previously with small G proteins Rnd3 (Rio et al., 2013).

In 2010, Zhou and his colleagues detected an interaction between 14-3-3 and myosin II to regulate its distribution and assembly in vegetative *Dictyostelium* cells (Zhou et al., 2010). Since an interaction between phosphorylated Ga2 and 14-3-3 has been detected, a possible regulation between Ga2 phosphorylation and myosin II may exist. The defect of cell streaming in Ga2(S113A)-YFP expressing cells (Figure 3.1C) strongly suggested a defect in cytoskeleton regulation. Immunostaining for myosin II mirrors this observation. Myosin II filaments were equally distributed in the front and the back of cells expressing Ga2-S113A (Figure 4.9), unlike Ga2-wt and Ga2-S113D expressing cells, which show a polarized myosin II distribution in the back end of migrating cells

The regulation of myosin II assembly during chemotaxis is not fully understood. Cyclic-AMP stimulation leads to increased myosin II filament formation in the cell cortex, reaching a peak in 30s and returning to basal level in 120s (de la Roche and Cote., 2001). Phosphorylation of G protein has been detected within 1 to 2 min after cAMP stimulation (Gundersen., 1997). Few studies reported the important role of cGMP signal in myosin II regulation. Cycle GMP level peaks at 10s after cAMP stimulation and returns to the basal levels within 40s (Liu and Newell., 1988). As cGMP level increase, myosin II translocates to the cell cortex (Liu et al., 1993; Liu and Newell., 1994). Also, increased cGMP level stimulates MHC kinases activity (Dembinsky et al., 1996). The action of MHC kinases leads to myosin II filaments disassembly, returning it to the cytosol. Three well-studied kinases have a functional significance in such regulation including myosin II heavy chain kinase A (MHCK A), Myosin II heavy chain-protein kinase C (MHC-PKC) and *Dictyostelium* PAKa, a member of the family of p21-activated kinases. MHCKA translocates to the cell cortex within 40s after cAMP stimulation and it is locally activated at the front of migrating cells, which lead to the myosin II disassembly in that area (Steimle et al., 2001). MHC-PKC translocate to the plasma membrane within 30s after cAMP stimulation and returns to the cytosol after 120s. Similar to the MHCKA, MHC-PKC acts on phosphorylation of MHC in the cell's leading edge (Dembinsky et al., 1996; Abu-Elneel et al., 1996). It has been shown that MHC-PKC binds 14-3-3 in the cytosolic fraction and this binding inhibit MHC-PKC activity (Matto-Yelin et a., 1997). However, PAKa translocates to the back of the cell cortex after cAMP stimulation and its activation inhibits the activity of MHCKA and MHC-PKC in the back which lead to delay of MHC phosphorylation in the back which in turn

resulting in the polarization of migrated cells. PAKa null cells have similar distribution of myosin II as Ga2S113A, however the development phenotype for both cell line is different (Chung and Firtel., 1999). Moreover, cAMP stimulation causes the translocation of PAKa to the cell cortex within 10s and return to the cytosol after 60s which is in the same time that Ga2 is being phosphorylated which likely excludes a possible regulation between PAKa and phosphorylated Ga2 (Chung and Firtel., 1999). Similar to the PAKa, both MHCKA and MHC-PKC act on myosin II regulation at the plasma membrane before phosphorylation of Ga2. Based on this regulation time, the myosin II distribution in Ga2S113A suggested that either the Ga2 signal in these cells persists longer resulting in increased cGMP and dysregulation of kinases activity and myosin II disassembly. Or, it is a sign of a new regulatory pathway of myosin II assembly/disassembly that is controlled directly or indirectly by Ga2 phosphorylation.

Our data support a model for Ga2 mode of action in the plasma membrane (Figure 6.1) whereby dense clusters of activated and phosphorylated Ga2 regulate the time-course of signaling which in turn leads to precise signaling that involves myosin II regulation. This model provides a new perspective on the dynamic membrane organization of Ga2, clusters function and regulation. However, evaluating the lifetime of Ga2 membrane clusters, stabilization mechanism and the involvement of membrane lipids in this dynamic are all important aspects for future investigation. In addition, still to be discovered are the protein kinase and specific phosphatase responsible for catalyzing Ga2 phosphorylation/dephosphorylation. Understanding of the catalytic mechanism of these reactions and how they are implicated in Ga2 membrane organization will move the field forward.

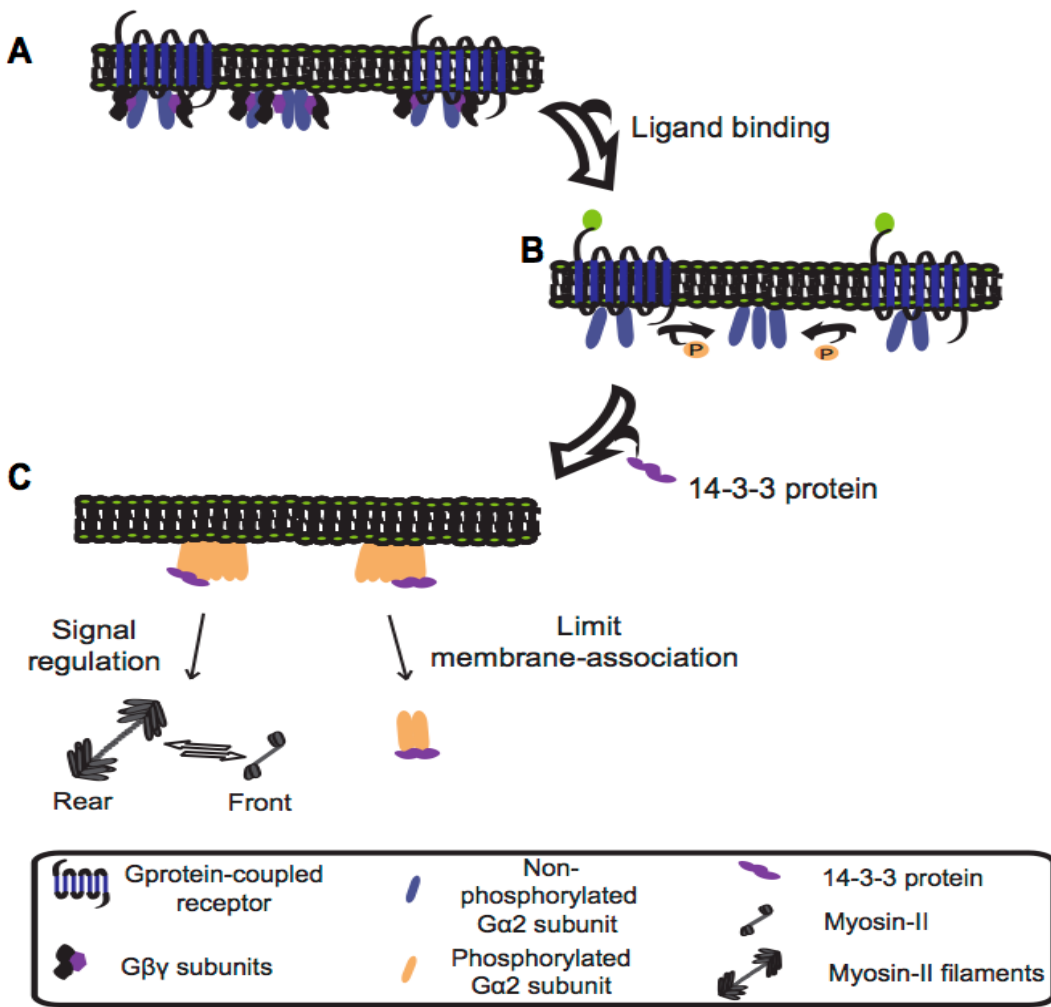


Figure 6.1. Model of G α 2 plasma membrane clustering. A. Represents membrane cluster pattern of the inactive/non-phosphorylated G α 2 where proteins tend to form more of the less dense clusters in the plasma membrane. B. Ligand binding to the receptor will initiate the phosphorylated state of G α 2 which (C) promotes the formation of denser clusters, decreasing the number of clusters per cell and facilitating an interaction with 14-3-3 protein. These dense clusters are critical to ensure precise signal regulation presented in Myosin II filaments disassembly in the front of the polarized cells as well as regulate the time-course of signaling by limiting plasma membrane association of G α 2.

REFERENCES

- Abu-Elneel K, Karchi M, Ravid S. Dictyostelium myosin II is regulated during chemotaxis by a novel protein kinase C.J. Biol. Chem.1996;271: 977-984.
- Alamer S, Kageyama Y, Gundersen RE (2018). Localization of palmitoylated and activated G protein α -subunit in *Dictyostelium discoideum*. Journal of Cellular Biochemistry.
- Alexander NS, Preininger AM, Kaya AI, Stein RA, Hamm HE, Meiler J. Energetic analysis of the rhodopsin-G-protein complex links the α 5 helix to GDP release. Nat Struct Mol Biol. 2014;21:56–63.
- Andreeva AV, Kutuzov MA, Voyno- Yasenetskaya TA. Scaffolding proteins in G-protein signaling. Journal of molecular signaling. 2007; 2: 13.
- Aragay AM, Quick MW. Functional regulation of Ga16 by protein kinase C. J Biol Chem.1999; 274:4807–4815.
- Axelrod D, Koppel DE, Schlessinger J, Elson E, Webb WW. Mobility measurement by analysis of fluorescence photobleaching recovery kinetics. Biophys J. 1976;16:1055–1069.
- Bagorda A, Mihaylov VA, Parent CA. Chemotaxis: moving forward and holding on to the past. *Thromb. Haemost.* 2006; 95:12-21.
- Baldwin JM. Structure and function of receptors coupled to G proteins. Curr Opinion Cell Biol. 1994;6:180–190.
- Baumgart T, Hess ST, Webb WW. Imaging coexisting fluid domains in biomembrane models coupling curvature and line tension. Nature. 2003; 425: 821–824.
- Benzing T, Yaffe MB, Arnould T, Sellin L, Schermer B, Schilling B, Schreiber R, Kunzelmann K, Leparc GG, Kim E et al. 14-3-3 interacts with regulator of G protein signaling proteins and modulates their activity. J. Biol. Chem. 2000;275: 28167-28172.
- Berman DM, Wilkie TM, Gilman AG. GAIP and RGS4 are GTPase-activating proteins for the Gi subfamily of G protein alpha subunits. Cell. 1996;86:445–452.
- Bosgraaf L, van Haastert PJ. The regulation of myosin II in Dictyostelium. Eur. J. Cell Biol. 2006;85: 969-979.
- Bravo-Cordero J, Hodgson L, Condeelis J. Spatial regulation of tumor cell protrusions by RhoC. Cell adhesion and migration. 2014;8(3).
- Brenner M, Thoms SD. Caffeine blocks activation of cyclic AMP synthesis n *Dictyostelium discoideum*. Dev Biol. 1984;101:136-46.

Bretschneider T, Othmer HG, Weijer CJ. Progress and perspectives in signal transduction, actin dynamics, and movement at the cell and tissue level: lessons from *Dictyostelium*. *Interface Focus*. 2016; 6:20160047.

Brewster R, Pincus SA , Safran PA. Hybrid lipids as a biological surface-active component, *Biophys. J.* 2009; 97:1087–1094.

Bunnell SC, Hong DI, Kardon JR, Yamazaki T, McGlade CJ, Barr VA, Samelson LE. T cell receptor ligation induces the formation of dynamically regulated signaling assemblies. *J. Cell Biol.* 2002;158:1263–1275.

Cai H., Katoh-Kurasawa M., Muramoto T., Santhanam B., Long Y., et al. , Nucleocytoplasmic shuttling of a GATA transcription factor functions as a development timer. *Science*. 2014; 343: 1249531.

Campi G, Varma R, Dustin ML. Actin and agonist MHC-peptide complex- dependent T cell receptor microclusters as scaffolds for signaling. *J. Exp. Med.* 2005; 202:1031-1036.

Carlier MF, Pernier J, Montaville P, Shekhar S, Kuhn S. Control of polarized assembly of actin filaments in cell motility. *Cell Mol. Life Sci.* 2015;72:3051–3067.

Caterina MJ, Hereld D, Devreotes PN. Occupancy of the *Dictyostelium* cAMP Receptor, cAR1, Induces a Reduction in Affinity Which Depends upon COOH-terminal Serine Residues *J. Biol. Chem.* 1995; 270: 4418–4423.

Cebecauer M, Owen DM, Markiewicz A, Magee AI. Lipid order and molecular assemblies in the plasma membrane of eukaryotic cells. *Biochem. Soc. Trans.* 2009; 37:1056-1060.

Cebecauer M, Spitaler M, Sergé A, Magee AI. Signalling complexes and clusters: functional advantages and methodological hurdles. *Journal of Cell Science*. 2010;123: 309-320.

Chan RK, Otte CA. Isolation and genetic analysis of *Saccharomyces cerevisiae* mutants supersensitive to G1 arrest by a factor and alpha factor pheromones. *Mol Cell Biol.* 1982a;2:11–20.

Chan RK, Otte CA. Physiological characterization of *Saccharomyces cerevisiae* mutant supersensitive to G1 arrest by a factor and alpha factor pheromones. *Mol Cell Biol.* 1982b; 2:21–29.

Charras G, Paluch E. Blebs lead the way: how to migrate without lamellipodia. *Nat Rev Mol Cell Biol.* 2008;9:730–736.

Chen CA, Manning DR. Regulation of G proteins by covalent modification, *Oncogene*. 2001;20:1643-1652.

Chen MY, Devreotes PN, Gundersen RE. Serine-113 is the Site of Receptor-Mediated Phosphorylation of the *Dictyostelium* G Protein α -subunit, Ga2. J. Biol. Chem. 1994;269: 20925-20930.

Cherezov V, Rosenbaum DM, Hanson MA, Rasmussen SG, Thian FS, Kobilka TS, Choi HJ, Kuhn P, Weis WI, Kobilka BK, Stevens RC. High-resolution crystal structure of an engineered human regulation β 2-adrenergic G protein-coupled receptor. Science. 2007;318:1258–1265.

Chini B, Parenti M. G-protein-coupled receptors, cholesterol and palmitoylation: facts about fats. J Mol Endocrinol. 2009; 42: 371-379.

Chung CY, Firtel RA. PAKa, a Putative PAK Family Member, Is Required for Cytokinesis and the Regulation of the Cytoskeleton in *Dictyostelium discoideum* Cells during Chemotaxis. The Journal of Cell Biology. 1999; 147:559-575.

Clainche L, Carlier MF. Regulation of actin assembly associated with protrusion and adhesion in cell migration. Physiol. Rev. 2008;88:489–513.

Clarke M, Kayman SC, Riley K. Density-dependent induction of discoidin-I synthesis in exponentially growing cells of *Dictyostelium discoideum*. Differentiation. 1987;34: 79-87.

Dan N, Pincus P, Safran SA. Membrane-induced interactions between inclusions. Langmuir. 1993; 9: 2768–2771.

Davis TL, Bonacci TM, Sprang SR, Smrcka AV. Structural and molecular characterization of a preferred protein interaction surface on G protein beta gamma subunits. *Biochemistry*. 2005; 44: 10593-10604.

De Keijzer S, Sergé A, van Hemert F, Lommerse P, Lamers G, Spaink H, Thomas Schmidt T, Snaar-Jagalska EA. spatially restricted increase in receptor mobility is involved in directional sensing during *Dictyostelium discoideum* chemotaxis. Journal of Cell Science. 2008;121:1750-1757.

De Keijzer S, Sergé A, van Hemert F, Lommerse P, Lamers G, Spaink H, Thomas Schmidt T, Snaar-Jagalska EA. spatially restricted increase in receptor mobility is involved in directional sensing during *Dictyostelium discoideum* chemotaxis. Journal of Cell Science. 2008;121:1750-1757.

De la Roche MA, Coate GP. Regulation of *Dictyostelium* Myosin I and II. Biochimica et Biophysica Acta. 2001;1525: 245-261.

Dembinsky A, Rubin H, Ravid S. Chemoattractant-mediated increases in cGMP induce changes in *Dictyostelium* myosin II heavy chain-specific protein kinase C activities, J. Cell Biol. 1996;134:911-921.

Depoil D, Fleire S, Treanor BL, WeberM, Harwood NE, Marchbank KL, Tybulewicz VL, Batista FD. CD19 is essential for B cell activation by promoting B cell receptor-antigen microcluster formation in response to membrane-bound ligand. *Nat. Immunol.* 2008;9: 63-72.

Devreotes P, Horwitz AR. Signaling Networks that Regulate Cell Migration. *Cold Spring Harb Perspect Biol.* 2015;7:a005959

De Vries L, Zheng B, Fischer T, Elenko E, Farquhar MG. The regulator of G protein signaling family. *Annu Rev Pharmacol Toxicol.* 2000; 40:235–271.

Douglass AD, Vale RD. Single-Molecule Microscopy Reveals Plasma Membrane Microdomains Created by Protein-Protein Networks that Exclude or Trap Signaling Molecules in T Cells. *Cell.* 2005; 121(6): 937–950

Drayer AL, van Haastert PJ. Transmembrane signalling in eukaryotes: a comparison between higher and lower eukaryotes. *Plant Mol Biol.* Dec. 1994;26:1239e1270.

Drews J. Genomic sciences and the medicine of tomorrow. *Nat Biotechnol.* 1996; 14:1516 –1518.

Dror RO, Mildorf TJ, Hilger D, Manglik A, Borhani DW, Arlow DH, Philippson A, Villanueva N, Yang Z, Lerch MT, Hubbell WL, Kobilka BK, Sunahara RK, Shaw DE. Structural basis for nucleotide exchange in heterotrimeric G proteins. *Science.* 2015;348:1361–1365.

Duc N, Kim H, Chung K. Recent Progress in Understanding the Conformational Mechanism of Heterotrimeric G Protein Activation. *Biomol Ther.* 2017;25:4-11.

Eichinger L, Pachebat JA, Glockner G, Rajandream MA, Sucgang R, Berriman M, et al. The genome of the social amoeba *Dictyostelium discoideum*. *Nature.* 2005; 435: 43–57.

Elzie C, Colby J, Sammons M, Janetopoulos C. Dynamic localization of G proteins in *Dictyostelium discoideum*. *J. Cell Science.* 2009;122: 2597-2603.

Etienne-Manneville S. Neighborly relations during collective migration. *Curr Opin Cell Biol.* 2014;30C: 51–59.

Fields TA, Casey PJ. Phosphorylation of G α by Protein Kinase C Blocks Interaction with the bg Complex. *J. Biol. Chem.* 1995; 270: 23119 –23125.

Flock T, Ravarani CN, Sun D, Venkatakrishnan AJ, Kayikci M, Tate CG, Veprintsev DB, Babu MM. Universal allosteric mechanism for G α activation by GPCRs. *Nature.* 2015;524:173–179.

Friedl P, Wolf K. Plasticity of cell migration: a multiscale tuning model. *J. Cell Biol.* 2010;188:11–19.

- Frisz JF, Lou K, ., Kraft ML. Direct chemical evidence for sphingolipid domains in the plasma membranes of fibroblasts. *Proc. Natl. Acad. Sci. USA.* 2012;110:613–622.
- Frisz JF, Klitzing HA, ., Kraft ML. Sphingolipid domains in the plasma membranes of fibroblasts are not enriched with cholesterol. *J. Biol. Chem.* 2013; 288:16855–16861.
- Funamoto S, Meili R, Lee S, Parry L, Firtel RA. Spatial and temporal regulation of 3-phosphoinositides by PI 3-kinase and PTEN mediates chemotaxis. *Cell.* 2002;109:611–623
- Gao Q, Wang Z. Classification of G-protein coupled receptors at four levels. *Protein Engineering, Design & Selection.* 2006;19: 511–516.
- Garbett D, Bretscher A. The surprising dynamics of scaffolding proteins. *Molecular biology of the cell.* 2014;25:2315-2319.
- Gentles A, Karlin S. Why are human G-protein- coupled receptors predominantly intronless? *Trends in Gen.* 1999; 15:47-8.
- Gerwert K, Mann D, Kotting C. Common mechanisms of catalysis in small and heterotrimeric GTPases and their respective GAPs. *Biol Chem.* 2017; 398: 523-533.
- Glick JL, Meigs TE, Miron A, Casey PJ. RGSZ1, a Gz-selective Regulator of G Protein Signaling Whose Action Is Sensitive to the Phosphorylation State of Gz α . *J. Biol.Chem.* 1998;273(40) 26008–26013.
- Good MC, Zalatan JG, Lim WA. Scaffold Proteins: Hubs for Controlling the Flow of Cellular Information. *Science.* 2011;332: 680-686.
- Goricanec D, Stehle R, Egloff P, Grigorie S, Plückthund A, Wagnere G, Hagn F. Conformational dynamics of a G-protein α subunit is tightly regulated by nucleotide binding. *Proc Natl Acad Sci USA.* 2016;113:E3629–E3638.
- Gorter E, Grendel F. On bimolecular layers of lipoids on the chromocytes of the blood. *J. Exp. Med.* 1925; 41: 439–443.
- Goswami D, Gowrishankar K, Bilgrami S, Ghosh S, Raghupathy R, Chadda R, Vishwakarma R, Rao M, Mayor S. Nanoclusters of GPI-anchored proteins are formed by cortical actin-driven activity. *Cell.* 2008; 135:1085–1097.
- Gowrishankar K, Ghosh S, Saha S, C R, Mayor S, Rao M. Active remodeling of cortical actin regulates spatiotemporal organization of cell surface molecules. *Cell.* 2012;149: 1353–1367
- Gudheti MV, Curthoys NM, Gould TJ, Kim D, Gunewardene MS, Gabor KA, Gosse JA, Kim CH, Zimmerberg J, Hess ST. Actin mediates the nanoscale membrane organization of the clustered membrane protein influenza hemagglutinin. *Biophys. J.* 2013; 104: 2182–2192.

Gundersen R. Phosphorylation of the G Protein α -Subunit, Ga2, of Dictyostelium discoideum Requires a Functional and Activated Ga2. *Journal of Cellular Biochemistry*. 1997;66:268–276.

Gundersen RE, Devreotes PN. In vivo Receptor Mediated Phosphorylation of a G Protein in *Dictyostelium*. *Science*. 1990; 248: 591-593.

Hall RA, Premont RT, Lefkowitz RJ. Heptahelical receptor signaling: beyond the G protein paradigm. *J.Cell Biol.* 1999;145:927-32

Harding A, Hancock JF Ras nanoclusters: combining digital and analog signaling. *Cell Cycle*. 2008;7:127-134.

Harris T, Awrey D, Cox B, Ravandi A, Tsang A, Chi-Hung Siu C. Involvement of a Triton-insoluble Floating Fraction in *Dictyostelium* Cell-Cell Adhesion. *The Journal Of Biological Chemistry*.2001;276:18640–18648.

Henis YI, Hancock JF, Prior IA. Ras acylation, compartmentalization and signaling nanoclusters. *Mol Membrane Biol*. 2009; 26:80-92.

Hepler JR, Berman DM, Gilman AG, Kozasa T. RGS4 and GAIP are GTPase-activating proteins for $G_{q\alpha}$ and block activation of phospholipase C β by γ -thio-GTP- $G_{q\alpha}$. *Proc Natl Acad Sci USA*. 1997; 94:428–432.

Hereld D, Vaughan R, Kim JY, Borleis J, Devreotes P. Localization of ligand-induced phosphorylation sites to serine clusters in the C-terminal domain of the *Dictyostelium* cAMP receptor, cAR1. *J. Biol. Chem.* 1994; 269: 7036–7044.

Hess ST, Girirajan TPK, Mason MD. Ultra-High Resolution Imaging by Fluorescence Photoactivation Localization Microscopy. *Biophysical Journal*. 2006; 91:4258-4272.

Hess ST, Gould TJ, Gudheti MV, Maas SA, Mills KD, Zimmerberg J. Dynamic clustered distribution of hemagglutinin resolved at 40 nm in living cell membranes discriminates between raft theories. *PNAS*. 2007;104(44): 17370–17375.

Huang C, Hepler JR, Gilman AG, Mumby SM. Attenuation of G_i - and G_q -mediated signaling by expression of RGS4 or GAIP in mammalian cells. *Proc Natl Acad Sci USA*. 1997; 94:6159–6163.

Huang YE, Iijima M, Parent CA, Funamoto S, Firtel RA, Devreotes PN. Receptor mediated regulation of PI3Ks confines PI(3,4,5)P3 to the leading edge of chemotaxing cells. *Mol. Biol. Cell*. 2003; 14: 1913–1922.

Hurley JH, Boura E, Carlson LA, Rózycki B. Membrane budding. *Cell*. 2010;143: 875–887.

Iijima M, Devreotes P. Tumor suppressor PTEN mediates sensing of chemoattractant gradients. *Cell*. 2002;109:599–610.

Inagaki N, Katsuno H. Actin waves: Origin of cell polarization and migration? *Trends in Cell Biology*. 2017;27(7):515-526.

Itoh Y, Cai K, Khorana HG. Mapping of contact sites in complex formation between light-activated rhodopsin and transducin by covalent crosslinking: Use of a chemically preactivated reagent. *Proc Natl Acad Sci USA*. 2001;98:4883–4887.

Janetopoulos C, Jin T, Devreotes P. Receptor-mediated activation of heterotrimeric G-proteins in living cells. *Science*. 2001; 291: 2408-2411.

Janetopoulos C, Ma L, Devreotes PN, Iglesias PA. The chemoattractant-induced PI(3,4,5)P₃ accumulation is regulated by a local excitation, global inhibition mechanism. *Mol. Biol. Cell*. 2004;15: 402A.

Jaqaman K, Grinstein S. Regulation from within: the cytoskeleton in transmembrane signaling. *Trends Cell Biol*. 2012;22:515–526.

Jaqaman K, Kuwata H, Touret N, Collins R, Trimble WS, Danuser G, Grinstein S. Cytoskeletal control of CD36 diffusion promotes its receptor and signaling function. *Cell*. 2011;146:593–606.

Jiao X, Zhang N, Xu X, Oppenheim J, Jin T. Ligand-Induced Partitioning of Human CXCR1 Chemokine Receptors with Lipid Raft Microenvironments Facilitates G-Protein-Dependent Signaling. *Molecular and Cellular Biology*. 2005; 25:5752–5762.

Jin T, Zhang N, Long Y, Parent CA, Devreotes PN. Localization of the G protein $\beta\gamma$ complex in living cells during chemotaxis. *Science*. 2000;287:1034-1036.

Johnson RL, Saxe CL, Gollop R, Kimmel AR, Devreotes PN. Identification and targeted gene disruption of cAR3, a cAMP receptor subtype expressed during multicellular stages of *Dictyostelium* development. *Genes Dev*. 1993;7:273–282.

Khan SM, Sleno R, Gora S, Zylbergold P, Laverdure J, Labbé J, Miller GJ, Hébert TE, Barker EL. The expanding roles of G $\beta\gamma$ subunits in G protein-coupled receptor signaling and drug action. *Pharmacol Rev*. 2013; 65(2):545–577

Klein PS, Sun TJ, Saxe CL, Kimmel AR, Johnson RL, Devreotes PN. A chemoattractant receptor controls development in *Dictyostelium discoideum*. *Science*. 1988;241:1467–1472.

Konyakhina TM, Goh SL, Amazon J, Heberle FA, Wu J, Feigenson GW. Control of a nanoscopic-to-macroscopic transition: modulated phases in four- component DPSC/DOPC/POPC/Chol, giant unilamellar vesicles, *Biophys. J.* 2011;101: L08–L10.

Kozasa T, Gilman AG. Protein Kinase C Phosphorylates G12 α and Inhibits Its Interaction with G $\beta\gamma$. *J. Biol. Chem.* 1996; 271:12562-12567.

Kreppel L, Fey P, et al. dictyBase: a new *Dictyostelium discoideum* genome database. Nucleic Acids Res. 2004; 32:D332–D333.

Kumagai A, Hadwiger JA, Pupillo M, Firtel RA. Molecular genetic analysis of two G alpha protein subunits in *Dictyostelium*. J. Biol. Chem. 1991; 266:1220-1228.

Kusumi A, Fujiwara TK, Chadda R, Xie M, Tsunoyama TA, Kalay Z, Kasai RS, Suzuki KG. Dynamic organizing principles of the plasma membrane that regulate signal transduction: commemorating the fortieth anniversary of Singer and Nicolson's fluid-mosaic model. Annu. Rev. Cell Dev. Biol. 2012; 28, 215–250.

Kusumi A, Ike H, Nakada C, Murase K, Fujiwara T. Single-molecule tracking of membrane molecules: plasma membrane compartmentalization and dynamic assembly of raftophilic signaling molecules. Semin. Immunol. 2005; 17: 3–21.

Lambright DG, Noel JP, Hamm HE, Sigler PB. Structural determinants for activation of the alpha-subunit of a heterotrimeric G protein. Nature. 1994;369:621–628.

Lambright DG, Snodek J, Bohm A, Skiba N, Hamm H, Sigler P. The 2.0 Å crystal structure of a heterotrimeric G protein. Nature. 1996; 379:311–319.

Lange Y, Swaisgood MH, Ramos BV, Steck TL. Plasma membranes contain half the phospholipid and 90% of the cholesterol and sphingomyelin in culture human fibroblasts. The Journal of Biological Chemistry. 1989; 264:3786–3793.

Lazennec G, Richmond A. Chemokines and chemokine receptors: new insights into cancer-related inflammation. Trends Mol Med. 2010; 16:133–144.

Lee E, Taussig R, Gilman AG.. The G226A mutant of Gs- α highlights the requirement for dissociation of G-protein subunits. J. Biol. Chem. 1992;267: 1212-1218.

Lefkowitz RJ, Whalen EJ. beta-arrestins: traffic cops of cell signaling. Curr Opin Cell Biol. 2004;16(2):162-8.

Leibler S, Andelman D. Ordered and curved meso-structures in membranes and amphiphilic films, J. de Physique. 1987; 48: 2013–2018.

Lingwood D, Simons K. Lipid Rafts As a Membrane- Organizing Principle. Science. 2010 January 1;327.

Lipowsky R. Budding of membranes induced by intramembrane domains. J.de Physique II. 1992; 2:1825–1840.

Lippincott-Schwartz J, Snapp E, Kenworthy A. Studying protein dynamics in living cells. Nat. Rev. Mol. Cell. Biol. 2001; 2: 444–456.

Liu G, Kuwayama H, Ishida S, Newell PC. The role of cyclic GMP in regulating myosin during chemotaxis of *Dictyostelium*: Evidence from a mutant lacking the normal cyclic GMP response to cyclic AMP. *J. Cell Sci.* 1993;106:591-596.

Liu G, Newell PC. Evidence that cyclic GMP regulates myosin interaction with the cytoskeleton during chemotaxis of *Dictyostelium*. *J. Cell Sci.* 1988; 90:123-129.

Liu G, Newell PC. Regulation of myosin regulatory light chain phosphorylation via cyclic GMP during chemotaxis of *Dictyostelium*. *J. Cell Sci.* 1994;107:1737-1743.

Liu W, Matingly R, Garrison, J. Transformation of Rat-i fibroblasts with the v-src oncogene increases the tyrosine phosphorylation state and activity of the a subunit of Gq/G11. *Proc. Natl. Acad. Sci. USA.* 1996; 93:8258-8263.

Liu Y, Berre M, Lautenschlaeger F, Maiuri P, Callan-Jones A, Heuze M, Takaki T, Voituriez R, Piel M. Confinement and Low Adhesion Induce Fast Amoeboid Migration of Slow Mesenchymal Cells. *Cell.* 2015; 160: 659–672.

Lorentzen A, Kinkhabwala A, Rocks O, Vartak N, Bastiaens P. Regulation of Ras Localization by Acylation Enables a Mode of Intracellular Signal Propagation. *Science Signaling.* 2010;140:ra68.

Louis JM, Ginsburg GT, Kimmel AR. The cAMP receptor CAR4 regulates axial patterning and cellular differentiation during late development of *Dictyostelium*. *Genes Dev.* 1994;8:2086–2096.

Lounsbury KM, Casey PJ, Brass LF, Manning DR. Phosphorylation of Gz in Human Platelets SELECTIVITY AND SITE OF MODIFICATION. *J. Biol Chem.* 1991; 266: 22051–22056.

Lounsbury KM, Schlegel B, Poncz M, Brass LF, Manning DR. Analysis of Gz α by Site-directed Mutagenesis. *J. Biol. Chem.* 1993; 268: 3494 –3498.

Luo HR, Huang YE, Chen JC, Saiardi A, Iijima M, Ye K, Huang Y, Nagata E, Devreotes P, Snyder SH. Inositol pyrophosphates mediate chemotaxis in *Dictyostelium* via pleckstrin homology domain-PtdIns(3,4,5)P3 interactions. *Cell.* 2003;114:559-572.

Marivin A, Leyme A, Parag-Sharma K, DiGiacomo V, Cheung AY, Nguyen LT, Dominguez I, Garcia-Marcos M. Dominant-negative G α subunits are a mechanism of dysregulated heterotrimeric G protein signaling in human disease. *Sci Signal.* 2016; 9(423).

Matto-Yelin M, Aitken A, Ravid S. 14–3-3 Inhibits the *Dictyostelium* Myosin II Heavy-Chain-specific Protein Kinase C Activity by a Direct Interaction: Identification of the 14–3-3 Binding Domain. *Molecular Biology of the cell.* 1997; 8:1889-1899.

Michaelson D, Ahearn I, Bergo M, Young S, Philips M. Membrane Trafficking of Heterotrimeric G Proteins via the Endoplasmic Reticulum and Golgi. *Molecular Biology of the Cell*. 2002;13: 3294–3302.

Muller-Taubenberger A, Lupas AN, Li H, Ecke M, Simmeth E, Gerisch G. Calreticulin and calnexin in the endoplasmic reticulum are important for phagocytosis. *EMBO Journal*. 2001;20(23): 6772-6782

Murakoshi H, Iino R, Kobayashi T, Fujiwara T, Ohshima C, Yoshimura A, Kusumi A. Single-molecule imaging analysis of Ras activation in living cells. *Proc. Natl. Acad. Sci. USA*. 2004;101: 7317-7322.

Murase K, Fujiwara T, Umemura Y, Suzuki K, Iino R, Yamashita H, Saito M, Murakoshi H, Ritchie K, Kusumi A. Ultrafine membrane compartments for molecular diffusion as revealed by single molecule techniques. *Biophys. J.* 2004;86:4075–4093.

Noda K, Saad Y, Grahem RM, Karnik SS. The high affinity state of the $\beta 2$ -adrenergic receptor requires unique interaction between conserved and non-conserved extracellular loop cysteines. *J Biol Chem*. 1994;269: 6743–6752.

Noel JP, Hamm HE, Sigler PB. The 2.2 Å crystal structure of transducin-alpha complexed with GTPyS. *Nature*. 1993;366: 654–663.

Nourshargh S, Alon R. Leukocyte migration into inflamed tissues. *Immunity*. 2014; 41(5):694-707.

Offermanns S, Hu Y-H and Simon MI. $\text{G}\alpha 12$ and $\text{G}\alpha 13$ Are Phosphorylated during Platelet Activation. *J. Biol.Chem*. 1996; 271: 26044-26048.

Okae H, Iwakura Y. Neural tube defects and impaired neural progenitor cell proliferation in $\text{G}\beta\alpha 1$ -deficient mice. *Dev. Dyn.* 2010; 239: 1089–1101.

Okaichi K, Cubitt A, Pitt G, Firtel R. Amino acid substitutions in the *Dictyostelium* $\text{G}\alpha$ Subunit $\text{G}\alpha 2$ produce dominant negative phenotypes and inhibit the activation of Adenylyl Cyclase, Guanylyl Cyclase, and Phospholipase C. *Molecular Biology of the Cell*. 1992; 3(7): 735-47.

Othmer H G, Schaap P. Oscillatory cAMP signaling in the development of *Dictyostelium discoideum*. *Comments Theor Biol*. 1998;5:175–282.

Owen DM, Gaus K. Imaging lipid domains in cell membranes: the advent of super-resolution fluorescence microscopy. *Front. Plant Sci*. 2013; 4; 503.

Owen DM, Williamson DJ, Magenau A, Gaus K. Sub-resolution lipid domains exist in the plasma membrane and regulate protein diffusion and distribution. *Nat. Commun.* 2012; 3: 1256.

Palmieri B, Yamamoto T, Brewster RC, Safran SA. Line active molecules promote inhomogeneous structures in membranes: theory, simulations and experiments, *Adv. Coll. Interf. Sci.* 2014; 208: 58–65.

Pfeifer A, Nurnberg B, Kamm S, Uhde M, Schultz G, Ruth P, Hofmann F. Cyclic GMP-dependent Protein Kinase Blocks Pertussis Toxin-sensitive Hormone Receptor Signaling Pathways in Chinese Hamster Ovary Cells. *J. Biol.Chem.* 1995; 270(16):9052-9059.

Pierce KL, Premont RT, Lefkowitz RJ. Seven-transmembrane receptors. *Nat. Rev. Mol. Cell Biol.* 2002;3:639-650

Pike L. Rafts defined: a report on the Keystone symposium on lipid rafts and cell function. *Journal of Lipid Research.* 2006;47.

Pingret J, Journet E, Barker DG. Rhizobium Nod factor signaling: evidence for a G protein-mediated transduction mechanism. *Plant Cell.* 1998;10:659- 71.

Pitt GS, Milona N, Borleis J, Lin KC, Reed RR, Devreotes PN. Structurally distinct and stage-specific adenylyl cyclase genes play different roles in *Dictyostelium* development. *Cell.* 1992; 69: 305-315.

Poppleton H, Sun H, Fulgham D, Bertics P, Pate TB. Activation of G_a by the Epidermal Growth Factor Receptor Involves Phosphorylation. *J. Biol.Chem.* 1996;271(12):6947–6951.

Prior IA, Muncke C, Parton RG, Hancock JF. Direct visualization of Ras proteins in spatially distinct cell surface microdomains. *The journal of cell Biology.* 2003;160:165-170.

Probst W, Synder LA, Schuster DI, Brosius J,Sealfon SC. Sequence alignment of the G-protein coupled receptor superfamily. *DNA Cell Biol.* 1992;11:1–20.

Rajagopal K, Lefkowitz RJ, Rockman HA. When 7 transmembrane receptors are not G protein-coupled receptors. *J. Clin. Invest.* 2005;115:2971–2974.

Rajendran L, Simons K. Lipid rafts and membrane dynamics. *Journal of Cell Science.* 2005;118: 1099-1102.

Rayermann S, Rayermann G, Merz A, Keller S. Hallmarks of reversible phase separation in living, unperturbed cell membranes. *Biophysical Journal.* 2017; 112: 522a.

Ridley AJ, Schwartz MA, Burridge K, Firtel RA, Ginsberg MH, Borisy G, Parsons JT, Horwitz AR. Cell migration: integrating signals from front to back. *Science.* 2003;302:1704-1709.

Riou P, Kjær S, Garg R, Purkiss A, George R, Cain RJ, Bineva G, Reymond N, McColl B, Thompson AJ, O'Reilly N, McDonald NQ, Parker PJ, Ridley AJ. 14-3-3 Proteins Interact with a Hybrid Prenyl-Phosphorylation Motif to Inhibit G Proteins. *Cell*. 2013;153:640-653.

Ross EM, Gilman AG. Biochemical properties of hormone-sensitive adenylate cyclase. *Annu Rev Biochem*. 1980;49:533-564.

Ross EM, Wilkie TM. GTPase-activating proteins for heterotrimeric G proteins: regulators of G protein signaling (RGS) and RGS-like proteins. *Annu. Rev. Biochem.* 2000; 69: 795–827.

Rot A, von Andrian UH. Chemokines in innate and adaptive host defense: basic chemokine grammar for immune cells. *Annu Rev Immunol*. 2004; 22:891-928.

Rotblat B, Prior IA, Muncke C, Parton RG, Kloog Y, Henis YI, Hancock JF. Three separable domains regulate GTP-dependent association of H-ras with the plasma membrane. *Mol Cell Biol*. 2004;24, 6799–6810.

Roy AA, Baragli A, Bernstein LS, Hepler TE, Chidiac P. RGS2 interacts with Gs and adenylyl cyclase in living cells. *Cell Signal*. 2006;18:336–348.

Ruppel KM, Willison D, Kataoka H, Wang A, Zheng YW, Cornelissen I, Yin L, Xu SM, Coughlin SR. Essential role for Ga13 in endothelial cells during embryonic development. *Proc. Natl. Acad. Sci. U. S. A.* 2005;102:8281–8286.

Sadik CD, Luster AD. Lipid-cytokine-chemokine cascades orchestrate leukocyte recruitment in inflammation. *J Leukoc Bio*. 2012; 91(2): 207–215.

Saxe CL, Ginsburg GT, Louis JM, Johnson R, Devreotes PN, Kimmel AR. CAR2, a prestalk cAMP receptor required for normal tip formation and late development of *Dictyostelium discoideum*. *Genes Dev*. 1993;7:262–272.

Saxe CL, Yu Y, Jones C, Bauman A, Haynes C. The cAMP receptor subtype cAR2 is restricted to a subset of prestalk cells during *Dictyostelium* development and displays unexpected DIF 1 responsiveness. *Dev. Biol*. 1996; 174:202–213.

Schneider IC, Haugh JM. Quantitative elucidation of a distinct spatial gradient-sensing mechanism in fibroblasts. *The Journal of Cell Biology*. 2005;171(5): 883–892.

Schulkes C, Schaap P. cAMP-dependent protein kinase activity is essential for pre-aggregative gene expression in *Dictyostelium*. *FEBS Lett*. 1995;368:381–384.

Scott JK, Huang, SF, Gangadhar BP, Samoriski GM, Clapp P, Gross RA, Taussig R, Smrcka AV. Evidence that a protein–protein interaction ‘hot-spot’ on heterotrimeric G protein β subunits is used for recognition of a subclass of effectors. *EMBO J*. 2001; 20: 767–776.

Sengupta P, Jovanovic-Talisman T, Skoko D, Renz M, Veatch SL, Lippincott-Schwartz J. Probing protein heterogeneity in the plasma membrane using PALM and pair correlation analysis. *Nat. Methods.* 2011;8: 969–975.

Servant G, Weiner OD, Neptune ER, Sedat JW, Bourne HR. Dynamics of a chemoattractant receptor in living neutrophils during chemotaxis. *Mol. Biol. Cell.* 1999;10:1163-1178.

Shim JY, Ahn KH, Kendall DA. Molecular basis of cannabinoid CB1 receptor coupling to the G protein heterotrimer Gai β : identification of key CB1 contacts with the C-terminal helix α 5 of Gai. *J Biol Chem.* 2013;288:32449–32465.

Shorr RGL, Lefkowitz RJ, Caron MG. Purification of the β -adrenergic receptor. Identification of the hormone-binding subunit. *J Biol Chem.* 1981;256:5820–5826.

Siderovski DP, Willard FS. The GAPs, GEFs, and GDIs of heterotrimeric G-protein alpha subunits. *Int J Biol Sci.* 2005;1: 51-66.

Sieber JJ, Willig KI, Kutzner C, Gerding-Reimers C, Harke B, Donnert G, Rammner B, Eggeling C, Hell SW, Grubmuller H, Lang T. Anatomy, dynamics of a supramolecular membrane protein cluster. *Science.* 2007;317: 1072–1076.

Silveira LA, Smith JL, TAN JL, Spudich JA. MLCK-A, an unconventional myosin light chain kinase from Dictyostelium, is activated by a cGMP-dependent pathway. *PNAS.*1998;95:13000-13005.

Simons K, van Meer G. Lipid sorting in epithelial cells. *Biochemistry* 1988;27:6197–6202.

Singer SJ, Nicolson GL. The fluid mosaic model of the structure of cell membranes. *Science.* 1972; 175: 720–731.

Smith AJ, Daut J, Schwappach B. Membrane proteins as 14-3-3 clients in functional regulation and intracellular transport. *Physiology.* 2011;26: 181-191.

Souza GM, da Silva AM, Kuspa A. Starvation promotes *Dictyostelium* development by relieving PufA inhibition of PKA translation through the YakA pathway. *Development.* 1999;126:3263–3274.

Souza GM, Lu S, Kuspa A. YakA, a protein kinase required for the transition from growth to development in *Dictyostelium*. *Development.* 1998;125:2291–2302.

Steimle PA, Yumura S, Co^{te} G. P, Medley QG, Polyakov MV, Leppert B, Egelhoff TT. Recruitment of a myosin heavy chain kinase to actin-rich protrusions in *Dictyostelium*. *Current Biology.* 2001;11:708-713.

Steven R, Zhang L, Culotti J, Pawson T. The UNC-73/Trio RhoGEF-2 domain is required in separate isoforms for the regulation of pharynx pumping and normal neurotransmission in *C. elegans*. *Genes Dev.* 2005;19: 2016–2029.

Strader CD, Fong TM, Tota MR, Underwood D, Dixon RA. Structure and function of G protein-coupled receptors. *Annu Rev Biochem.* 1994;63:101-32.

Strassheim D, Malbon C. Phosphorylation of Gia2 Attenuates Inhibitory Adenylyl Cyclase in Neuroblastoma Glioma Hybrid(NG-108-15) Cells. *J. Biol.Chem.* 1994; 269(19):14307-14313.

Sun B, Firtel RA. A Regulator of G Protein Signaling-containing Kinase Is Important for Chemotaxis and Multicellular Development in *Dictyostelium*. *Molecular Biology of the cell.* 2003;14:1727-1743.

Sun TJ, Devreotes PN.. Gene targeting of the aggregation stage cAMP receptor cAR1 in *Dictyostelium*. *Genes Dev.* 1991; 5:572–582.Swaney KF, Huang CH, Devreotes PN. Eukaryotic chemotaxis: a network of signaling pathways controls motility, directional sensing, and polarity. *Annu Rev Biophys.* 2010;39: 265e289.

Syrovatkina V, Alegre K O, Dey R, Huang X. Regulation, Signaling, and Physiological Functions of G-Proteins. *J Mol Biol.* 2016; 428: 3850–3868.

Szczepk M, Beyrière F, Hofmann KP, Elgeti M, Kazmin R, Rose A, Bartl FJ, von Stetten D, Heck M, Sommer ME, et al. Crystal structure of a common GPCR-binding interface for G protein and arrestin. *Nat Commun.* 2014;5:4801.

Taddei ML, Giannoni E, Comito G, Chiarugi P. Microenvironment and tumor cell plasticity: an easy way out. *Cancer Lett.* 2013; 341: 80–96.

Taddei ML, Giannoni E, Morandi A , Ippolito L , Ramazzotti M , Callari M , Gandellini P, Chiarugi P. Mesenchymal to amoeboid transition is associated with stem-like features of melanoma cells. *Cell Communication and Signaling.* 2014;12:24.

Takeda M, Leser GP, Russell CJ, Lamb RA . Influenza virus hemagglutinin concentrates in lipid raft microdomains for efficient viral fusion. *Proc Natl Acad Sci USA.*2003;100:14610 –14617.

Tang L, Franca-Koh J, Xiong Y, Chen MY, Long Y, Bickford RM, Knecht DA, Iglesias PA, Devreotes PN. tsunami, the *Dictyostelium* homolog of the Fused kinase, is required for polarization and chemotaxis. *Genes Dev.* 2008;22:2278–2290.

Tang Y, Lv P, Sun Z, Han L, Zhou W. 14-3-3 β Promotes Migration and Invasion of Human Hepatocellular Carcinoma Cells by Modulating Expression of MMP2 and MMP9 through PI3K/Akt/NF- κ B Pathway. *PLoS ONE.*2016;11.

Thomsen A, Plouffe B, Cahill TJ, Shukla AK, Tarrasch JT, Dosey AM, Kahsai AW, Strachan RT, Pani B, Mahoney JP, Huang L, Breton B, Heydenreich FM, Sunahara

RK, Skiniotis G, Bouvier M, Lefkowitz RJ. GPCR-G Protein-b-Arrestin Super-Complex Mediates Sustained G Protein Signaling. *Cell*. 2016; 166: 907–919.

Tian T, Harding A, Inder K, Plowman S, Parton RG, Hancock JF Plasma membrane nanoswitches generate high-fidelity Ras signal transduction. *Nat. Cell Biol.* 2007; 9:905–914.

Tozluoglu M, Tournier AL, Jenkins RP, Hooper S, Bates PA, Sahai E. Matrix geometry determines optimal cancer cell migration strategy and modulates response to interventions. *Nat. Cell Biol.* 2013; 15: 751–762.

Trusov Y, Chakravorty D, Botella J. Diversity of heterotrimeric G-protein subunits in plants. *BMC Research Notes*. 2012;5:608.

Tuteja N. Signaling through G protein coupled receptors. *Plant Signaling & Behavior*. 2009; 4: 942-947.

Tysona R , Zatulovskiyb E, Kayb R , Bretschneider T. How blebs and pseudopods cooperate during chemotaxis. *PNAS*. 2014;111(32): |11703–11708.

Umemori H, Inoue T, Kume S, Sekiyama N, Nagao M, Itoh H, Nakanishi S, Mikoshiba K, Yamamoto T. Activation of the G Protein Gq/1 1 Through Tyrosine Phosphorylation of the a Subunit. *Science*.1997; 276.

Ursell TS, Klug WS, Phillips R Morphology and interaction between lipid domains. *Proc Natl Acad Sci USA*. 2009; 106:13301–13306.

Valiyaveetil FI, Zhou Y, MacKinnon R Lipids in the structure, folding, and function of the KcsA K⁺ channel. *Biochemistry*. 2002; 41: 10771–10777.

Van Hemert F, Lazova M, Snaar-Jagaska E, Schmidt T. Mobility of G proteins is heterogeneous and polarized during chemotaxis. *Journal of Cell Science*. 2010;123(17):2922-2930.

Veltman DM, Roelofs J, Engel R, Visser AJ, Van Haastert PJ. Activation of soluble guanylyl cyclase at the leading edge during Dictyostelium chemotaxis. *Mol Biol Cell*. 2005;16:976–983

Vorotnikov AV, Tyurin-Kuzmin P. Chemotactic signaling in mesenchymal cells compared to amoeboid cells. *Genes & Diseases*. 2014; 1: 162–173.

Wall MA, Coleman DE, Lee E, Iniguez-Lluhi JA, Posner BA, Gilman AG, Sprang SR. The structure of the G protein heterotrimer G α 1 β 1 γ 2. *Cell*. 1995; 83: 1047–1058.

Wang J, Frost JA, Cobb MH, Ross EM. Reciprocal Signaling between Heterotrimeric G Proteins and the p21-stimulated Protein Kinase. *J. Biol.Chem.* 1999; 274(44): 31641–31647,

- Watson. Biological membranes. Essays Biochem. 2015; 59: 43–70.
- Watts D, Ashworth J. Growth of Myxamoebae of the Cellular Slime Mould *Dictyostelium discoideum* in Axenic Culture. The Biochemical Journal. Vol.1970;119(2):171-174.
- Weiser DC, Pyati UJ, Kimelman D. Gravin regulates mesodermal cell behavior changes required for axis elongation during zebrafish gastrulation. Genes Dev. 2007; 21: 1559–1571.
- Westfield GH, Rasmussen SG, Su M, Dutta S, DeVree BT, Chung KY, Calinski D, Velez-Ruiz G, Oleskie AN, Pardon E, Chae PS, Liu T, Li S, Woods VL, Steyaert J, Kobilka BK, Sunahara RK, Skiniotis G. Structural flexibility of the $\text{G}\alpha_s$ α -helical domain in the $\beta 2$ -adrenoceptor G_s complex. Proc. Natl. Acad. Sci. U.S.A. 2011;108:16086–16091.
- Wettschureck N, Moers O A, Offermann S. Mouse models to study G-protein-mediated signaling. Pharmacol. Ther. 2004; 101:75–89.
- Wettschureck N, Offermanns. Mammalian G Proteins and Their Cell Type Specific Functions. Physiol Rev. 2005;85: 1159–1204.
- White J, Helenius A, Gething MJ. Haemagglutinin of influenza virus expressed from a cloned gene promotes membrane fusion. Nature. 1982; 300:658 – 659.
- Williams SL, Lutz S, Charlie NK, Vettel C, Ailion M, et al. Trio's Rho-specific GEF domain is the missing Galphqa effector in *C. elegans*. Genes Dev. 2007;21: 2731–2746.
- Wilson RL, Frisz JF, Klitzing H, Zimmerberg J, Weber PK, Kraft ML. Hemagglutinin clusters in the plasma membrane are not enriched with cholesterol and sphingolipids. Biophysical Journal. 2015;108:1652-1659.
- Wu L, Valkema R, Van Haastert PJ, Devreotes PN. The G protein beta subunit is essential for multiple responses to chemoattractants in *Dictyostelium*. J. Cell Biol. 1995;129:1667–1675.
- Xiao Z, Zhang N, Murphy DB, Devreotes PN. Dynamic distribution of chemoattractant receptors in living cells during chemotaxis and persistent stimulation. J. Cell Biol. 1997;139:365-374.
- Xu X, Meier-Schellersheim M, Jiao X, Nelson LE, Jin T. Quantitative imaging of single live cells reveals spatiotemporal dynamics of multistep signaling events of chemoattractant gradient sensing in *Dictyostelium*. Mol. Biol. Cell. 2005; 16: 676–688.
- Yao XQ, Grant BJ. Domain-opening and dynamic coupling in the α -subunit of heterotrimeric G proteins. Biophys.J. 2013;105:L08–10.
- Yethiraj A, Weisshaar JC. Why are lipid rafts not observed in vivo? Biophys. J. 2007;93:3113.

Ye Y, Yang Y, Cai X, Liu L, Wu K, Yu M. Down-regulation of 14-3-3 Zeta Inhibits TGF- β 1-Induced Actomyosin Contraction in Human Trabecular Meshwork Cells Through RhoA Signaling Pathway. *iOVS*. 2016;57: 719-30.

Yokosuka T, Sakata-Sogawa K, Kobayashi W, Hiroshima M, Hashimoto-Tane A, Tokunaga M, Dustin ML, Saito T. Newly generated T cell receptor microclusters initiate and sustain T cell activation by recruitment of Zap70 and SLP- 76. *Nat. Immunol.* 2005; 6:1253-1262.

Yuen IS, Jain R, Bishop JD, et al. A density-sensing factor regulates signal transduction in *Dictyostelium*. *J. Cell Biol.* 1995;129:1251–1262.

Yumura S, Fukui YY. Spatiotemporal dynamics of actin concentration during cytokinesis and locomotion in *Dictyostelium*. *Journal of Cell Science*.1998;111: 2097-2108.

Yu Y, Saxe CL.. Differential distribution of cAMP receptors cAR2 and cAR3 during *Dictyostelium* development. *Dev. Biol.* 1996;173:353–356.

Zernecke A, Weber C Chemokines in the vascular inflammatory response of atherosclerosis. *Cardiovasc Res.* 2010;86: 192-201.

Zhai P, Yamamoto M, Galeotti J, Liu , Masurekar M, Thaisz J, Irie K, Holle E, Yu X, Kupershmidt S et al. Cardiac-specific overexpression of AT1 receptor mutant lacking G α q/G α i coupling causes hypertrophy and bradycardia in transgenic mice. *J. Clin. Invest.* 2005;115:3045–3056.

Zheng B, Ma YC, Ostrom RS, Lavoie C, Gill GN, Insel PA, Huang XY, Farquhar MG. RGS-PX1, a GAP for Galphas and sorting nexin in vesicular trafficking. *Science*. 2001; 294:1939-1942.

Zhou Q, Kee Y, Poirier CC, Jelinek C, Osborne J, Divi S, Surcel A, Will ME, Eggert US, Muñller-Tauberberger A, Iglesias PA, Cotter RJ, Robinson DN. 14-3-3 Coordinates Microtubules, Rac, and Myosin II to Control Cell Mechanics and Cytokinesis. *Current Biology*.2010; 20:1881-1889 .

Zigmond SH, Joyce M, Borleis J, Bokoch GM, Devreotes PN. Regulation of actin polymerization in cell-free systems by GTP γ S and Cdc42. *J Cell Biol.* 1997;138:363–374.

BIOGRAPHY OF THE AUTHOR

Sarah Alamer was born in Al-Ahsa, Saudi Arabia on October 6th, 1984. She graduated from the Third High School in 2003. In 2008, she graduated from King Faisal University (KFU) with a Bachelor's degree in Biology. After graduating, Sarah was hired by KFU to teach biology laboratory. KFU offered her, after one year, a full scholarship to obtain a Master's and PhD degree. She received a Master degree in Microbiology from University of Maine in August 2013. Sarah started Graduate School of Biomedical Science and Engineering (GSBSE) program at UMaine in fall 2013. She is a candidate for the Doctor of Philosophy degree in Biomedical Sciences from the University of Maine in August 2018.